Optimising the power quality control of a distributed generation power system

C.P. du Rand

Dissertation submitted in partial fulfillment of the requirements for the degree

Magister Ingeneriae

in Electrical and Electronic Engineering at the North-West University

Supervisor: Prof. G. van Schoor

Potchefstroom

2004

Opsomming

Verspreide generasie of generators (VG) verwys na die opwekking van elektriese drywing op 'n kleiner skaal (produksie wissel in grootte van 'n paar kW tot menige MW) deur 'n eenheid wat nie deel is van 'n sentrale voorsiener nie. Hierdie eenheid (of eenhede op 'n netwerk) is nader aan die las waaraan dit elektrisiteit voorsien. VG tegnologie kan in die behoeftes van 'n groot verskeidenheid van gebruikers voorsien, met toepassings in die residensiële (sonselle), kommersiële (brandstofselle) en industriële sektore (turbines).

Drywingskwaliteit en beheer speel 'n belangrike rol in hierdie VG netwerke. Drywingskwaliteit het 'n groot bekommernis geword vir elektrisiteitsvoorsieners, vir hul kliënte, en vir die vervaardigers van elektriese toerusting, a.g.v. die negatiewe impak wat drywingskwaliteitsteurnisse op stelselbetroubaarheid en-operasie het. Groot hoeveelhede data, vaagheid in die data, en die oneindige hoeveelheid variasies van stelselkonfigurasies dra als by tot die kompleksiteit van drywingskwaliteitanalise en-diagnose. Hierdie kompleksiteit het die behoefte vir gesofistikeerde hulpmiddels genoodsaak om stelselingenieurs te help. Kunsmatige intelligensie (KI) blyk die mees geskikte hulpmiddel vir drywingskwaliteit toepassings te wees.

Die verhandeling voorsien aan die leser 'n oorsig oor VG en drywingskwaliteitprobleme in kragnetwerke. 'n Gedeeldte van 'n huidige kragnetwerk word gemodelleer en ge-evalueer. Twee VGs word op strategiese posisies aan die netwerk gekoppel met die doel om drywingskwaliteit parameters te optimeer. Die Kunsmatige Neurale Netwerk (KNN) metode van KI word in hierdie navorsing gebruik omdat dit ideaal gepas is vir patroonherkenning. Die KNN word gebruik vir die patroonherkenning van die laste en selekteer dan die uitsette van die VGs. Die opleidingsdata vir die KNN word geskep d.m.v. 'n kostefunksie. Die kostefunksie bepaal die optimale toestande van die VGs vir 'n spesifieke insettoestand. Die kostefunksie gebruik die gemiddelde spanningsafwyking van die toelaatbare gebied (V_{avg}), die gemiddelde spanningsafwyking van die ideaal (V_{ideal}), die koste van produksie (C_T) en die netwerk aktiewe verliese (P_L) as parameters vir optimering. Na hierdie optimeringsproses word die KNN opgelei met die willekeurig rangskikte opleidingsdata.

Die aanpasbare gedrag van die KNN beheerder word ondersoek en vergelyk met die geval waar daar geen beheer toegepas word nie. Uit hierdie ondersoeke is daar gevind dat die KNN beheerder sinvolle besluite kon neem, selfs vir laspatrone buite die opleidingsversameling. Die gedrag van die KNN beheerder is egter baie afhanklik van die integriteit van die opleidingsdata. Verdere verfyning en kontinue opdatering van die opleidingsversameling m.b.t. die operasionele gebiede van die laste word aanbeveel vir verdere navorsing. Die gevolgtrekking wat gemaak kan word uit hierdie navorsing is dat

dit sinvol is om VGs met KNN beheer in 'n elektriese kragnetwerk te plaas om die drywingskwalitiet te optimeer.

Dankbetuigings

Eerstens en die belangrikste, die Hemelse Vader, vir die verstand en die geleentheid om die studie te kon doen. Sonder Hom by my, sou niks moontlik gewees het nie.

Prof. G. van Schoor vir sy bekwame leiding en geduld tydens die studie.

My familie en vriende vir hul ondersteuning en begrip gedurende die studie

M-Tech Industrial vir die finansiële ondersteuning met die studie.

Die Skool vir Elektriese en Elektronies Ingenieurswese by die Noordwes Universiteit vir die geleentheid om die studie te kon doen.

ESKOM vir die gevallestudievoorstel en die hulp met die kragnetwerk.

Contents

Chapter 6 Evaluation of the cost function and ANN controller

Chapter 7 Conclusion and Recommendations

Annexures

Bibliography

List of Abbreviations

ac	alternating current
AI	Artificial intelligence
ANN	Artificial neural network
ANFS	Artificial neuro-fuzzy system
AVDP	Average voltage deviation from permitted
AVDI	Average voltage deviation from ideal
AVR	Automatic voltage regulator
CF	Cost function
CHP	Combined heat and power
dc	direct current
DG	Distributed generation/Distributed generators
ES	Expert system
FFT	Fast fourier transform
FL	Fuzzy logic
GA	Generic algorithms
GUI	Graphical user interface
kW	kilowatt
LFC	Load frequency control
LTC	Load tap changer
MLP	Multilayer perceptron
MVA	Mega volt ampere
MVAr	Mega volt ampere reactive
MW	Megawatt
NNT	Neural network toolbox
OPF	Optimum power flow
PBMR	Pebble bed modular reactor
PF	Power factor
PQ	Power quality
pu	per unit
RLC	Combination of resistive, inductive and capacitive elements
rms	root-mean-square
SLG	Single line-to-ground
SPS	SimPowerSystems
SVR	Step voltage regulator

List of Symbols

α	ANN momentum constant
η	ANN learning rate parameter
$\varphi(\bullet)$	Neuron activation function
δ	Voltage phase angle on network busses
$\angle I_L$	Load current phase angle
$\angle V_{gen}$	Generator/source voltage phase angle
$\angle V_L$	Load voltage phase angle
b_k	Neuron bias
B_{00}, B_{0i}, B_{ij}	Power flow loss coefficients
C_T	Total cost of generation
C(F/km)	Line capacitance in Farad per kilometer
d_{norm}	Normalised data point
d_{min}	Minimum normalisation value
d_{max}	Maximum normalisation value
e_{ij}	Output of neuron j for i^{th} training value
H	Hermittian matrix
I_L	Load current magnitude
k	Number of subsets in training data
L(H/km)	Line inductance in Henry per kilometer
n	Number of load combinations
n_d	Number of load busses
n_g	Number of generator busses
nv	Normalisation value
N	Number of network busses
P_D	Total active load of system
P_G	Total active power generation of all generation plants
P_{gen}	Generator/source active power
P_i	Active power generation of plant i
P_L	Total system active power losses
P_{load}	Load active power
Q_{gen}	Generator/source reactive power
Q_{load}	Load reactive power
R(Ω/km)	Line resistance in ohm per kilometer
V_{avg}	Average voltage deviation from permitted range

V_{gen}	Generator/source voltage magnitude
V_i	Voltage at network bus i
V_i^*	Desired voltage range at network bus i
V_{ideal}	Average voltage deviation from ideal
v_{ideal}	Ideal voltage at network bus i
V_L	Load voltage magnitude
w_{km}	Neuron synaptic weights
x_m	Neuron inputs
Y_{bus}	Network bus admittance matrix
Z_{bus}	Network bus impedance matrix

List of Figures

List of Tables

Chapter 1 - Introduction

The aim of this chapter is to introduce distributed generation (DG) to the reader as an emerging technology in the power industry. DG can provide energy solutions to customers that are more cost-effective, more environmentally friendly, or provide higher power quality (PQ) and reliability than conventional solutions. PQ plays an important role in power networks and with the aid of DG and the proper control tools that incorporates artificial intelligence (AI), PQ can be analysed and controlled. This chapter gives a short overview of DG and AI, thus motivating the purpose of the study. Furthermore an overview of the dissertation is given.

1.1 Distributed generation

DG is a new approach in the electricity industry and the relevant literature shows there is no generally accepted definition for DG [1]. In the literature, a large number of terms and definitions are used for DG. The *Institute of Electrical and Electronic Engineers (IEEE)* defines DG as "The generation of electricity by facilities sufficiently smaller than central generating plants as to allow interconnection at nearly any point in a power system".

DG is currently being used by some customers to provide some or all of their electricity needs. In some instances, DG technologies can be more cost effective than conventional solutions. There are many different potential applications for DG technologies. For example, some customers use DG to reduce demand charges imposed by their electric utility, while others use it to provide premium power or reduce environmental emissions. DG can also be used by electric utilities to enhance both their distribution and existing power systems.

Current technologies for distributed generation vary widely. A summary of current technologies is shown in table 1.1. Some of these technologies are discussed in chapter 2.

Technology	Typical size per module
1. Combined gas turbine	35 – 400 MW
2. Internal combustion engines	5 kW – 10 MW
3. Combustion turbine	1 – 250 MW
4. Micro turbines	35 kW – 1 MW
Renewable sources	
5. Small hydro	1 – 100 MW
6. Micro hydro	25 kW – 1 MW
7. Wind turbine	200 W – 3 MW
8. Photovoltaic cells	20 W – 100 kW
9. Solar thermal	1 – 80 MW
10. Biomass, e.g. based on gasification	100 kW – 20 MW
11. Fuel cells	1 kW – 5 MW
12. Geothermal	5 – 100 MW
13. Ocean energy	100 kW – 1 MW
14. Battery storage	500 kW – 5 MW

Table 1.1 Technologies for distributed generation.

1.2 The power quality problem

Electric power quality (PQ) has become a topic of increasing interest since the late 1980's. This interest involves all the parties concerned with PQ in the power business: firstly, the utility companies which is the origin of the electricity, the customers who use the electricity and the manufacturers of electric equipment. According to Ibrahim and Morcos [2], the growing concern is due to the following reasons:

a) End-user load equipment has become more sensitive to power quality due to many microprocessor-based controls;
b) Complexity of industrial processes. The restart-up of these industries is a very costly affair;
c) Development of sophisticated power electronic equipment used for improving system stability, operation, and efficiency. These devices are a major source of bad power quality and are themselves vulnerable to bad PQ;
d) Complex interconnection of systems, which results in more severe consequences if any one component fails;

e) Continuous development of high performance equipment: Such equipment is more susceptible to power disturbances.

Power quality problems can be defined as any problem in power due to current, voltage or frequency deviations that result in the failure or malfunction of the customers' equipment [3]. Alternative definitions for PQ are used within the power industry, reflecting the different viewpoints of the parties involved. From a supplier and equipment manufacturer's point of view, PQ is a perfect sinusoidal waveform with no distortion (consistent in voltage magnitude and frequency) and no noise on the grounding system. The customers' point of view may be that PQ is simply the power that works for their equipment without damaging it.

While each of these viewpoints is clearly different, a definition that is properly focused is difficult to establish. A definition based upon the PQ parameters is also not feasible, because different PQ parameters will apply to different power network scenarios. To establish a PQ definition that is acceptable to all the parties is a field of interest on its own. As the appropriate literature suggests, the following PQ attributes are affected with the connection of DGs onto the power grid [4],[5]:

a) Islanding;
b) Steady state voltage regulation;
c) Harmonic distortion;
d) Reverse power flow effects;
e) Direct current injection;
f) Over-voltage conditions;
g) System losses;
h) Voltage unbalance;
i) Under-voltage conditions; and
j) Flicker.

The PQ parameters that are applicable for the purpose of this research are defined in chapter 2. The use of DG in power networks has positive and negative effects on the PQ [3]. Concerning voltage regulation, the response due to the use of discrete tap changing devices like regulators is not effectively smooth and fast. Impedance compensation devices like shunt capacitors may cause harmonic problems, whilst series capacitors may result in resonance and ferroresonance (in transformers). From the point of view of power system losses, electric power systems incorporate generation plants and loads that are interconnected by long transmission lines. These systems can suffer from significant losses [6]. It is therefore necessary to study the effect of integrated DG units on PQ control in the electric power system.

The literature suggests that DG offers the following benefits for PQ problems [5]:

a) Harmonic content produced by the generators are limited to below acceptable limits. This is primarily an equipment vendor design issue;
b) DGs can have a beneficial impact on flicker caused by other loads if they are operated as controlled voltage sources;
c) DG does not inject DC current into the grid;
d) DG can counter the effect of ripple current, which is proportional to the amount of voltage unbalance.
e) DG can be effective in counteracting voltage regulation problems because of its ability to impact the active and reactive power flow.

1.3 Artificial intelligence and power quality

Previous research has shown that AI tools are very suitable for PQ analysis and control. An important application of AI is the development of a PQ analysis and control system. According to Ibrahim and Morcos [2], AI techniques are suitable for PQ applications for the following reasons:

a) Knowledge about PQ is dispersed and fragmented;
b) PQ experts are scarce in the electric power industry;
c) Endless number of system configurations, making each PQ problem unique in its characteristics and diagnosis;
d) Large domain analysis of PQ (equipment, standards, and methodologies);
e) Distributed PQ monitoring systems that gather a huge amount of data, which is not feasible for a human expert to analyse;
f) Large amount of data that require not only intelligent analysis but also intelligent data management;
g) Imprecision of data, making conventional programs fail to identify PQ problems;
h) PQ diagnosis requires expertise in a wide variety of power topics. AI tools can combine knowledge in several domains.

These PQ parameters can be optimised and controlled with the aid of AI tools. AI tools include expert systems (ES), artificial neural networks (ANN), fuzzy logic (FL), and newer techniques like adaptive neuro-fuzzy systems (ANFS) and generic algorithms (GA). The algorithms and feasibility of these tools are discussed in chapter 2.

1.4 Problem statement

The aim of this study is to control the quality of power through the optimal utilisation of DGs in an electric power network. A scenario (part of a power network) needs to be investigated to determine the PQ control parameters. An ANN controller needs to be developed to assess the state of the power network (load conditions) and control the output of the DGs to optimise the PQ parameters. The block diagram in figure 1.1 illustrates the principal of the connection between the proposed ANN, the DGs and the power network.

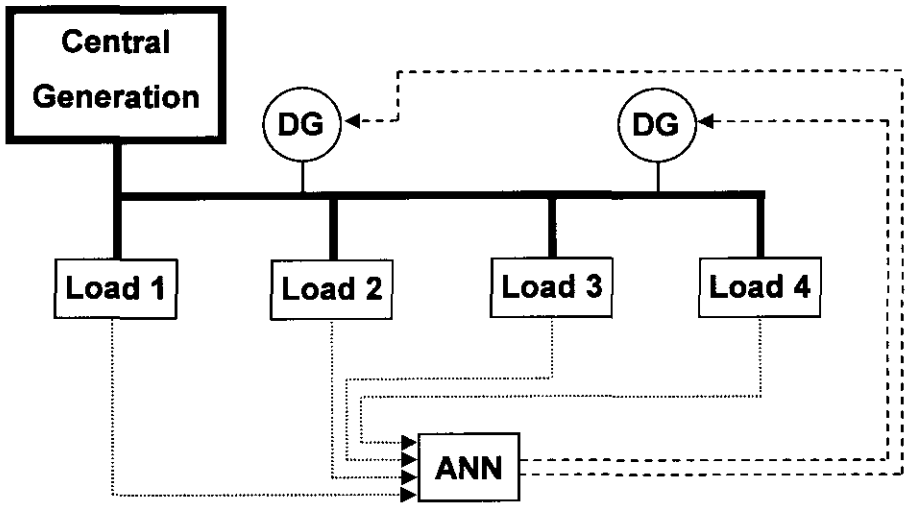

Figure 1.1 Block diagram of the power network with ANN controller.

The ANN controller will typically use the active and reactive power flows of the loads as input and the output will be the optimal operating levels of the DGs.

1.5 Methodology

The power network under consideration, different DG technologies and typical interconnection methodologies are firstly evaluated to assess their impact on the PQ parameters. Based on this assessment, the PQ parameters applicable to this study is identified and evaluated. The voltage and power loss sensitivities of the power network are evaluated to determine the optimal connection points of the DGs. Also, the different control types are reviewed and a control type for the DGs is selected.

To optimise the PQ parameters identified, a cost function (CF) is developed to analyse the condition

of the power network and select the optimal operating states of the DGs. The CF is developed from the basis of a well-known topic: "Reactive power flow optimisation [25], [26]". The active power flow of the system is optimised which results in optimised active power losses. Data is developed by the CF from the different load conditions. Loads are varied from minimum to maximum load capacity.

Based on the data developed by the CF, an AI controller is developed for the DGs. The different AI technologies are firstly reviewed to identify the most suitable. The AI controller is trained with the network data and optimised. Several techniques are used to optimise and determine the topology of the AI controller. The controller is finally integrated into the system and the network conditions are evaluated for the DGs with an AI controller.

1.6 Overview of dissertation

The dissertation begins with a proposed definition of DG in **Chapter 2**. The different applications of DG are discussed emphasizing the potential interest of electric utilities and their customers to employ DG technology. The chapter gives insight into DG technologies by explaining the operating principles, applications and pros/cons of these technologies. Different PQ phenomena are also discussed and investigated for the purpose of the PQ control parameters. Lastly, an introduction to ANNs is given and discussed. For the purpose of this study, only the ANN is used as AI control tool.

To evaluate the control of PQ in an electric power network, a scenario is modelled. The model includes the interconnected electric power network and the DG sources. **Chapter 3** discusses the modelling of the power network from the applicable scenario. The scenario forms part of an existing ESKOM (S.A. electric power utility) network. The simulation evaluates the steady state conditions of the network and assesses the condition of the network at different points. The simulation is interactive and allows power-flow analysis of the system. Steady state voltage and current information is gathered and used to calculate PQ parameters to provide the necessary information about network condition.

Chapter 4 focuses on the development of the training data for the ANN controller. A cost function is firstly developed to determine the optimal output conditions of the DGs for a particular load pattern. The cost function comprises four objective functions:

a) The average voltage deviation from the permitted range (V_{avg});
b) The average voltage deviation from ideal (V_{ideal});
c) The power network active losses (P_L);
d) The generation costs (C_T).

The objective is to control V_{avg} to meet certain criteria while at the same time minimising V_{ideal}, P_L, and C_T. The training load patterns are restricted to an acceptable size of three operating states for each load in the power system. This ultimately leads to a data set size with 2187 load combinations, each evaluated by the cost function. This ordered training set resulted in the characteristic training patterns of the network.

The training and optimisation of the ANN controller is done in **Chapter 5**. The topology of the ANN is determined by two methods: the network growing method and the leave-one-out method. Both methods identified a topology of 14:24:4 representing 14 input layer neurons, 24 hidden layer neurons and 4 output layer neurons. The training is done off-line with a randomly arranged training set, as discussed in the literature. Through a process of optimisation, the optimal training set is identified which gives the ANN controller the ability to learn as much about the load patterns as possible. The optimal learning parameters are identified and results in improved generalisation capability of the ANN. The optimised ANN controller is proved to control the DGs successfully.

In **Chapter 6**, the adaptive behaviour of the ANN controller for the DGs is evaluated. The ANN controller is shown to closely mimic the response of the cost function for the load patterns trained with. The ability of the ANN controller to adapt its output for new load patterns in the electric power system is also investigated. The ANN controlled cases are compared to the cases where no control is active i.e. the DGs run at full generation capacity and to the optimal decision of the cost function. It is found that the ANN controller can sensibly adapt to the new load patterns and make meaningful decisions.

Chapter 7 concludes the dissertation. The main conclusion of this dissertation is that it is viable to use DGs with ANN control to optimise the power quality in an electric power system. The performance of the ANN controller is however strongly dependent on the training data. Further research is recommended in the refinement and updating of the training data. Power quality issues other than the problems addressed in this research, are also an area for future exploration. An integrated control scheme (DG, tap-changer and capacitor bank control schemes) that assists other regulating devices is also suggested for further investigation.

Chapter 2 - Distributed generation

2.1 Introduction

In any power system, the need for improvement and upgrading is unavoidable. This is due to a competitive electric power industry and the constant advancement in technology. The goal in any competitive market is ultimately lower electricity prices and higher energy efficiency. Distributed Generation (DG) has emerged as potentially the future of small-scale power generation, an alternative to the old central generation plant model.

This chapter firstly gives a proposed definition for DG and an overview of the different DG technologies. The issues and applications of the DG technologies are discussed to point out the necessity for DG in power systems. The different power quality (PQ) phenomena are discussed and the most suitable PQ terms for this study are highlighted. The chapter lastly gives an overview of the operation of Artificial Neural Networks (ANNs).

2.2 Distributed generation: A definition

A study by the *Electric Power Research Institute* (EPRI) indicates that by 2010, 25% of the new generation will be distributed [7]. Distributed generation (DG) is a new approach in the electricity industry and the relevant literature shows that there is no generally accepted definition for DG [1] or the definitions used are inconsistent. Some countries define DG based on the power level, whereas others define DG as facilities that directly supply consumer loads. Other countries define DG as having some basic characteristic (for example, using renewables). In regards to the rating of DG power units, the following different definitions are currently used:

- The *Electric Power Research Institute* (EPRI) defines DG as generation from 'a few kilowatts up to 50 MW' [7];
- The *Gas Research Institute defines* DG as being 'typically between 25 kW and 25 MW' [8];
- *Preston and Rastler* defines the size as 'ranging from a few kilowatts to over 100 MW' [9];
- *The International Conference on Large High Voltage Electric Systems* (CIGRE) defines DG as 'smaller than 100 MW' [10];

Due to the large variations in the definitions used in the literature, the following different issues have to be discussed to define DG more precisely:

- **Purpose:** There is an agreement among different organizations regarding the definition of the purpose of DG.

  Definition *- The purpose of distributed generation is to provide a source of electric power.*

  According to this definition, DG can be the only source of electric power, or complement the existing power network.

- **Location:** The location of DG is defined as an electric power source near the load or on the customer side of the meter.

  Definition *- The installation and operation of electric power generation units connected directly to the power network near the load or connected to the network on the customer side of the meter.*

  The idea of DG is to locate generation close to the load, hence on the distribution network or on the customer side of the meter.

- **Rating of a DG unit:** The maximum possible rating of the DG source is often used within the definition of DG, but is not relevant as the different technologies get better and more powerful everyday. The rating of a DG power source is thus not relevant for the definition.

- **Technology:** The term DG is often used in combination with a certain generation technology category, e.g. renewable energy technology. The definition of DG is not limited to specific types of energy sources. Current technologies for DG vary widely. A summary of current technologies is shown in chapter 1. A detailed technical description of some technologies is presented in the next section.

- **Environmental impact:** DG technologies are described as environmentally friendlier than centralized generation. The environmental impact of the DG technology is however not relevant for the definition.

- **Ownership:** It is frequently mentioned that DG has to be owned by independent power producers or by the customers themselves, to qualify as DG. Large power generation companies have become more and more interested in DG and there is no obvious reason why DG should be limited to independent ownership, thus the ownership is not relevant.

2.2.1 Proposed definition for distributed generation

Different definitions regarding DG are used in the literature. These variations in the definition can cause confusion. Therefore, a general definition is formulated after studying the various factors surrounding DG:

> ***Definition*** *- DG is a modular electric power source sufficiently smaller than central generation that is used in applications that benefit the electric power network, the utility customer, and the electric utility.*

This definition does not define the rating of the generating source, as the maximum rating depends on the local power network conditions, e.g. voltage level. It is however useful to suggest categories of different ratings for DG. The following categories are suggested:

- ***Micro DG:*** *1 W to 5 kW;*
- ***Small DG:*** *5 kW to 5 MW;*
- ***Medium DG:*** *5 MW to 50 MW; and*
- ***Large DG:*** *50 MW < 200 MW (PBMR).*

2.3 Issues surrounding distributed generation

DG is currently being used by some customers to provide some or all of their electricity needs. There are many different potential applications for DG technologies. Some customers use DG to reduce demand charges imposed by their electric utility, while others use it to provide premium power or reduce environmental emissions. Many other applications for DG solutions exist. The following is a list of those of potential interest to electric utilities and their customers.

2.3.1 Continuous power/stand alone

In this application, the DG technology is operated at least 6,000 hours a year to allow a facility to generate some or all of its power on a relatively continuous basis. Important DG characteristics for continuous power include:

- High electric efficiency;
- Low maintenance costs;
- Low installation costs.

DG is currently being utilized in a continuous power capacity for industrial applications such as food manufacturing, plastics, rubber, metals and chemical production.

2.3.2 Combined heat and power (CHP)

This application is also referred to as cooling, heating, and power or cogeneration. This DG technology is operated at least 6,000 hours per year to allow a facility to generate some or all of its power. A portion of the DG waste heat is used for water heating, space heating, steam generation or other thermal needs. Important DG characteristics for CHP include:

- High useable thermal output (leading to high overall efficiency);
- Low maintenance costs;
- Low emissions.

As with Continuous Power, CHP is most commonly used by industry clients.

2.3.3 Peaking power/peak saving power

In a peaking power application, DG is operated between 200-3000 hours per year to reduce overall electricity costs. Units can be operated to reduce the utility's demand charges, to defer buying electricity during high-price periods. Important DG characteristics for peaking power include:

- Low installation costs;
- Quick start-up;
- Low fixed maintenance costs.

The most common applications are in educational facilities, lodging, miscellaneous retail sites and some industrial facilities with peaky load profiles.

2.3.4 Green power

DG units can be operated by a facility to reduce environmental emissions from generating its power. Important DG characteristics for green power applications include:

- Low emissions;
- High efficiency;
- Low variable maintenance costs.

Applications for green power are mostly found near areas that are nature preservations or at facilities in highly polluted areas.

2.3.5 Premium power/grid support

DG is used to provide power at higher level of reliability and quality than typically available from the grid. Customers typically demand uninterrupted power for a variety of applications, and for this reason, premium power is broken down into three categories:

- **Emergency power system** This independent system automatically provides electricity within a specified period to replace the normal source if it fails. The system is used to power critical devices whose failure would result in property damage and threatened health and safety. Customers include apartment, office and commercial buildings, hotels, schools, and a wide range of public gathering places.

- **Standby power system** This independent system provides electricity to replace the normal source if it fails and thus allows the customer's entire facility to continue to operate satisfactorily. Such a system is critical for clients like airports, fire and police stations, military bases, prisons, water supply and sewage treatment plants and dairy farms.

- **True premium power system** Clients who demand uninterrupted power, free of all power quality problems such as frequency variations, voltage transients, dips, and surges, use this system. Power of this quality is not available directly from the grid; it requires both power conditioning equipment and standby power. Alternatively, DG technology can be used as the primary power source and the grid as a backup. This technology is used by mission critical systems like airlines, banks, insurance companies, communications stations and hospitals.

Important DG characteristics for premium power include:

- Quick start-up;
- Low installation costs;
- Low fixed maintenance costs.

2.3.6 Transmission and distribution deferral

In some cases, placing DG units in strategic locations can help delay the purchase of new transmission or distribution systems and equipment (for example distribution lines and substations).

Important DG characteristics for transmission and distribution include:

- Low installation costs;
- Low fixed maintenance costs.

Figure 2.1 shows a DG network developed on the applications mentioned in this section. Some of the benefits of making use of these applications are:

i. Customer benefits

- Ensures reliability of energy supply;
- Provides the right energy solution at the right location;
- Provides the power quality needed in many industrial applications;
- Enables savings on electricity rates during high-cost peak power periods;
- Provides a stand-alone power option for areas where transmission and distribution infrastructure does not exist or is too expensive to build; and
- Allows power to be delivered in environmentally sensitive areas by having a high efficiency and near-zero pollutant emissions.

ii. Supplier benefits

- Avoids major investments in transmission and distribution system upgrades by placing new generation near the customer;
- Offers options in remote areas without transmission and distribution systems.

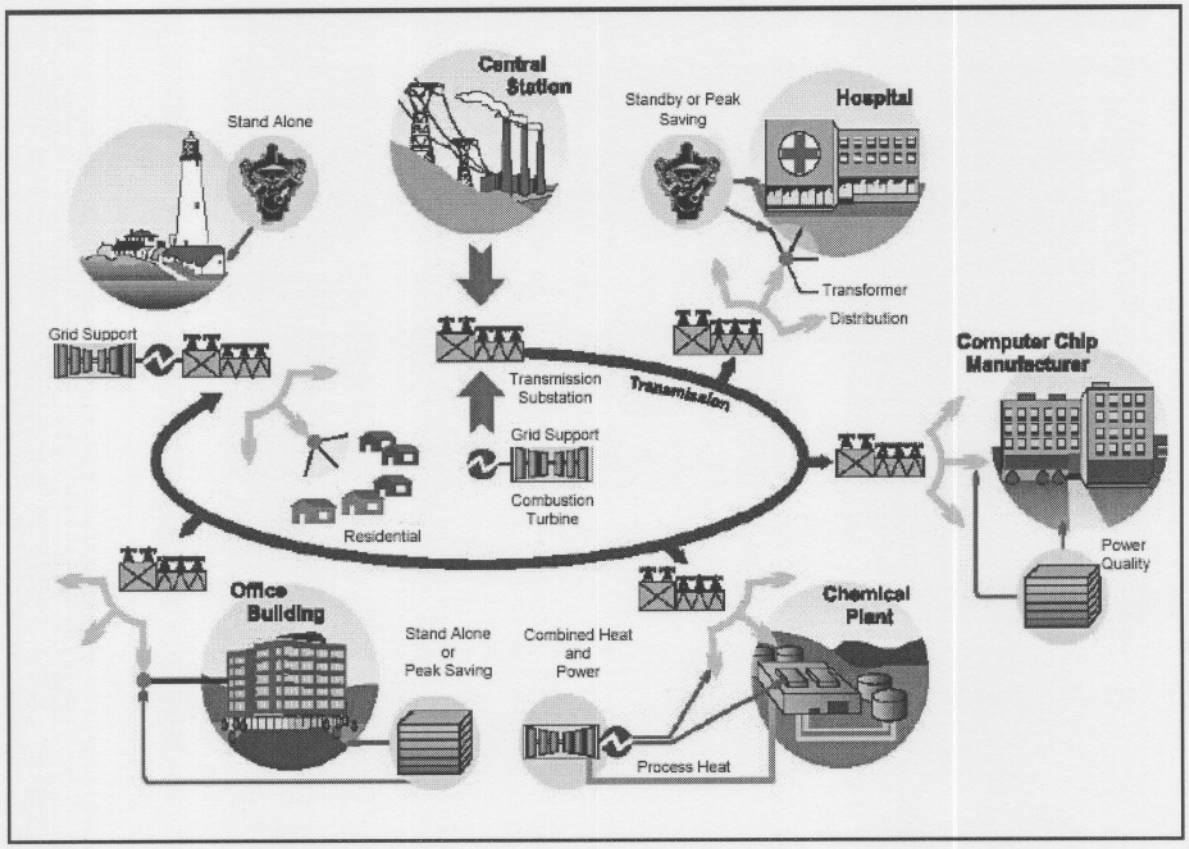

Figure 2.1 A small power network with DG applications.

2.4 Distributed generation technologies

DG technologies can meet the needs of a wide range of users, with applications in the residential, commercial, and industrial sectors. A summary of DG technologies is provided in this section [11]. The technologies include reciprocating engines, micro turbines, gas turbines, combustion turbines, fuel cells, photovoltaics, and wind turbine systems. For each technology its operation and advantages/disadvantages are discussed.

2.4.1 Reciprocating engines

Almost all engines used for power generation are four-stroke and operate in four cycles (intake, compression, combustion, and exhaust). The process begins with fuel and air being mixed. Some engines are turbo-charged or supercharged to increase engine output, meaning that the intake air is compressed by a small compressor in the intake system. The fuel/air mixture is introduced into the combustion cylinder, and then compressed as the piston moves toward the top of the cylinder. As the

piston nears the top of its movement, a spark is produced that ignites the mixture. The pressure of the hot, combusted gases drives the piston down the cylinder. Energy in the moving piston is translated to rotational energy by a crankshaft. As the piston reaches the bottom of its stroke, the exhaust valve opens and the combusted gases is expelled from the cylinder by the rising piston. Table 2.1 lists the advantages and disadvantages.

Advantages	Disadvantages
Good electrical efficiencies (up to 45%)	Atmospheric emissions (mainly Nox)
Quick start-up	Frequent maintenance intervals
Ease of operation and maintenance	Noise and vibration
High reliability	Inability to start itself from zero RPM
Inexpensive	

Table 2.1 Advantages and disadvantages of reciprocating engines.

2.4.2 Micro turbines

Micro turbines are typically in the size range of 35 kW to 1 MW. Micro turbines consist of a compressor, combustor, turbine, and generator. Most designs are single-shaft and use a high-speed generator producing variable voltage, variable frequency alternating current (AC) power. An inverter is employed to produce 50 Hz AC power. Most micro turbine units are currently designed for continuous-duty operation. Micro turbines have no gearbox, and the turbine and generator are on the same shaft. The distinctions of micro turbines are the presence of a recuperator used to heat the input air to keep internal temperature high and the use of air bearings. Micro turbines can be divided in two general classes:

- recuperated micro turbines, which recover the heat from the exhaust gas to boost the temperature of combustion and increase the efficiency; and
- unrecuperated (or simple cycle) micro turbines, which have lower efficiencies, but also lower capital costs.

Table 2.2 lists the advantages and disadvantages.

Advantages	Disadvantages
Compact size and light weight	High initial cost
Relatively high reliability	Maintenance skill requirements
Low maintenance needs	Noise and vibration
Low emissions	Moderate ratio for fuel consumption/efficiency

Table 2.2 Advantages and disadvantages of micro turbines.

2.4.3 Gas turbines

Gas turbines are based on the Brayton or Joule cycle, which consists of four processes:

- compression with no heat transfer;
- heating at constant pressure;
- expansion with no heat transfer; and
- a closed cycle system, cooling at constant pressure.

In open cycle gas turbines, the fourth step does not exist since inlet air is taken from the atmosphere and the exhaust is dumped to atmosphere. Due to its higher temperature, there is more energy available from the expansion process than is expended in the compression. The net work delivered to drive a generator is the difference between the two. The thermal efficiency of the gas turbine is a function of the pressure ratio of the compressor, the inlet temperature of the power turbine, and any parasitic losses (especially the efficiency of the compressor and power turbine).

In closed cycle gas turbines, the fuel is not physically ignited. The fuel is heated and passed through stages of turbos and compressors. The kinetic energy from the fuel is converted to mechanical energy and then to electrical energy by a generator. The system can be a single shaft system (only one turbo/compressor combination) or a twin or three shaft system. The Pebble Bed Modular Reactor (PBMR) is a three shaft closed cycle gas turbine system. Figure 2.2 shows a flow diagram of the system and figure 2.3 a picture of the micro plant.

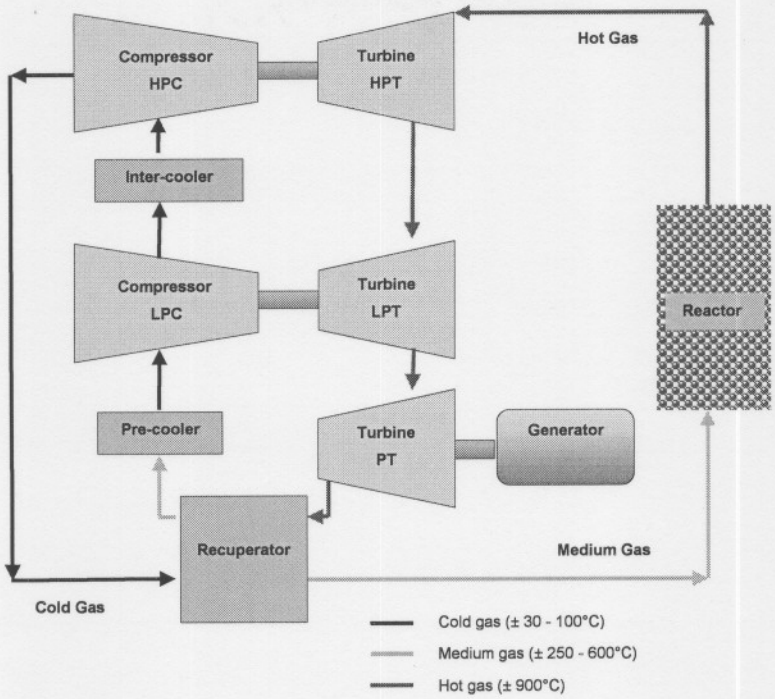

Figure 2.2 Flow diagram of a three shaft closed cycle gas turbine.

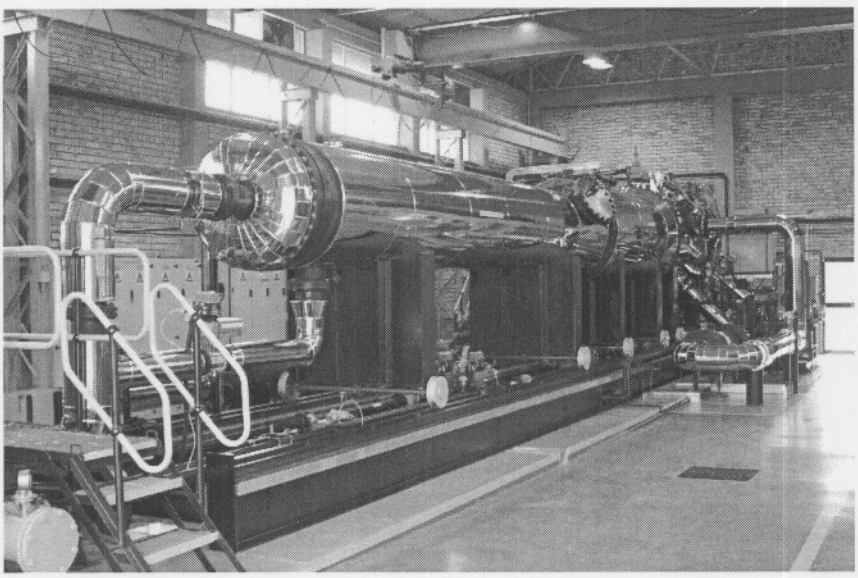

Figure 2.3 A closed cycle gas turbine (the PBMR).

Table 2.3 lists the advantages and disadvantages of gas turbines.

Advantages	Disadvantages
It is modular and adjustable	High initial cost
Relatively high reliability	Maintenance skill requirements
It is cost efficient	Noise and vibration
Low emissions	Moderate ratio for fuel consumption/efficiency
Short construction lead-time	

Table 2.3 Advantages and disadvantages of a gas turbine.

2.4.4 Combustion turbines

A combustion turbine is a device in which air is compressed and a fuel is ignited. The combustion products expand directly through the blades in a turbine to drive an electric generator. The compressor and turbine usually have multiple stages and axial blading. This differentiates them from smaller micro turbines that have radial blades and are single staged. Combustion turbines typically range in size from about 1 MW up to 200 MW. Table 2.4 lists the advantages and disadvantages.

Advantages	Disadvantages
Short start time	Low electric efficiency
Multi-fuel capability	Small system cost and efficiency not as good as larger systems
Proven reliability and availability	
Low emissions	
High efficiency and low cost (large systems).	
High power-to-weight ratio	

Table 2.4 Advantages and disadvantages of a combustion turbine.

2.4.5 Fuel cells

There are many types of fuel cells, but each uses the same basic principle, to generate power. A fuel cell consists of two electrodes (an anode and a cathode) separated by an electrolyte. Hydrogen fuel is fed into the anode, while oxygen (or air) enters the fuel cell through the cathode. With the aid of a catalyst, the hydrogen atom splits into a proton (H+) and an electron. The proton passes through the electrolyte to the cathode, and the electrons travel through an external circuit connected as a load,

creating a DC current. The electrons continue on to the cathode, where they combine with hydrogen and oxygen, producing water and heat. Table 2.5 lists the advantages and disadvantages.

Advantages	Disadvantages
High efficiency	High initial cost
Low pollution	Fuel sensitivity
Low noise and vibration	Lack of maintenance experience
Low emissions	Absence of a long history of commercial usage

Table 2.5 Advantages and disadvantages of fuel cells.

2.4.6 Photovoltaics

A photovoltaic cell is composed of several layers of different materials. The top layer is a glass cover to protect the cell from weather conditions. This is followed by an anti-reflective layer. The main layers are two semiconductor layers, creating the electron current. Photovoltaic cells, or solar cells, convert sunlight directly into electricity. The cells produce DC electricity. Photovoltaic cells are assembled into flat plate systems that can be mounted on rooftops or other sunny areas. However, the cost is currently too high for bulk power applications. Table 2.6 lists the advantages and disadvantages.

Advantages	Disadvantages
No dangerous emissions	Decisive importance of weather conditions
Can be used in remote areas	High initial costs
Good system scalability (arrays can be built in sizes less than 0,5 w)	Additional equipment required (energy storage devices, ac converters)
PV have a few moving parts	Strong site dependence
Little maintenance	

Table 2.6 Advantages and disadvantages of photovoltaics.

2.4.7 Wind turbines

Wind turbines are packaged systems that include a rotor, generator, turbine blades, and coupling device. As the wind blows through the blades, the air exerts aerodynamic forces that cause the blades to turn the rotor. Most systems have a gearbox and generator in a single unit behind the turbine

blades. The output of the generator is processed by an inverter that changes the electricity from DC to AC so that the electricity can be used. Wind conditions limit the amount of electricity that the turbines are able to generate, and the minimum wind speed required for electricity generation determines the turbine rating. Coastlines and hills are among the best places to locate a wind turbine, as these areas typically have more wind. Table 2.7 lists the advantages and disadvantages.

Advantages	Disadvantages
No dangerous emissions	Decisive importance of weather conditions
Can be used in remote areas	High initial costs
Minimal land use - the land below each turbine can be used for example animal grazing	Additional equipment required (energy storage devices, ac converters)
Little maintenance	Strong site dependence

Table 2.7 Advantages and disadvantages of wind turbines.

Table 2.8 shows a summary of the suitability of the DG technologies discussed for the different applications discussed in the previous section.

Application	Reciprocating Engines	Micro Turbines	Gas Turbines	Combustion Turbines	Fuel Cells	Photovoltaics	Wind Turbines
Continuous	☺	😐	😐	😐	☺	😐	☹
CHP	😐	😐	☺	☺	😐	☹	☹
Peaking	☺	😐	😐	😐	☹	☹	☹
Green	☹	☹	☹	☹	☺	☺	☺
Premium	😐	😐	😐	😐	☺	☹	☹

Application Fit: ☺ = good 😐 = moderate ☹ = poor

Table 2.8 The suitability of DG technologies for the different power applications.

2.5 Distributed generation and power quality

A major issue related to interconnection of DG onto the power grid is the potential impacts on the quality of power provided to other customers connected to the grid. The main reason for PQ analysis in power systems is purely of economical value. The economic impacts are on utilities (main grid or DG), their customers and suppliers of load equipment. The electrical utilities are concerned with PQ

issues as to maintain customer expectations and customer confidence. Customers and suppliers of load equipment are concerned because modern equipment is much more sensitive to voltage deviations. The main attributes that define PQ in systems with DG are:

- **Voltage regulation** – Maintaining the voltage at the point of delivery within an acceptable range.
- **Flicker** - Rapid and repetitive changes in voltage, which has the effect of causing unacceptable variations in light output.
- **Voltage imbalance** – Each phase of the grid voltage does not have identical voltage magnitude, and a 120° phase separation between each phases.
- **Harmonic distortion** - The injection of currents having frequency components that are multiples of the fundamental frequency.
- **Direct current injection** - This can cause saturation and heating of transformers and motors. This can also cause these passive devices to produce unacceptable harmonic currents.
- **System losses** - The active power losses in the power system (transformers, lines etc.).

While the common term for describing this section is PQ, it is actually the quality of the voltage that is being addressed. In engineering terms, power is the rate of energy delivered and is proportional to the product of the voltage and the current. In most DG power systems, only the voltage is controlled and there is no control over the current that loads might draw. Therefore, the standard would be to maintain an acceptable supply voltage at all times. Any disturbance in the magnitude, frequency and purity of the supply voltage waveform, is a PQ problem.

2.5.1 Classification of electromagnetic phenomena (Power quality disturbances)

PQ refers to a wide spectrum of electromagnetic phenomena that describe the voltage and current at any given point in the system. The categorisation of electromagnetic phenomena is shown in table 2.9 [4]. The reason for the categories and their descriptions are important to be able to classify the measurements. The main reasons for the categories are that there are different ways to solve a PQ problem for a particular variation and for analysis purposes. A short overview of the PQ phenomena is given in this section. Annexure A gives a summary of all the PQ terminology. Table 2.9 shows a classification of all the PQ phenomena.

	Categories	Duration	Voltage Magnitude
1.	**Transients**		
	• Impulsive	1 ns - > 1 ms	
	• Oscillatory	5 μs - 50 ms	0 - 4 pu
2.	**Short duration variations**		
	• Instantaneous ***sag***	0.5 - 30 cycles	0.1 - 0.9 pu
	• Instantaneous ***swell***	0.5 - 30 cycles	1.1 - 1.8 pu
	• Momentary ***interruption***	0.5 cycles - 3 s	< 0.1 pu
	• Momentary ***sag***	30 cycles - 3 s	0.1 - 0.9 pu
	• Momentary ***swell***	30 cycles - 3 s	1.1 - 1.4 pu
	• Temporary ***interruption***	3 s - 1 min	< 0.1 pu
	• Temporary ***sag***	3 s - 1 min	0.1 - 0.9 pu
	• Temporary ***swell***	3 s - 1 min	1.1 - 1.2 pu
3.	**Long duration variations**		
	• Interruption sustained	> 1 min	0.0 pu
	• Undervoltages	> 1 min	0.8 - 0.9 pu
	• Overvoltages	> 1 min	1.1 - 1.2 pu
4.	**Voltage imbalance**	steady state	0.5 - 2 %
5.	**Waveform distortion**		
	• DC offset	steady state	0 - 0.1 %
	• Harmonics	steady state	0 - 20 %
	• Interharmonics	steady state	0 - 2 %
	• Notching	steady state	
	• Noise	steady state	0 - 1 %
6.	**Voltage fluctuations**	intermittent	0.1 - 7 %
7.	**Power frequency variations**	<10s	

Table 2.9 PQ phenomena classification.

2.5.1.1 Transients

The term *transient* is used for a phenomenon or a quantity that varies between two consecutive steady states during a time interval that is short compared to the time scale of interest. Transients can be classified into two categories, *impulsive* and *oscillatory*. These terms reflect the wave shape of a current or voltage transient.

An *impulsive transient* is a sudden, non-power frequency change in the steady state condition of voltage, current, or both, that is unidirectional in polarity (primarily either positive or negative). The most common cause of impulsive transients is lightning.

An *oscillatory transient* is a sudden, non-power frequency change in the steady state condition of voltage, current, or both, that includes both positive and negative polarity values. An oscillatory transient consists of a voltage or current whose instantaneous value changes polarity rapidly. Back-to-back capacitor energization results in oscillatory transient currents. This phenomenon occurs when a capacitor bank is energized in close electrical proximity to a capacitor bank already in use. Figure 2.4 shows an oscillatory transient.

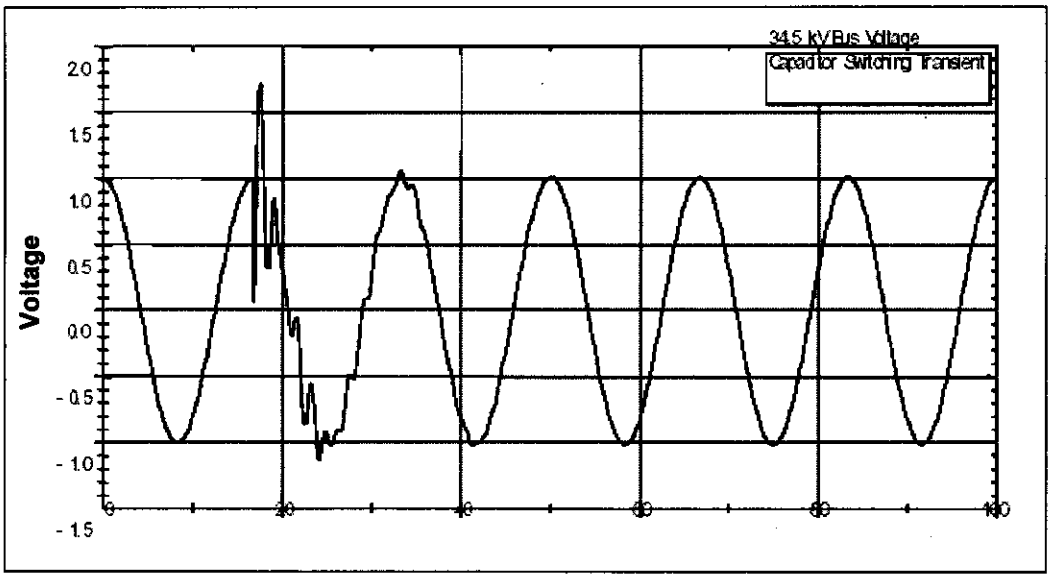

Figure 2.4 Oscillatory transient caused by capacitor-bank energization.

2.5.1.2 Short duration voltage variations

The short duration variation is the general category of events that last for a period that is greater than 0.5 cycles, but less than or equal to 1 minute. These voltage variations are usually caused by fault

conditions, such as the energization of large loads that require a starting current that is a multiple of the operating current (motors). Figure 2.5 shows a time scale of the characterized groups of short duration voltage variations. These groups can be classified into two categories, *sags* and *swells*.

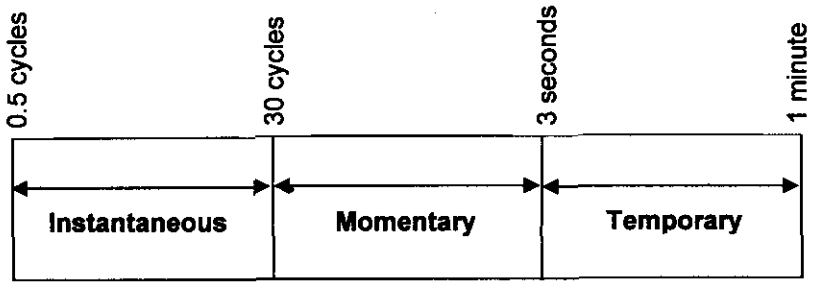

Figure 2.5 Time scale of short duration voltage variations.

A sag is a decrease between 0.1 and 0.9 pu in rms voltage or current at the power frequency. Voltage sags are usually associated with system faults but can also be caused by switching of heavy loads or starting of large motors. Figure 2.6 shows a voltage sag that can be associated with a single line-to-ground (SLG) fault.

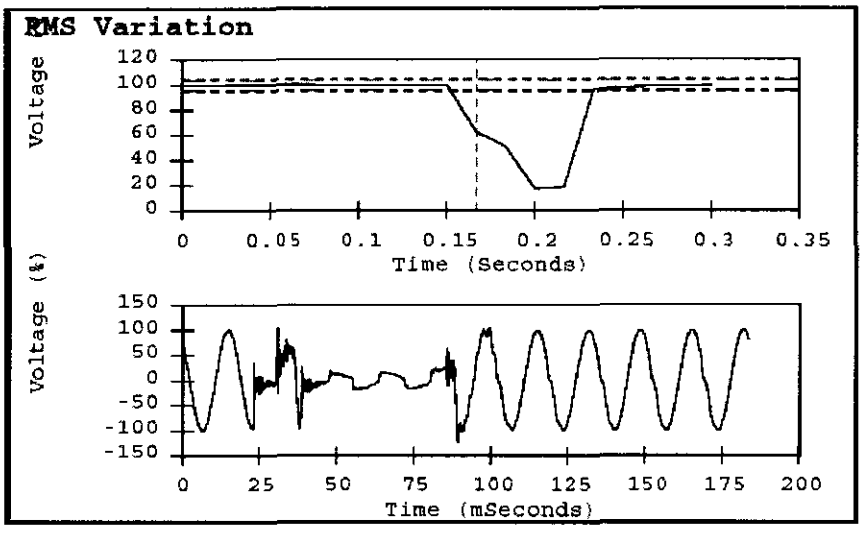

Figure 2.6 Instantaneous voltage sag caused by a SLG fault.

A swell is an increase between 1.1 - 1.8 pu in rms voltage or current at the power frequency. As with sags, swells are usually associated with system fault conditions or switching off a large load or large capacitor bank. A swell can occur due to a SLG fault on the system resulting in a temporary voltage rise on the unfaulted phases. Figure 2.7 illustrates a voltage swell caused by a SLG fault.

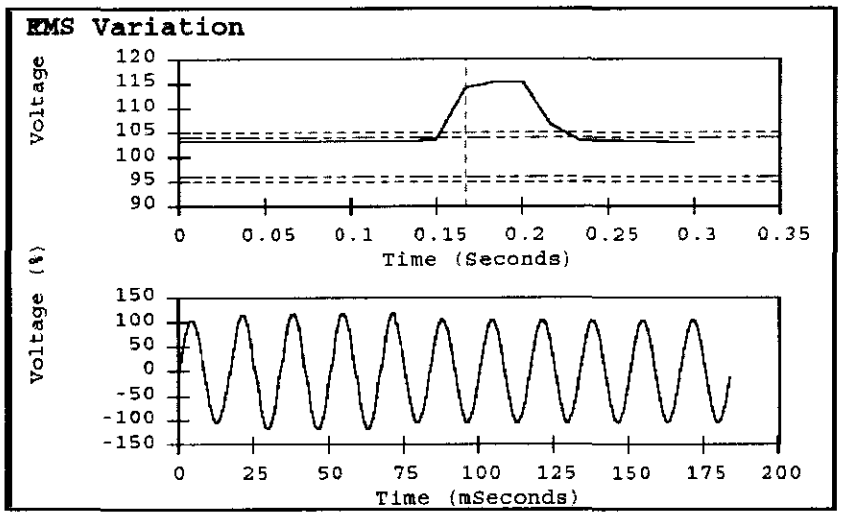

Figure 2.7 Instantaneous voltage swell caused by a SLG fault.

2.5.1.3 Long duration voltage variations

Long duration voltage variations is variations of the rms voltage from the nominal voltage for a time greater than 1 min. Long duration voltage variations can be either overvoltages or undervoltages. These variations are generally not the result of system faults, but are caused by load variations.

An overvoltage refers to a measured voltage having a value greater than the nominal voltage for a period greater than 1 min. Typical values are 1.1 to 1.2 pu. Overvoltages can be the result of a load switching off or variations in the reactive compensation in the system. Poor voltage regulation capabilities or control results in this PQ phenomenon. Figure 2.8 shows a typical overvoltage waveform.

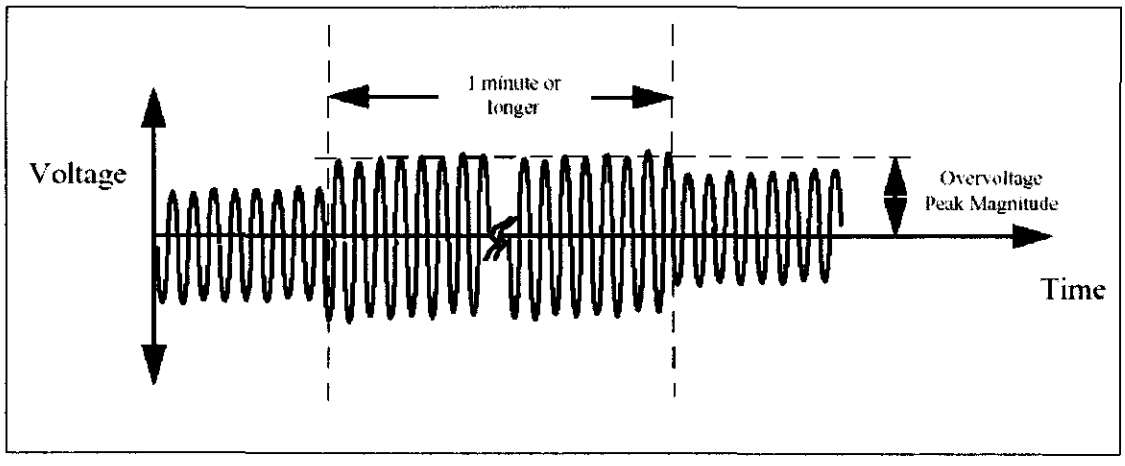

Figure 2.8 Overvoltage waveform.

An undervoltage refers to a measured voltage having a value less than the nominal voltage for a period greater than 1 min. Typical values are 0.8 - 0.9 pu. Undervoltages are the result of the inverse events that cause overvoltages. A load switching on can cause an undervoltage until voltage regulation equipment can bring the voltage back to optimum values. Overloaded systems can also result in undervoltages.

2.5.1.4 Voltage imbalance

Voltage imbalance is sometimes defined as the maximum deviation among the three phases from the average three-phase voltages or currents, divided by the average of the three-phase voltages or currents. This ratio is usually expressed as a percentage.

Voltage imbalance = 100 x (maximum deviation from average voltage/average voltage)

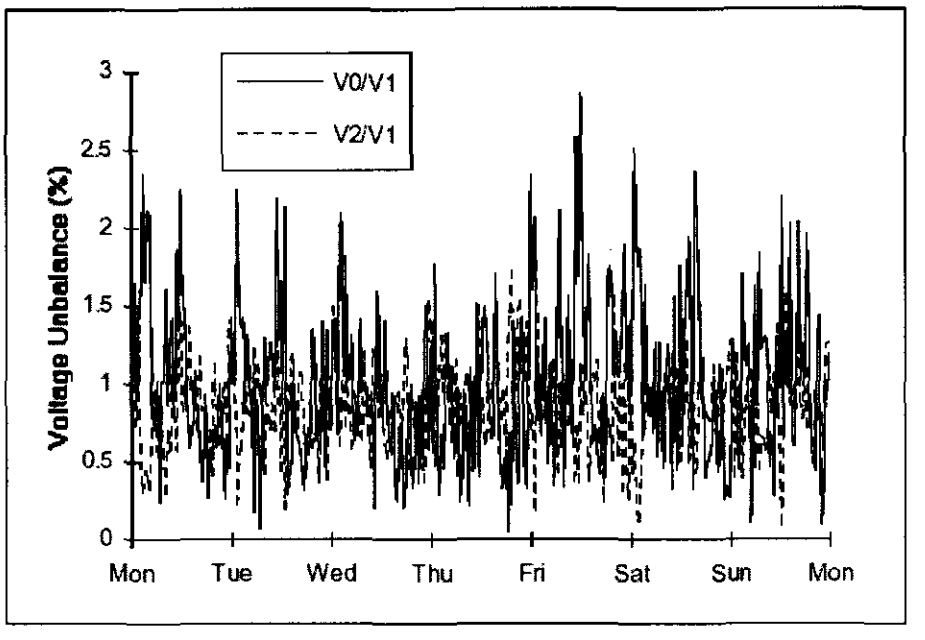

Figure 2.9 Imbalance for a feeder measured over a week.

2.5.1.5 Waveform distortion

A waveform distortion can be classified as a steady state deviation from an ideal sine wave of power frequency characterized by the spectral content of the deviation.
The *DC offset* is the presence of a dc voltage or current in an ac power system. This phenomenon can occur as the result of half-wave rectification.

Harmonics are sinusoidal voltages or currents having frequencies that are integer multiples of the frequency at which the supply system is designed to operate (fundamental frequency). Harmonics combine with the fundamental voltage or current, and produce waveform distortion. Harmonic distortion exists due to the nonlinear characteristics of devices and loads in the system. Figure 2.10 illustrates the harmonic content in the input current of a speed drive.

Interharmonics are voltages or currents having frequency components that are not integer multiples of the frequency at which the supply system is designed to operate. The main sources of interharmonic waveform distortion are static frequency converters, cyclo-converters, induction motors and arcing devices.

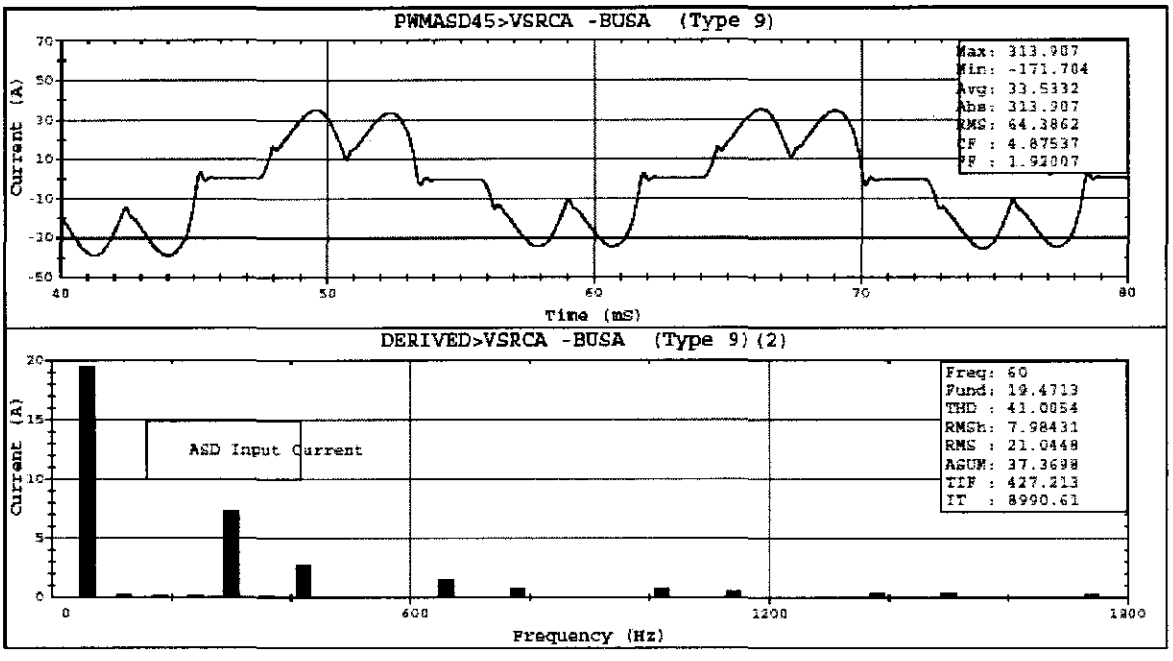

Figure 2.10 Current waveform and harmonic spectrum for an adjustable speed drive input current.

Notching is a periodic voltage disturbance caused when current is commutated from one phase to another. During this period, there is a momentary short circuit between two phases. Three-phase converters that produce continuous dc current are the most cause of notching.

Noise is defined as unwanted electrical signals superimposed upon the power system voltage or current. These signals are usually on the phase conductors or neutral conductors. Noise can be caused by power electronic devices such as solid-state rectifiers and switching power supplies.

2.5.1.6 Voltage fluctuations

Voltage fluctuations are random changes in the voltage magnitude. These changes normally do not exceed the voltage ranges from 0.95 pu to 1.05 pu. Loads that exhibit continuous, rapid variations in load current magnitude can cause fluctuations referred to as *flicker*. Arc furnaces are the most common cause of voltage fluctuations in power systems. Figure 2.11 shows voltage fluctuations caused by an arc furnace and figure 2.12 an example of voltage flicker.

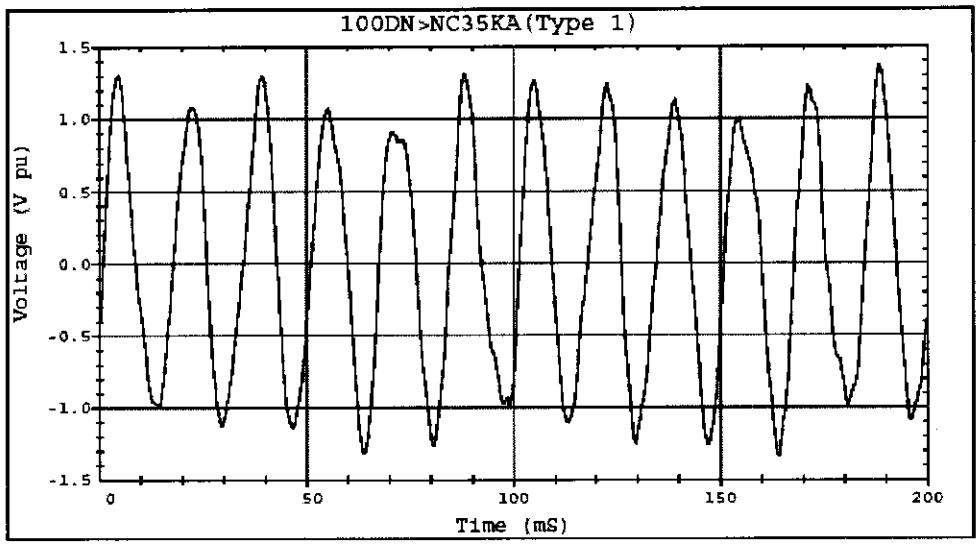

Figure 2.11 Voltage fluctuations caused by arc furnace operation.

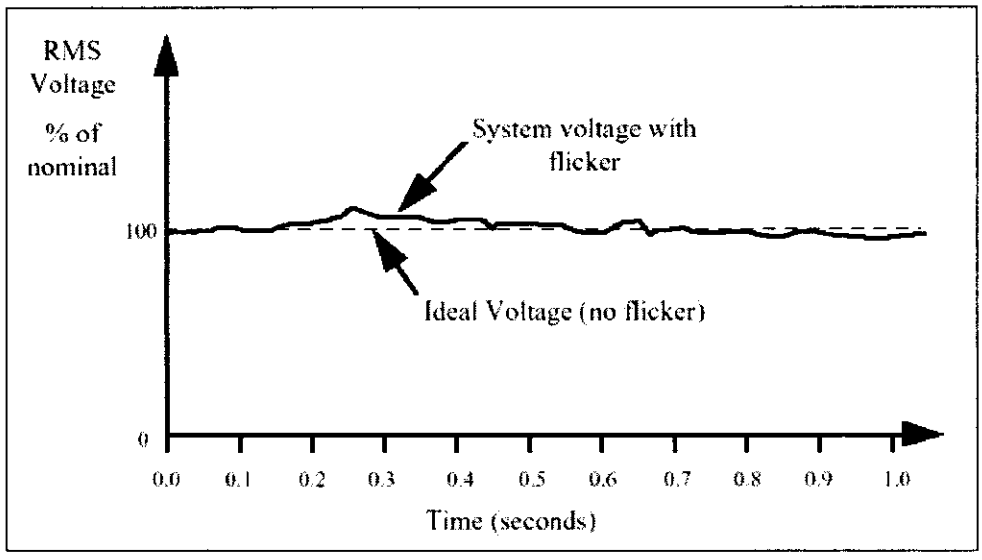

Figure 2.12 Voltage flicker.

2.5.1.7 Power frequency variations

Power frequency deviations are defined as the deviation of the power system frequency from its fundamental value (e.g. 50 Hz). This can be an increase or decrease in the power frequency. The power system frequency is directly related to the rotational speed of the generators on the system. At any instant, the frequency depends on the balance between the load and the capacity of the available generation. When this dynamic balance changes, small changes in frequency occur. The size and duration of the frequency shift depends on the load characteristics and the response of the generators to load changes.

2.5.2 Improving the power quality

Without DG, power flow is always unidirectional, and decreasing in real power (kW) magnitude with increasing distance from the generating source. The addition of DG to a power system can shift power flow patterns and can make it difficult to maintain adequate voltage regulation [12]. The main objective of the power delivery system is to supply customers with an acceptable voltage, which is within a prescribed range. Two voltage ranges are specified by ANSI C84.1, (American National Standards Institute):

- Range A, covering normal operation;
- Range B, covering a wider range for less frequent events.

Normal variations in load and DG operation fall in the category covered by Range A. The NRS 048 [13] standard in South Africa demands that voltage regulation must comply within ±5 % of the nominal voltage level for voltage levels above 500 V This result in a range from 0.95 pu - 1.05 pu of the base voltage. Improving the voltage profile of the grid (minimising PQ indices like overvoltages and undervoltages) is thus possible with DG penetration and adequate control techniques. These PQ indices are likely to occur when large loads are switched on and off the power grid.

2.6 Distributed generation and artificial intelligent control tools

The control techniques chosen for DG control will mainly depend on the type of application the unit is used for and the control parameters. According to Ibrahim and Morcos [2], AI techniques are suitable for PQ analysis and control. Controlling the DG power source is important because the control mode will determine the following:

- Has the DG application goals been achieved (PQ control, back-up, power saving etc.)?
- Is the DG a profitable investment?

The DG application goal for this study is PQ control. The fundamental goal of the control scheme is to determine the output control parameters of the DGs for a specific network condition. This section gives a short overview of the different AI techniques and types of control. The operation and internal structure of ANNs are also described. Most DG systems have properly engineered internal control systems (speed governing systems, exciter control etc.) which are not discussed.

2.6.1 Artificial intelligence techniques for DG

2.6.1.1 Expert systems (ES)

ES uses knowledge and reasoning procedures to solve problems that are difficult and require significant human expertise for their solution. Just like human experts, ES are designed to be an expert in one knowledge domain. An advantage of ES is the explanation facility (used when there is a lack of PQ knowledge resources).

2.6.1.2 Fuzzy logic (FL)

Fuzzy set theory provides a means for representing uncertainties. Fuzzy logic seems to be most successful in two kinds of situations:

- In models where understanding is limited or vague; or
- Processes where human reasoning and human decision-making are inextricably involved.

Fuzzy logic rule-based systems use a collection of fuzzy conditional statements (rules). This means that fuzzy logic rule-based system identifiers, is generally model-free paradigms. Fuzzy logic rule-based systems are nonlinear function approximators, and any nonlinear function can be approximated to any desired precision [14].

2.6.1.3 Artificial neural networks (ANNs)

A neural network is a massively parallel distributed processor made up of several computing units, which is able to store experimental knowledge and to learn from examples and generalize. Generalization refers to the network producing *reasonable* outputs for inputs not encountered during training (learning) [15]. This means that the system has to be retrained with the new "knowledge" to

optimise the precision of the system. The network learns from examples by constructing an input-output mapping for the problem at hand. With this kind of interconnected internal structure, it is able to represent functions and to learn these functions.

2.6.1.4 Adaptive nero-fuzzy systems (ANFS)

Adaptive nero-fuzzy systems combine the learning abilities of ANNs and the excellent knowledge representation and reasoning of fuzzy logic. ANFS are derived from a general category of intelligent networks known as adaptive networks, like ANNs. ANFS is an effective tool for tuning the membership functions and minimizing the output error measure of a FL system.

Artificial intelligence has been applied to several PQ problems [16]. The following applications are summarised as follows:

- ANNs have been used to classify PQ patterns and the cause of the disturbance.
- ANNs have been used to classify events into PQ events (sags, swells, distortions, interruptions etc.) and non-PQ events.
- Fuzzy-ES systems have been used to diagnose PQ problems. FL is combined into these systems because of the imprecision and fuzziness of the data.
- ANN-ES systems have been used to classify PQ disturbances into respective classes (ES) while the ANN decided the cause of the disturbance (individual ANNs each trained for only one class of disturbance).

As discussed in chapter 4, the main goal of the control scheme is to optimally control the DGs. The input to the control scheme is based on pattern-recognition and ANNs emerged as powerful pattern-recognition tools [2]. For the purpose of this research, ANNs is chosen as AI control technique.

2.6.2 Control Types for DG

2.6.2.1 Threshold Control

In threshold control, the DGs run whenever a facility's electrical load is greater than the predetermined threshold. The number of DGs initially installed is equal to the difference between the annual peak and the threshold divided by the nominal power output of each installed unit:

$$\text{Number installed} = (kW_{peak} - kW_{threshold})/kW_{per\ unit}$$

If the electrical load of the facility is greater than the threshold, then the number of DGs operating is equal to the number to reduce the grid load to the threshold limit:

$$\text{Number operating} = (kW_{building} - kW_{threshold})/kW_{per\ unit}$$

A problem with this type of control is deciding where to assign the threshold limit. A *high* limit means that the DGs is used only for peak saving (operating hours is small). A *low* limit means the DGs run more often and is a characteristic of base loading. A threshold of *zero* means the DGs will try to operate whenever possible.

2.6.2.2 Net metering control

In this metering scenario, the electrical meter runs backwards if excess electricity is produced on-site. If the meter reaches zero, buyback rates apply.

2.6.2.3 Cooling/heating priority control

This type of control is mainly used for on-site generation. DG units will be deployed as co-generators to satisfy a cooling or a heating load. In this mode of control, the DGs operate primarily to satisfy these loads, and the satisfaction of the electrical load is a secondary benefit.

2.6.2.4 Optimal control

This type of control is mainly used for on-site DGs. On-site generation is operated using an algorithm that reduces the operating cost such that the cost to the facility is minimized every hour. The cost of the grid electricity and locally produced electricity are compared each hour; and when the former is more expensive, the on-site DGs are operated.

2.6.2.5 Complete optimisation

Optimal control is sufficient for performing optimization-based control. An optimization routine must be able to keep track of all data acquired a period and provide cost estimates for the period. In this period, the optimization routine determines the capacity of DG needed for that period. A prediction of the load data for that period is usually required.

2.6.2.6 Regulation control

The objective of this control type is to regulate parameters in the system. The DG can control the

following parameters:

- Real power;
- Reactive power;
- Frequency;
- Voltage magnitude;
- PF.

The main goal is to deliver power to the load as reliably and economically as possible while maintaining the voltage and frequency within permissible limits. This control is most common at sensitive loads that are susceptible for voltage fluctuations. Frequency is mainly affected by changes in real power, whilst the voltage magnitude is mainly affected by changes in reactive power [17], [18]. Thus, the real and reactive powers must be controlled separately. The two techniques used to control the real and reactive powers are:

- Load frequency control (LFC); and
- Automatic voltage regulator (AVR).

The LFC controls the real power and the frequency of the system and the AVR controls the reactive power and the voltage magnitude of the system. LFC is the basis of any large interconnected power system, and has made operation of such large systems possible.

Another type of control technique is power factor (PF) control, where the DG is fixed ate a set PF. The PF is typically around unity. This mode allows the unit to follow the system voltage, with no attempt to regulate it. The reactive power follows the real power output so that the PF remains relatively constant while the real power is varied. While in the grid-dependent mode (connected to the grid), the DG operates at near unity power factor.

2.6.3 System voltage control

Kundur [19] identifies the main objectives of system voltage control as:

- Voltage at the terminals of all equipment should be kept within acceptable limits, to avoid damage and malfunction;
- Keep voltages close to the values for which stabilising controls are designed for;
- Minimize reactive power flows, to reduce active and reactive power losses.

The control of voltage in transmission systems are divided in three strategies, i.e. normal, preventive and emergency state control. Preventive and emergency state control are mostly focused on contingency plans in case of outage of major components or lines which may force the system to become unstable. Normal state control deals with the voltage regulation issues of the system in the normal state (all system components operational). A brief overview of the three control types for normal state control follows in the next paragraph [19], [20].

- **Primary Control** is used to keep the terminal voltages of the generators close to reference values given by the operators or secondary controllers. Also, tap changers and their controllers belong to primary control layer.

- **Secondary Control** acts on a time scale of seconds to a minute and within certain regions of a power network. The network is divided in geographic regions. The aim of this control is to keep an appropriate voltage profile in a region, reduce circulating reactive power flows, and maximise reactive reserves.

- **Tertiary Control** acts system wide on a time scale of about ten to thirty minutes. This control type is based on the OPF (optimum power flow). The desired network conditions are specified in the form of a cost function, which main goal is to minimise system losses and regulate voltage profiles close to the rated values. The main control variables are generator voltage setpoints and switching orders of compensation devices such as shunt capacitors.

2.6.4 Advantages of DG control

Control and communication of DG is necessary in power systems. These devices can usually be controlled from a central location or control centre. Figure 2.13 illustrates a communication and control network overlaying a power network with DG.

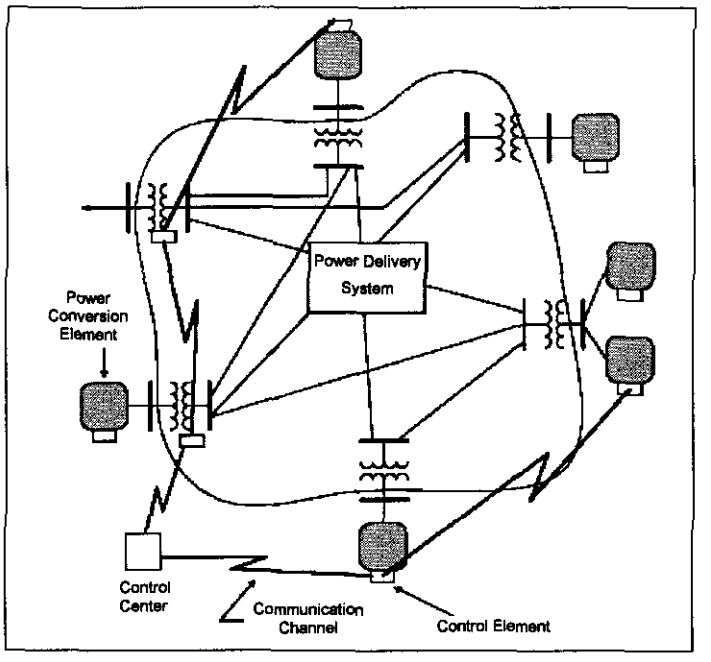

Figure 2.13 Communication and control of DG on a power network.

There are a number of advantages to providing control over the DG in the electric power system and they include:

- **Scheduled Dispatching**

  New DG technology has the capability to dispatch power quite rapidly to varying load conditions. The power dispatch of a 3-phase, 30 kW microturbine is shown in figure 2.14. The DG requires ±20 s to vary its power output from one third to full power.

- **Cold-Load Pickup**

  DG can be controlled to reduce the amount of load that has to be picked up by central generation after an outage or fault in the system.

- **Load Management**

  DG can be controlled to reduce the load during peak periods. By controlling the amount of power delivered by the DG, the stress on central generation and transmission lines can be relieved.

- **Voltage Regulation**

  By controlling and coordinating existing distribution elements with DG, improved voltage

profiles is possible. It may be necessary for distribution elements to be controlled to operate under different settings or modes when the DG is operable. If the equipment operates autonomously without control, undesirable conditions may occur and damage equipment.

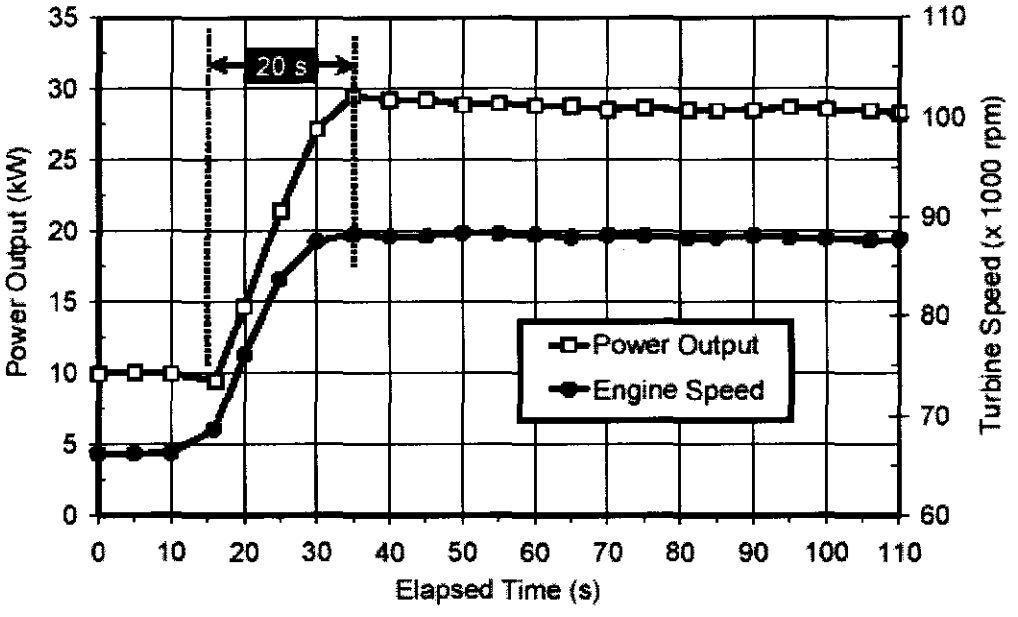

Figure 2.14 Power output of a 30 kW microturbine.

2.6.5 Artificial neural networks

Artificial neural networks (ANNs) consist of simple processing units operating in parallel. This concept is motivated from its inception that the human brain consists of billions of neurons functioning as a parallel processing unit. The human brain has the ability to learn from experience and adapt to its surrounding environment. From this principal, an ANN is constructed to model the way the human brain performs a task, mainly the process of *learning*.

The ANN is trained (the learning process) and adjusted so that a particular input leads to a target output. This process is called input-output mapping or supervised learning. It involves modification or adjusting the synaptic weights (values of the connections between elements) of the ANN. Figure 2.15 illustrates the process of training.

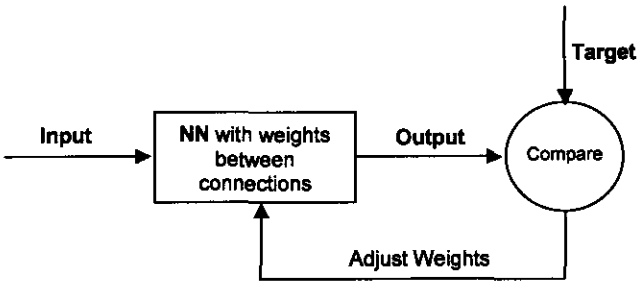

Figure 2.15 Training process of an ANN.

The benefits of using a NN are the following [15]:

- It can model non-linear input-output data, e.g. non-linear functions;
- The model is adaptive and can be retrained with data to adapt to a new surrounding;
- The network can provide information about the confidence of its decision. This can be used to improve the classification performance of the network.

To design an ANN, the model of a neuron itself is firstly discussed. The neuron is the simplest building block of an ANN and is fundamental to the operation thereof. The model consists of three basic elements [15]:

- A set of synapses that is each characterised by its own weight;
- An adder to sum the inputs;
- An activation function for limiting the outputs of the neuron.

Figure 2.16 shows the model of the neuron.

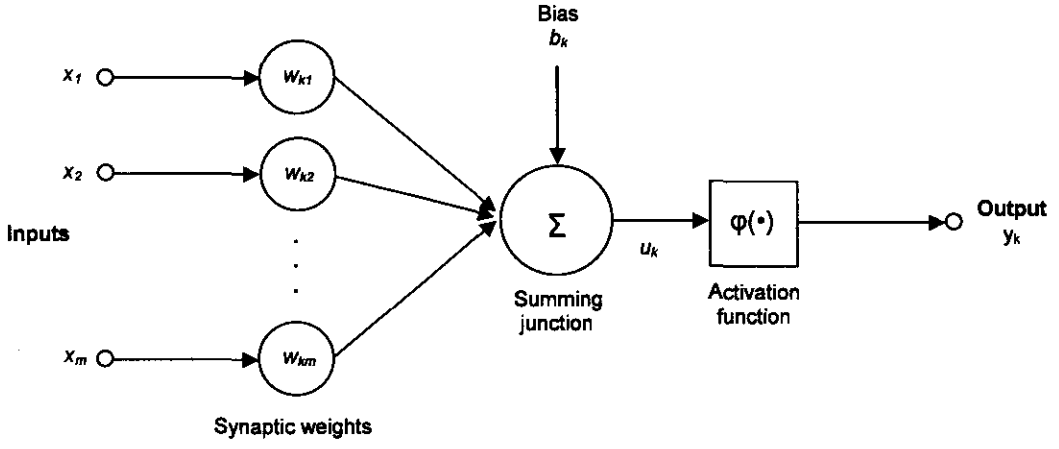

Figure 2.16 Nonlinear model of a neuron.

Figure 2.16 may be described in mathematical terms by the following equations:

$$u_k = \sum_{j=1}^{m} w_{kj} x_j \tag{2.1}$$

$$y_k = \varphi(u_k + b_k) \tag{2.2}$$

where $x_1, \ldots, x_m$ are the inputs; $w_{k1}, \ldots, w_{km}$ are the synaptic weights; u_k is the linear combiner output; b_k is the bias; $\varphi(\bullet)$ is the activation function and y_k is the output of the neuron.

The activation function, denoted by $\varphi(\bullet)$, is determined by the type of data the ANN is trying to learn. The tangential sigmoid function limits the output to between minus one and one, while the logarithmic sigmoid function limits the output of the neuron to between zero and one. Figure 2.17 shows the transfer functions.

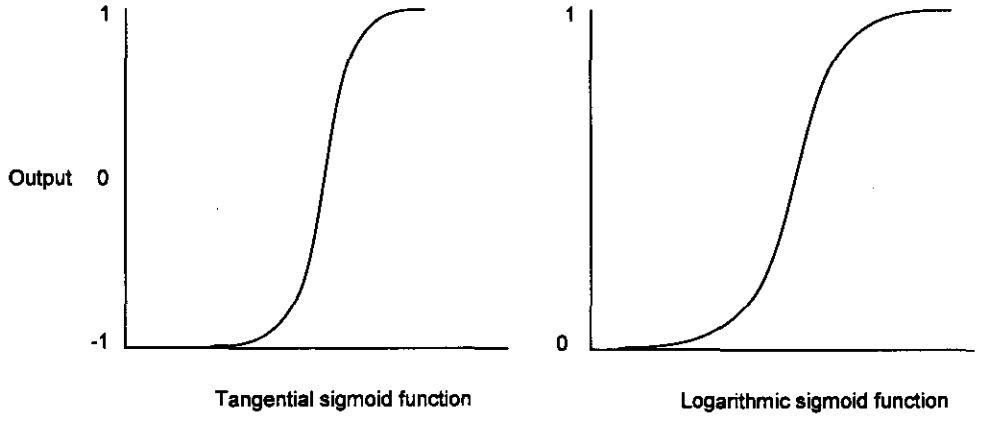

Figure 2.17 ANN activation functions.

The internal structure of the ANN is intimately linked with the learning algorithm that is used. The multilayer feedforward architecture has emerged as a suitable structure for the ANN. In this type of network architecture, the neurons are structured in layers. The input space is connected to the output space by means of a hidden layer. Every node in each layer is connected to every node in the next forward layer, but not to each other. Figure 2.18 shows the structure of a multilayer feedforward ANN. The training process and type of feedforward algorithm that is used are discussed in chapter 5.

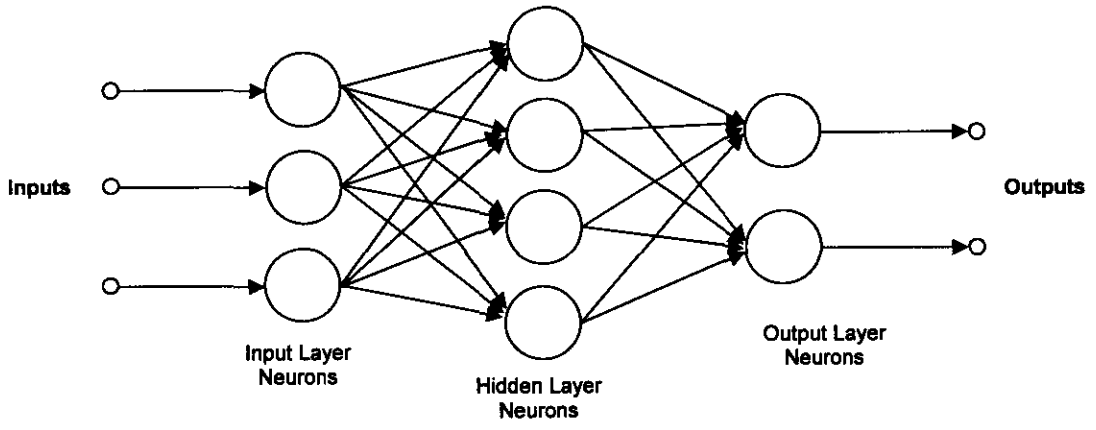

Figure 2.18 Internal structure of a multilayer feedforward neural network.

2.7 Conclusions

Existing DG technologies are described and the major benefits and issues of using DG are discussed. The different technologies are evaluated in terms of their contribution to the listed benefits and issues. A definition for DG is proposed as there is no consensus on a precise definition for the concept (it encompasses many technologies and many applications in different environments).

Electric PQ control is necessary in any power system to ensure effective operation of equipment and importantly to avoid damage to equipment. This means a consistent and controlled voltage magnitude and frequency. Many factors contribute to PQ problems, from lightning strikes to household computers, each resulting in different PQ phenomena. For the purpose of this study, the switching of large loads on a MVA power grid is investigated. This can result in PQ problems like overvoltages and undervoltages. Proper control of strategically placed DGs in the power grid may improve these conditions. The main control strategy of the DGs will focus on tertiary normal state control as discussed in section 2.6.3.

AI techniques have emerged as suitable solutions for the control scheme of DGs. The different AI techniques are discussed and evaluated. ANNs emerged as an appropriate AI control technique for the control of the DGs because of its ability to recognise patterns (e.g. the network load patterns as discussed in chapter 4). To control the PQ in the grid, regulation control is chosen to as control scheme for the DGs. Choosing this control type makes it possible to control the power, voltage and frequency in the power grid. A proper control scheme for the DGs will ensure that the power quality and stability of the power network will be maintained.

Chapter 3 - Electric power system model

3.1 Introduction

In this chapter, a simulation model is developed which integrates the DGs and the electric power system. The software environment chosen for the simulation platform is Matlab Simulink® and Matlab SimPowerSystems® (SPS). The electric power network scenario is provided by ESKOM and forms part of an existing electric power network. The impact and penetration of DG in the electric power system is investigated and some key issues include voltage regulation and electrical power losses. This simulation model forms the basis for the analysis of the electric power system.

3.2 Case study

The scenario used in this research is part of an ESKOM power network that is under revision. The network may have power quality problems in the near future, as the network is loaded to full capacity. The main transmission lines are rated at 275 kV ac. Sub transmission or distribution is rated at 132 kV ac for cities, towns and big customers (e.g. mines). Figure 3.1 shows the line diagram of the ESKOM network under revision and the substation names are shown in table 3.1.

Sub	Name	Base kV
A	Everest	275
B	Perseus	275
C	Harvard	275
D	Merapi	275
E	Boundary	275
F	Olien	275
G	Ferrum	275
H	Garona	275

Table 3.1 Substation names and voltage ratings of the electric power network.

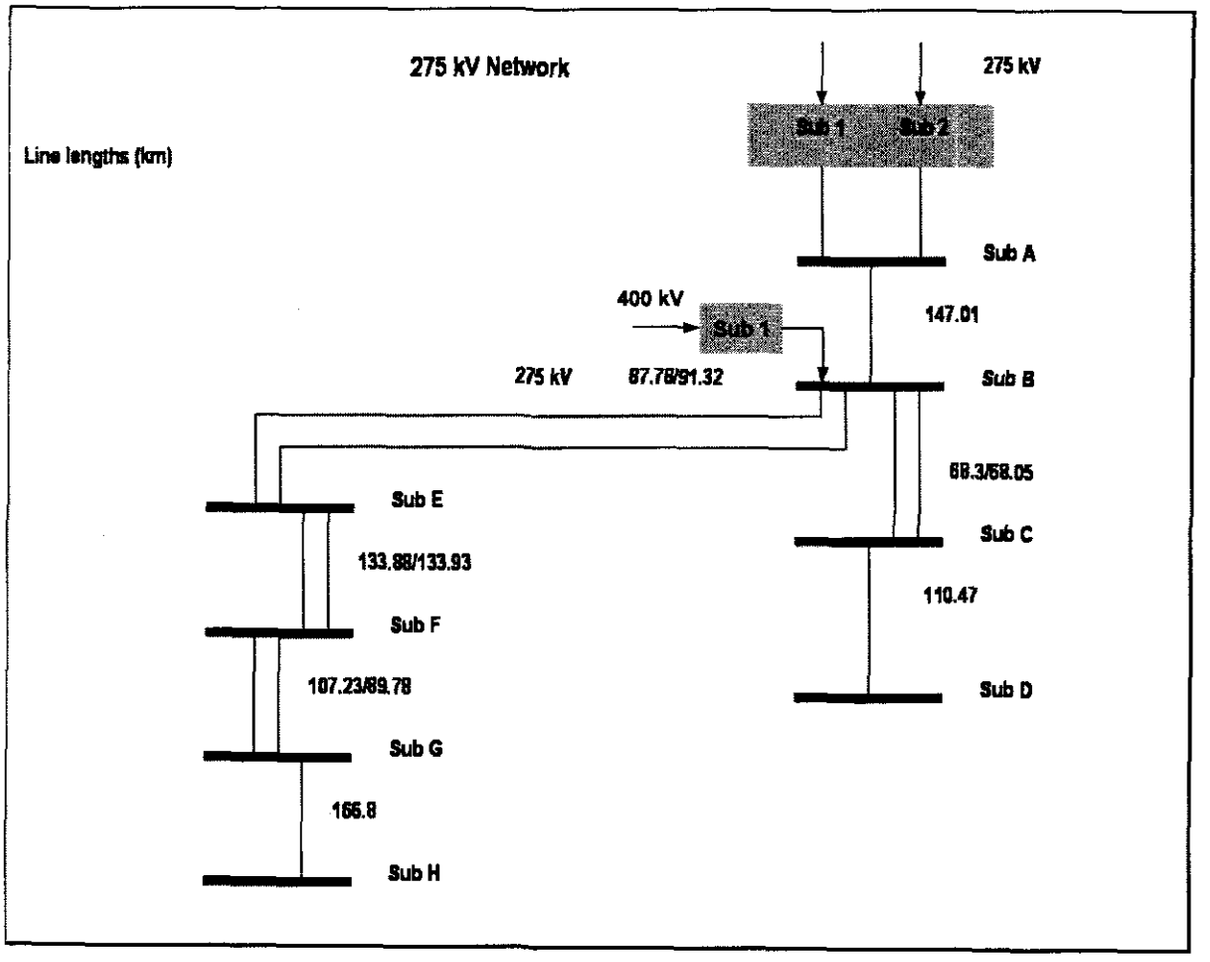

Figure 3.1 Line diagram of the ESKOM network.

The electric power network line, load, capacitor bank and substation data are shown in annexure B. The transformation of line data from R, X and B (pu) to R (Ω/km), L (H/km) and C (F/km) is also shown in Annexure B. This is done because the line modelling blocks of SPS uses the line R, L and C values. Figure 3.2 shows the line diagram of the network with the real load capacities, line lengths, bus numbers, transformer ratings and capacitor banks.

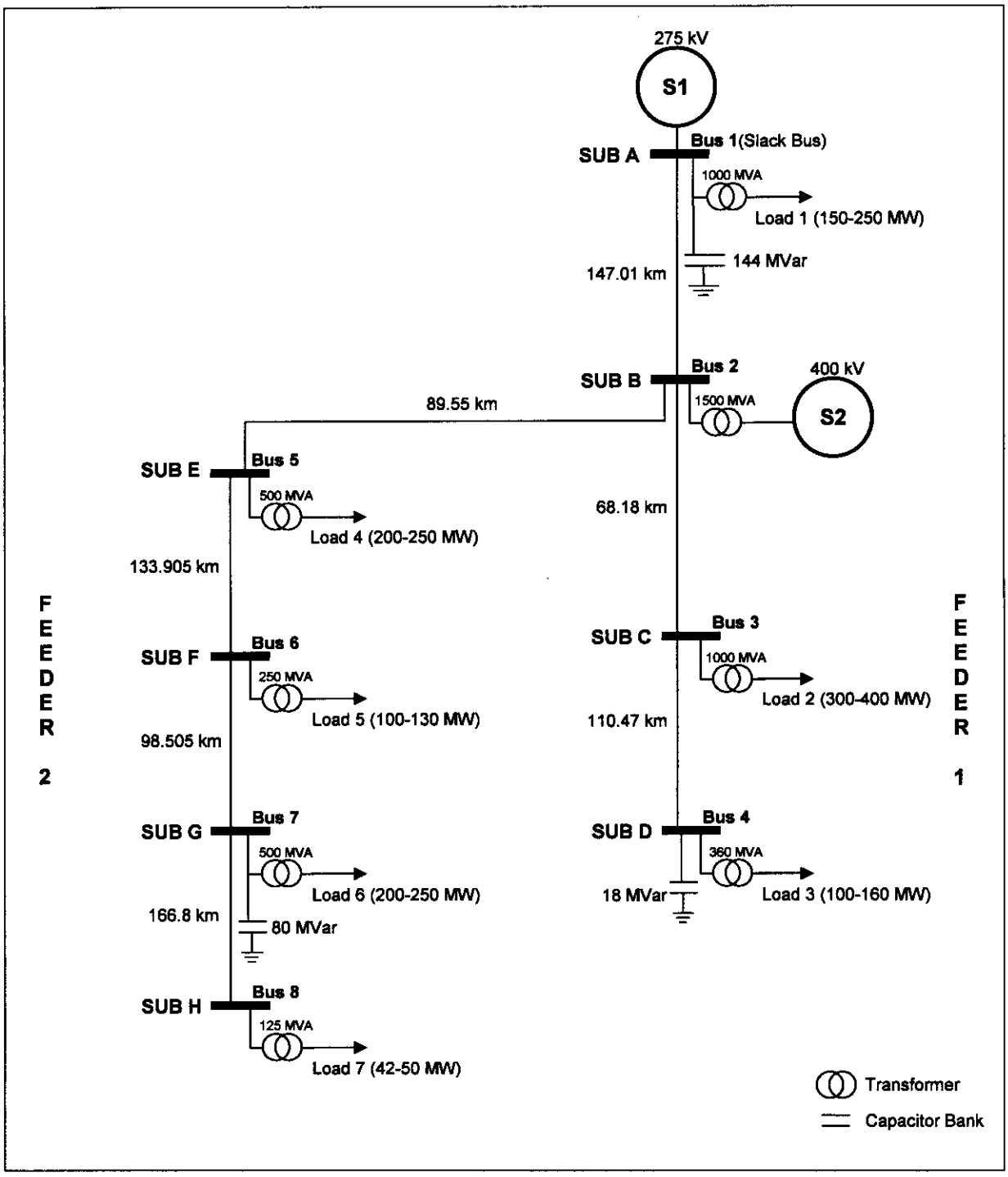

Figure 3.2 Line diagram of the ESKOM power network.

3.3 Simulation environment

Matlab6.5R13 [21] is a mathematical computing program with the capability of real time interfacing with external devices like monitoring devices and controllers. The full package constitutes several different computing toolboxes (control, neural networks, fuzzy logic, optimization, robust control etc.). Simulink is a toolbox of Matlab where complete systems can be modelled by means of blocksets. These blocksets are more user friendly than a string of programming code. The blocksets can be anything from simple connectors to advanced controllers with feedback and monitoring signals. SPS, which is a sub-toolbox of Simulink [22], constitutes the following sub-libraries:

- Electrical sources (dc, ac, current etc.) ;
- Elements (branches, lines, transformers, circuit breakers etc.);
- Power electronics (diodes, thyristors, bridge, mosfets etc.);
- Machines (regulators, dc, synchronous, asynchronous etc.);
- Connectors (ground, busbars etc.);
- Measurements (voltage, current, impedance, power etc.).

The part of the ESKOM power network is simulated using these libraries. Figure 3.3 shows the main draw window in Simulink.

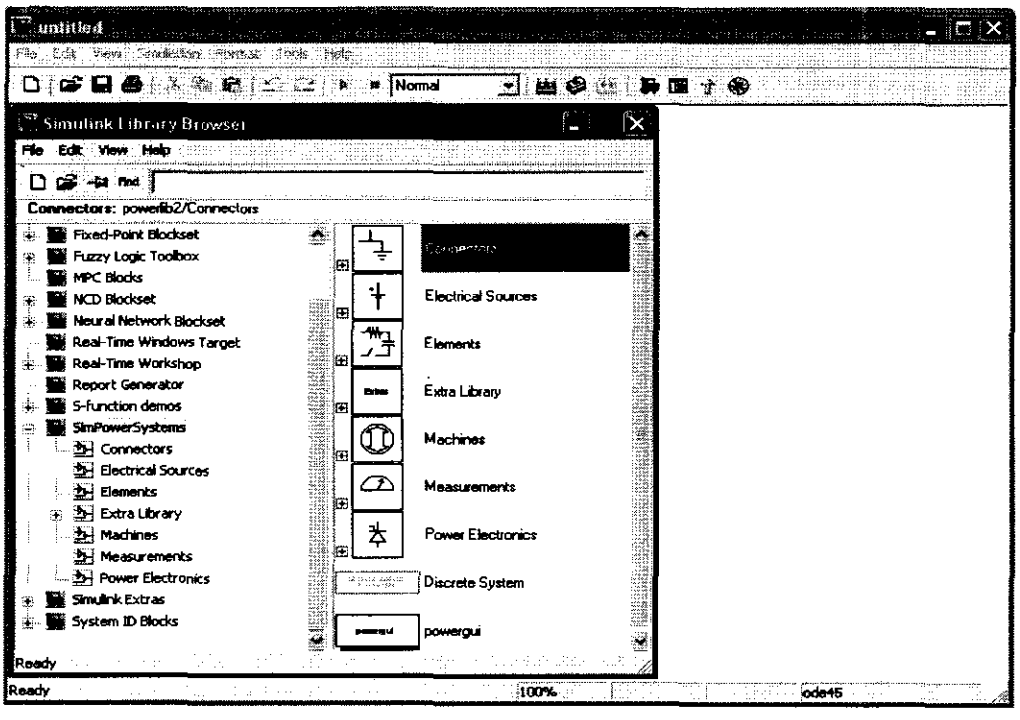

Figure 3.3 The main draw window in Simulink with the SPS library browser.

The power graphical user interface (GUI) in the library browser is used to provide a graphical user interface for the analysis of models created in Simulink. The power GUI allows you to evaluate and modify the initial states in order to start the simulation from any initial condition. It displays the steady state values of measured currents and voltages. The power GUI also performs load flow analyses and initialization of three phase networks containing machines so that the simulation starts in steady state. It also displays impedance versus frequency plots and FFT analyses of the system. The power GUI is used in the simulation to obtain the following data and results:

- steady state values of voltages and currents on each busbar; and
- load flow and machine initialisation to start the simulation in steady state.

Figure 3.4 shows the main window of the power GUI tool.

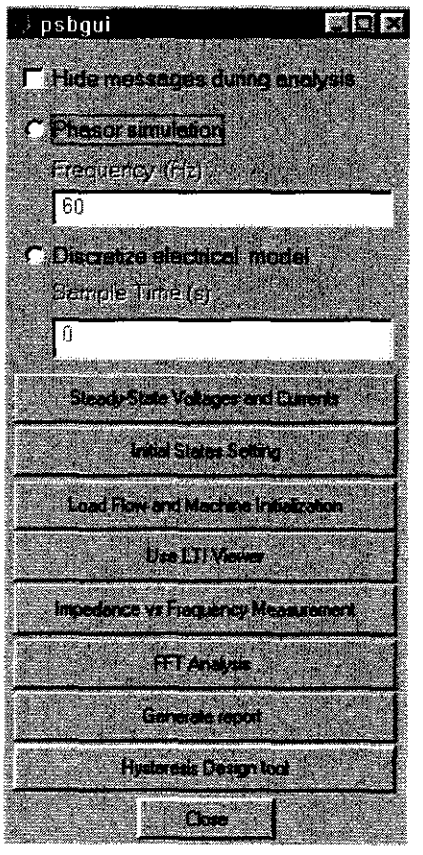

Figure 3.4 The main window of the power GUI.

3.4 Simulating the electric power network in Matlab

The power system under consideration is modelled in Simulink using SPS. The model constitutes the following building blocks:

- Feeding sources;
- Transmission lines;
- Loads;
- Transformers.

The network constitutes the following components:

- One 275 kV feeding source (275 kV transmission line);
- One 400 kV feeding source (400 kV transmission line);
- Seven 275 kV transmission lines;
- Three 275 kV capacitor banks;
- Seven 132 kV RLC loads;
- Seven 275 kV:132 kV transformer substations;
- One 400 kV:275 kV transformer substation;
- Two 30 kV:275 kV transformer substations;
- Two 30 kV ac generators;
- Two 30 kV resistive loads.

Since the study mainly focuses on an artificial control scheme for the DGs in the power system, the power system constitutes the following constraints:

- There is no unbalance in the system. All three phases are balanced;
- The transformer tap positions are not control variables, so all the transformer tap positions are fixed at 1 pu;
- The generators do not inject any harmonics into the system;
- The power system is evaluated in steady state only (evaluated only at the fundamental frequency 50 Hz);
- All the loads are linear at 50 Hz and rated at 132 kV;
- Double lines are modelled as single lines with the equivalent values and ratings;
- Synchronous generators are used for the DGs (capable of delivering large-scale power [18]).

3.4.1 The power system components

3.4.1.1 Voltage source (Feeding sources)

The grounded three-phase voltage source implements a pure three-phase sinusoidal voltage source with equivalent RLC impedance. This block is used to simulate a part of a power network feeding the existing network. It is typically used to simulate the network from the power station up to the point of connection. Figures 3.5 and 3.6 show the library block and the library dialog box of the voltage source.

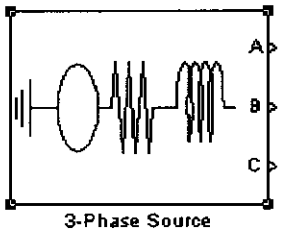

Figure 3.5 Simulink library block of a three-phase voltage source with equivalent RLC impedance.

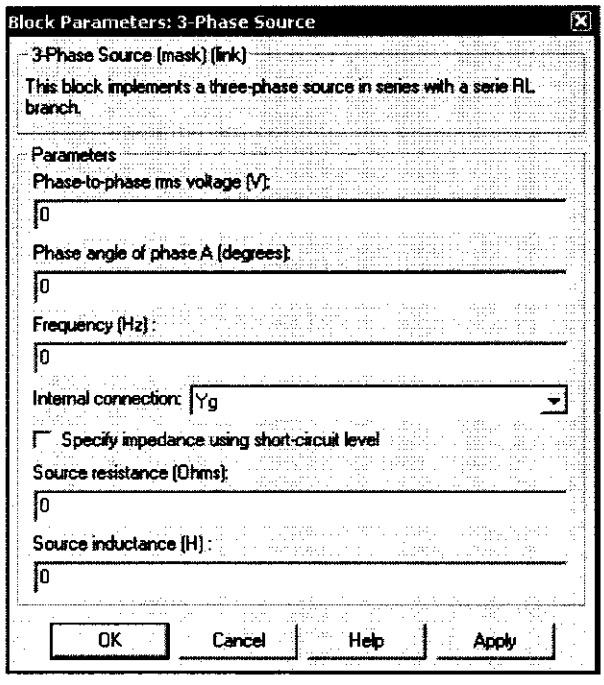

Figure 3.6 Dialog box parameters of a three-phase voltage source with equivalent RLC impedance.

3.4.1.2 Transmission line

The pi section transmission line implements a single-phase transmission line with parameters lumped in pi sections. For a transmission line, the resistance, inductance, and capacitance are uniformly distributed along the line. Figures 3.7 and 3.8 show the library block and the library dialog box of the transmission line.

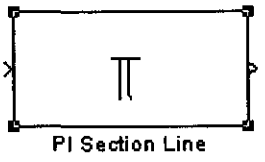

Figure 3.7 Simulink library block of a pi section transmission line.

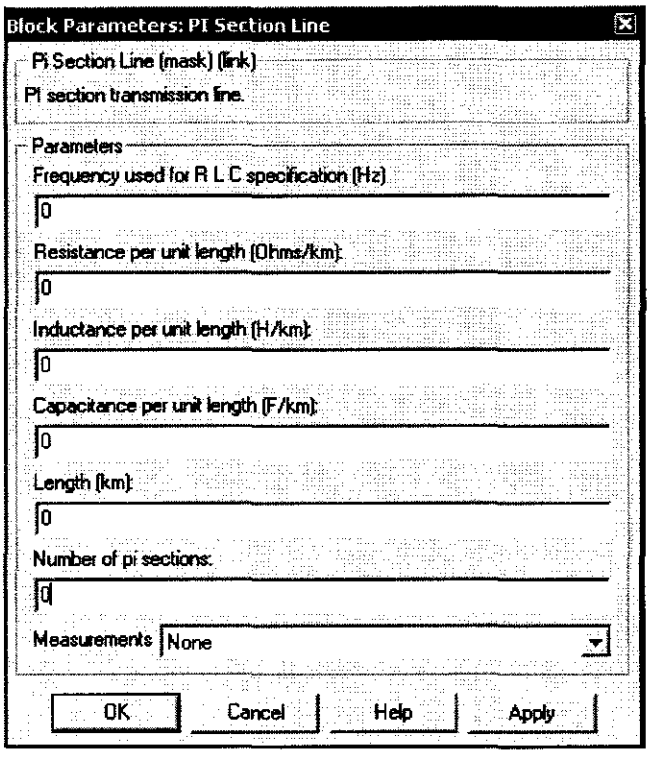

Figure 3.8 Dialog box parameters of a pi section transmission line.

3.4.1.3 Transformer

The three-phase transformer with two windings (three windings is used to eliminate harmonics) block implements a three-phase transformer using three single-phase transformers. The transformers in the network are used to step up the voltage at the generators from 15 kV to 275 kV (Δ - Yg) and to step down the voltage at the loads from 275 kV to 132 kV (Yg - Δ) [18]. Figures 3.9 and 3.10 show the library block and the library dialog box of the transformer.

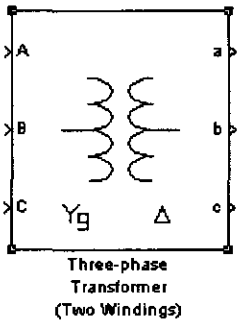

Figure 3.9 Simulink library block of a three-phase transformer.

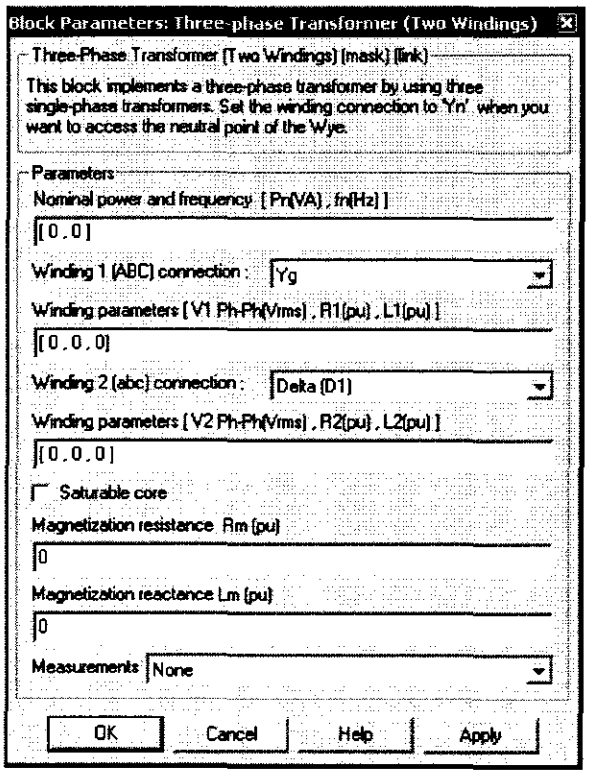

Figure 3.10 Dialog box parameters of a three-phase transformer.

3.4.1.4 Load

The series RLC load block implements a linear load as a series combination of R, L, and C elements. At the specified frequency, the load exhibits constant impedance and its power is proportional to the square of the applied voltage. Figures 3.11 and 3.12 show the library block and the library dialog box of the load.

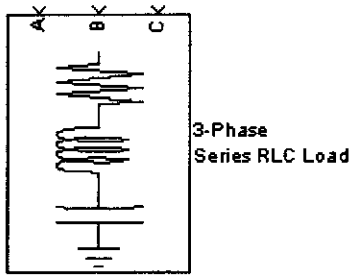

Figure 3.11 Simulink library block of a three-phase series RLC load.

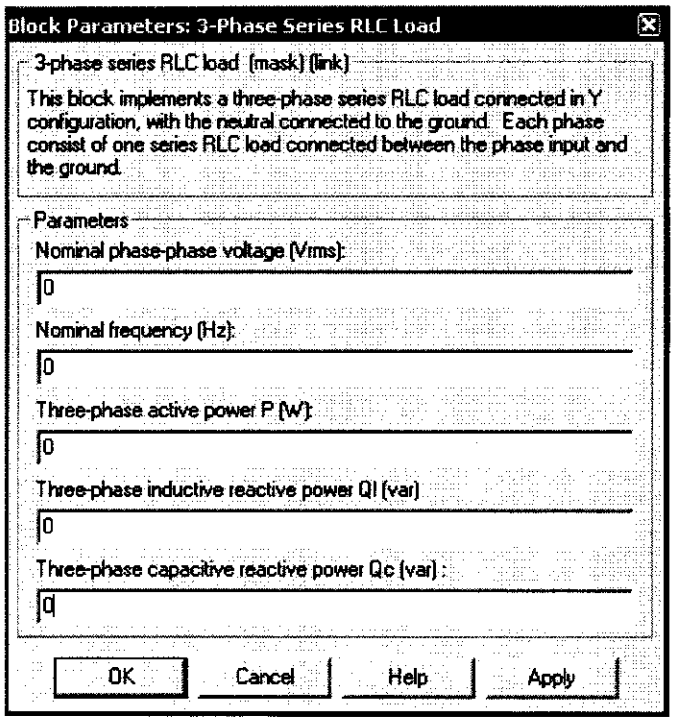

Figure 3.12 Dialog box parameters of a three-phase series RLC load.

3.4.1.5 Generator (DG)

The synchronous machine block models both the electrical and mechanical characteristics of a simple synchronous machine. The electrical system for each phase consists of a voltage source in series with a RL impedance, which implements the internal impedance of the machine. Figures 3.13 and 3.14 show the library block and the library dialog box of the generator.

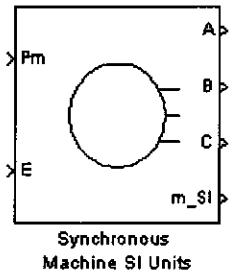

Figure 3.13 Simulink library block of a synchronous machine.

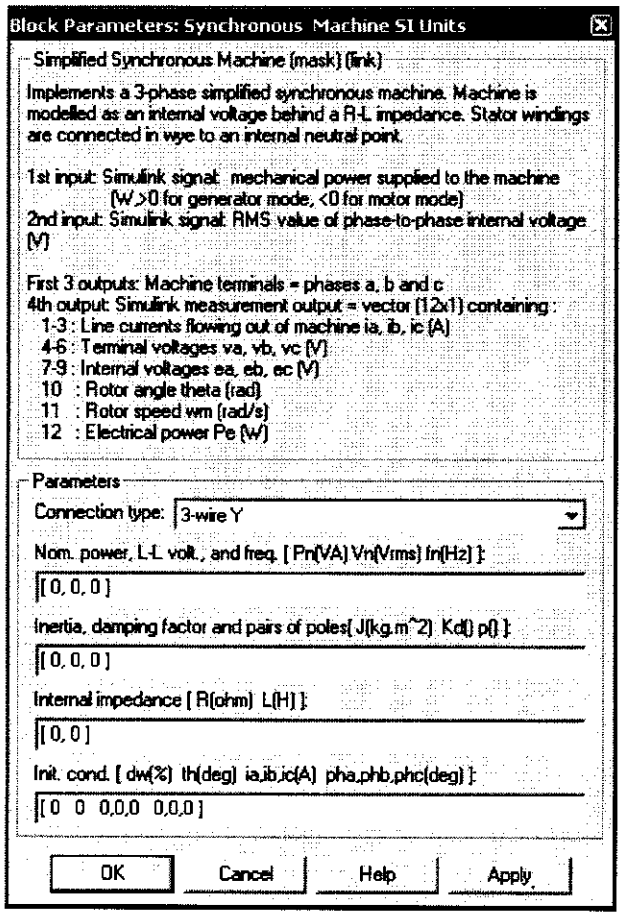

Figure 3.14 Dialog box parameters of a synchronous machine.

3.4.2 Placement of DGs in the electric power network

To optimise the power quality in the electric power system, a maximum of two DGs must be integrated into the existing network. The voltage profile of the network is firstly evaluated without any DGs for two steady state conditions, firstly at minimum load and secondly at full load. Table 3.2 shows the voltage profile of the power network at minimum and maximum load without the DGs (transformer tap positions are fixed at 1 pu).

Load	Bus 1	Bus 2	Bus 3	Bus 4	Bus 5	Bus 6	Bus 7	Bus 8
Min.	1.00	1.00	0.95	0.945	1.00	1.01	1.04	1.059
Max.	1.00	1.00	0.91	0.883	1.00	0.945	0.945	0.96

Table 3.2 Voltage profile of the power system at min. and max. load.

Table 3.2 shows that the voltage profiles of busses 3 and 4 are the worst. To select the optimal injection points of the generators, the DGs are placed randomly at the six busbars in the network (DGs are not placed at busses with a feeding source or on the same transmission feeder). The network active power losses are evaluated for the load conditions at full capacity. Table 3.3 shows the power losses for the randomly placed DGs. From these results, the weakest points are identified.

DG 1 (bus no.)	DG 2 (bus no.)	Total Power Loss (MW)
3	5	49.6099
3	6	53.8522
3	7	50.7263
3	8	51.8229
4	5	51.8207
4	6	52.7379
4	7	49.7470
4	8	49.9336

Table 3.3 Power losses of the network for the randomly placed DGs.

Busses 3 and 5 were observed to have minimum loss reduction and hence considered to be the sensitive busses. The results show that DG 1 must be placed at bus 3 and DG 2 at bus 5.

Figure 3.15 shows the final line diagram of the power network with the two integrated DGs.

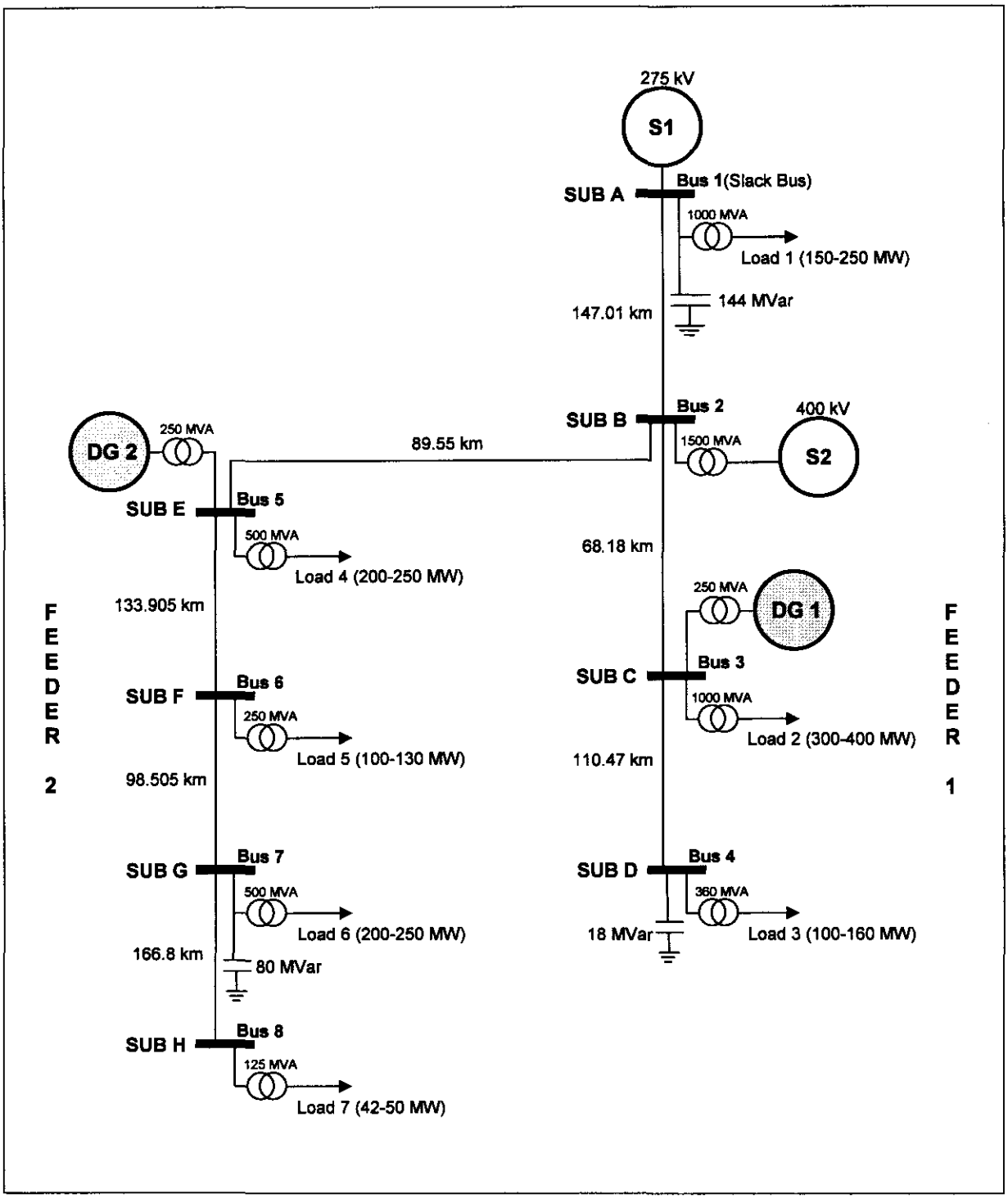

Figure 3.15 Line diagram of the ESKOM power network with the two integrated DGs.

3.4.3 Interconnection of the DGs on the grid

The DG can either be operated in parallel with the grid or on a switched, roll-over basis [23], [24]. In parallel operation, the DG and the grid are both always connected to each other and to the load. One advantage of this operation is that the outage of the primary supply causes no interruption of service. If the DG is supplying the power and fails, the grid instantaneously makes up the difference and no interruption of power flow to the load occurs. Similarly if the grid fails, the DG picks up the load. By contrast, in roll-over mode, only one of the sources is connected to the load at any one time. The connection is operated by the "flip of a switch". The disadvantage of this mode is that a brief interruption of service occurs when the primary power source fails. Figure 3.16 shows the operation and interconnection of DG on the power grid.

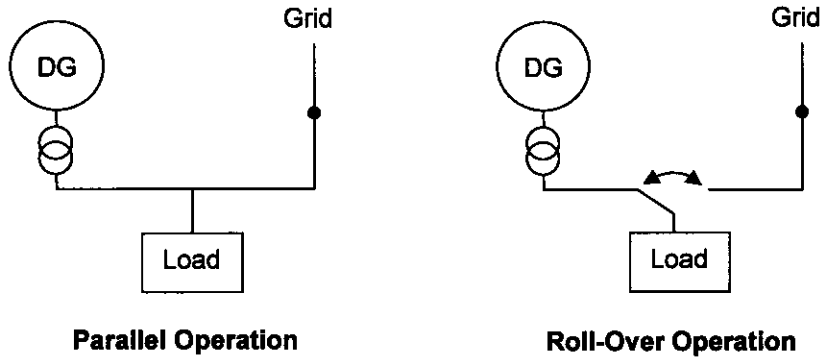

Figure 3.16 Operation and interconnection of DG on the power grid.

Parallel operation of DG with the power grid can solve voltage regulation problems [23]. As the load varies, the grid will support the DG and provide the instant transient response needed, allowing the DG to vary its output at its slow (compared to the power grid) rate. The result is far less variation in the supply voltage and improved power quality. The switching of large loads causes less voltage change than when served only by the power grid. Due to this advantage, parallel operation of the DGs is considered for the electric power network. The complete system as shown in figure 3.15 is modelled in Simulink with SPS. The Simulink model is shown in figure E.1 in Annexure E.

3.5 Conclusions

To evaluate the electric power system under revision, a simulation model is developed which integrate the DGs and the electric power system. The software environment chosen for the simulation platform is Matlab Simulink® and Matlab SimPowerSystems®. The strategic placement of the DGs in the power

system is important and the loss sensitivities of the busses are investigated. The results show that the DGs must be placed at busses 3 and 5. The interconnection issues surrounding DG are discussed and it is concluded that the DGs must operate in parallel with the electric power grid. The integrated model is lastly modelled in Simulink, which forms the basis for the analysis of the electric power system.

Chapter 4 - ANN data development

4.1 Introduction

This chapter focuses on the development of training data for the ANN controlling the DGs on the power grid. This procedure firstly involves the development of a cost function to determine the optimal output values for the DGs. The main goal of the cost function is to optimise the voltage profile of the system for a particular network condition. The cost function must also determine the level of contribution by each DG to minimise total system losses.

The cost function incorporates a voltage constraint and optimises the function until the point where the best voltage profile with minimum system losses is obtained. The final training set developed contains the operating parameters for each DG for the different load conditions of the network.

4.2 Development of the training data

4.2.1 Network parameters

The input space to the ANN must give some information about the network conditions and status. Many feedback parameters can be monitored in the power network, ranging from load conditions to generator power factors. For the purpose of this study, the load conditions are monitored on all the system busbars. This means that from the 132 kV substation transformers to the 220 V distribution systems are modelled as an entire load. To extract the most information from the minimum amount of measurements, the network parameters as given in table 4.1 are measured:

Measurement	Description
V_L	The load voltage magnitude
$\angle V_L$	The load voltage phase angle
I_L	The load current magnitude
$\angle I_L$	The load current phase angle

Table 4.1 The measured parameters for each load in the network.

Fundamental calculations can be made from these parameters. To calculate the active and reactive powers at the fundamental frequency, the following equations are used:

$$P_{load} = \frac{1}{T}\int_{t}^{t+T}(v(\varpi t)\times i(\varpi t))dt \tag{4.1}$$

$$Q_{load} = \frac{1}{T}\int_{t}^{t+T}(v(\varpi t)\times i(\varpi t - \pi/2))dt \tag{4.2}$$

with T = 1/fundamental frequency.

These calculations are done for every load in the network. All the calculated and measured parameters of the power network are listed in table 4.2.

Input parameter	Description
V_L	The load voltage magnitude
$\angle V_L$	The load voltage phase angle
I_L	The load current magnitude
$\angle I_L$	The load current phase angle
P_{load}	The load real power
Q_{load}	The load reactive power
V_{gen}	The generators/sources voltage magnitude
$\angle V_{gen}$	The generators/sources voltage phase angle
P_{gen}	The generators/sources real power
Q_{gen}	The generators/sources reactive power

Table 4.2 Measured and calculated parameters of the loads and sources in the network.

4.2.2 Power flow analysis

To develop a training data set for the ANN, a cost function is used to find the optimum generation levels of the DGs for the various input conditions. To ensure the credibility of the training data, the cost function must accurately represent the network model. To do this, a power flow solution of the power network is done using the Newton-Raphson Power Flow solution. This method is found to be more efficient than the Gauss-Seidel Power Flow solution [18]. To solve the power flow solution, the system is assumed to operate under balanced conditions and only a single-phase model is used. To solve the power flow of the system, four quantities are associated with each bus in the network:

- Voltage magnitude $|V|$;
- Phase angle δ;
- Real power P;
- Reactive power Q;

The system busses are classified into three different types [18]:

- **Slack Bus (Swing Bus)**
  This bus is taken as reference for the voltage magnitude and phase angle. The difference between the loads and the generated power caused by the network losses is made up by this bus.

- **Load Busses (P-Q Busses)**
  The real and reactive powers are specified at these busses. The voltage magnitude and phase angle of these busses are unknown.

- **Regulated Busses (P-V Busses)**
  These are the generator or voltage-controlled busses. The real power, voltage magnitude and limit of the reactive power are specified.

The following two equations describe the active and reactive powers on the busses (Newton-Raphson Power Flow solution):

$$\Delta P_i = \sum_{j=1}^{n} |V_i||V_j||Y_{ij}|\cos(\theta_{ij} - \delta_i + \delta_j) \tag{4.3}$$

$$\Delta Q_i = -\sum_{j=1}^{n} |V_i||V_j||Y_{ij}|\sin(\theta_{ij} - \delta_i + \delta_j) \tag{4.4}$$

with V_i = voltage magnitude of bus i
V_j = voltage magnitude of bus j
Y_{ij} = bus admittance matrix.

The Matlab program named **lfnewton** [18] is used to obtain the power flow solution for a given network condition. The credibility of this algorithm is validated against the power flow solution of SimPowerSystems. For this validation process, a test model is created in Matlab and the two simulations are compared. The results of the power flow solutions for the two different modelling environments (Newton-Raphson code vs. SimPowerSystems) are shown in Annexure C. The results

show close correlation, thus verifying the credibility of the Newton-Raphson method.

4.2.3 Power losses analysis

The first step in determining the optimal generation levels of the generators is to express the system losses in terms of the generators real power outputs. The method used to determine the system losses is known as *Kron's Power Loss* formula or the *B-coefficient* method [18].

The total power at bus i, denoted by S_i, is given by (4.5) as

$$S_i = P_i + jQ_i = V_i I_i^* \tag{4.5}$$

The total system losses are given as the summation over all the buses as

$$P_L + jQ_L = \sum_{i=1}^{n} V_i I_i^* = V_{bus}^T I_{bus}^* \tag{4.6}$$

with P_L = Real power losses of the system

Q_L = Reactive power losses of the system

V_{bus} = Column vector of the bus voltages

I_{bus} = Column vector of the injected bus currents

The bus currents in terms of the bus voltages is given as

$$I_{bus} = Y_{bus} V_{bus} \tag{4.7}$$

with Y_{bus} the bus admittance matrix. Solving equation (4.7) for Y_{bus} gives

$$V_{bus} = Y_{bus}^{-1} I_{bus} = Z_{bus} I_{bus} \tag{4.8}$$

with Z_{bus} the bus impedance matrix.

Also, Z_{bus} is symmetrical, therefore $Z_{bus}^T = Z_{bus}$. Substituting (4.8) into (4.6), results in

$$P_L + jQ_L = [Z_{bus} I_{bus}]^T I_{bus}^* = I_{bus}^T Z_{bus}^T I_{bus}^* = I_{bus}^* Z_{bus} I_{bus}^* \tag{4.9}$$

Equation (4.9) can be rewritten in index notion as

$$P_L + Q_L = \sum_{i=1}^{n}\sum_{j=1}^{n} I_i Z_{ij} I_j^* \tag{4.10}$$

The bus impedance matrix is also symmetrical ($Z_{ij} = Z_{ji}$), thus (4.10) becomes

$$P_L + jQ_L = \frac{1}{2}\sum_{i=1}^{n}\sum_{j=1}^{n} Z_{ij}(I_i I_j^* + I_j I_i^*) \tag{4.11}$$

Splitting (4.11) in the real and imaginary components, the power loss becomes

$$P_L = \frac{1}{2}\sum_{i=1}^{n}\sum_{j=1}^{n} R_{ij}(I_i I_j^* + I_j I_i^*) \tag{4.12}$$

$$Q_L = \frac{1}{2}\sum_{i=1}^{n}\sum_{j=1}^{n} X_{ij}(I_i I_j^* + I_j I_i^*) \tag{4.13}$$

with R_{ij} the real element and X_{ij} the imaginary element of the bus impedance matrix.

Since $R_{ij} = R_{ji}$, the real power given by (4.12) can be rewritten as

$$P_L = \sum_{i=1}^{n}\sum_{j=1}^{n} I_i R_{ij} I_j^* \tag{4.14}$$

The system real power loss (4.14) can be rewritten in matrix form as

$$P_L = I_{bus}^T R_{bus} I_{bus}^* \tag{4.15}$$

with R_{bus} the real component of the bus impedance matrix.

The total load current is expressed as the sum of all the individual load currents. This is done to obtain a general formula for the system power loss in terms of the generator powers.

$$I_D = I_{L1} + I_{L2} + \ldots + I_{Ln_d} \tag{4.16}$$

Assuming the individual bus currents vary as a constant complex fraction of the total load current, i.e.

$$I_{Lk} = l_k I_D \qquad k=1,2,\ldots,n_d \tag{4.17}$$

Taking the reference or slack bus as bus 1, the first row in (4.8) becomes

$$V_1 = Z_{11}I_1 + Z_{12}I_2 + \ldots + Z_{1n}I_n \tag{4.18}$$

If the number of generator busses is n_g and n_d is the number of load busses, equation (4.18) can be written in terms of the generator and load currents as

$$V_1 = \sum_{i=1}^{n_g} Z_{1i}I_{gi} + \sum_{k=1}^{n_d} Z_{1k}I_{Lk} \tag{4.19}$$

Substituting I_{Lk} from (4.17) into (4.19), the results in

$$V_1 = \sum_{i=1}^{n_g} Z_{1i} + I_D \sum_{k=1}^{n_d} l_k Z_{1k} = \sum_{i=1}^{n_g} Z_{1i}I_{gi} + I_D T \tag{4.20}$$

with $T = \sum_{k=1}^{n_d} l_k Z_{1k}$

If we define I_0 as the current flowing away from bus 1, with all other currents set to zero, then

$$V_1 = -Z_{11}I_0 \tag{4.21}$$

Substituting (4.21) in (4.20) and solving I_D, results in

$$I_D = -\frac{1}{T}\sum_{i=1}^{n_g} Z_{1i}I_{gi} - \frac{1}{T}Z_{11}I_0 \tag{4.22}$$

Substituting I_D from equation (4.21) into (4.17), the load currents then become

$$I_{Lk} = -\frac{l_k}{T}\sum_{i=1}^{n_g} Z_{1i}I_{gi} - \frac{l_k}{T}Z_{11}I_0 = \rho_k \sum_{i=1}^{n_g} Z_{1i}I_{gi} + \rho_k Z_{11}I_0 \tag{4.23}$$

with $\rho = -\frac{l_k}{T}$

Substituting the generator currents with the above relation in matrix form, yields the matrix C

$$I_{bus} = CI_{new} \tag{4.24}$$

Substituting (4.24) into (4.15) yields

$$P_L = [CI_{new}]^T R_{bus} C^* I_{new}^* = I_{new}^T C^T R_{bus} C^* I_{new}^* \tag{4.25}$$

Given S_{gi} the complex power at bus *i*, the generator current becomes

$$I_{gi} = \frac{S_{gi}^*}{V_i^*} = \frac{P_{gi} - jQ_{gi}}{V_i^*} = \frac{1 - j\dfrac{Q_{gi}}{P_{gi}}}{V_i^*} P_{gi} = \psi_i P_{gi} \tag{4.26}$$

with $\psi_i = \dfrac{1 - j\dfrac{Q_{gi}}{P_{gi}}}{V_i^*}$

If the current I_0 is added to the column vector current in (4.26), it becomes

$$I_{new} = \psi P_{G1} \tag{4.27}$$

Substituting (4.27) into (4.25), the loss equation results in

$$P_L = [\psi P_{G1}]^T C^T R_{bus} C^* \psi^* P_{G1}$$

$$= P_{G1}^T \psi^T C^T R_{bus} C^* \psi^* P_{G1}^* \tag{4.28}$$

$$= P_{G1}^T H P_{G1}^* \tag{4.29}$$

with $H = \psi^T C^T R_{bus} C^* \psi^*$

The real power loss is found from the real part of the complex resultant matrix above. *H* is a *Hermittian* matrix and is symmetrical. The real part is obtained from

$$\Re[H] = \frac{H + H^*}{2} \tag{4.30}$$

(4.30) represents the system *loss coefficients* or *B-coefficients*. *Kron's Loss Formula* can thus be written as

$$P_L = \sum_{i=1}^{n} \sum_{j=1}^{n} P_i B_{ij} P_j + \sum_{i=1}^{n} B_{0i} P_i + B_{00} \tag{4.31}$$

4.2.4 Cost function development

When transmission lines are long and the load density areas are very low (loads are far from one another), transmission or system losses become a major factor in determining the optimal generation levels of the DGs. Optimal generation levels influence the following factors:

- Generator efficiencies;
- Bus tension profile (effective bus voltages);
- Transmission or system losses;
- Fuel costs.

This means that the generation levels are determined by expressing these variables in terms of the generator output powers. The input to a DG or generation plant is usually measured in Btu/h (British thermal units per hour) and the output in MW (delivered power). Figure 4.1 shows an input-output curve of a DG or known as a heat-rate curve.

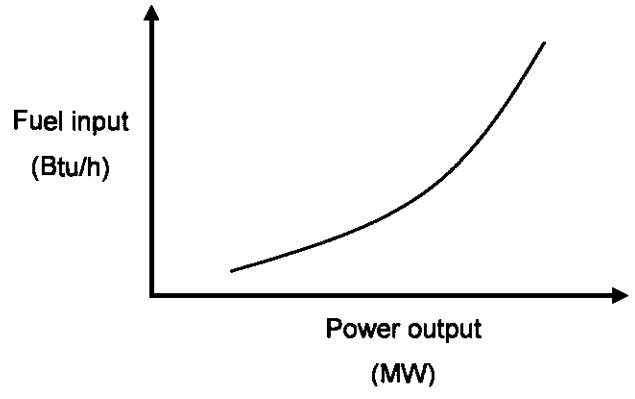

Figure 4.1 Heat-rate curve of a DG unit.

The heat-rate curve can be converted to a fuel-cost curve by changing the ordinate of the heat-rate curve [18]. Figure 4.2 shows the fuel-cost curve of the DG.

This relationship can be represented by a quadratic function of the real power generation by the DG

$$C_i = c_i + b_i P_i + a_i P_i^2 \tag{4.32}$$

with a_i, b_i, c_i constants

P_i the output powers of the DGs

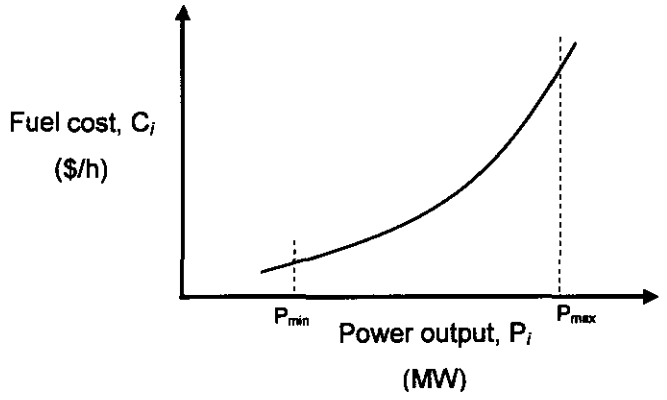

Figure 4.2 Fuel-cost curve of a DG unit.

The following objective functions that are considered for the cost function are [18], [25], [26]:

4.2.4.1 Generation costs

For a system with i generating units, the production costs as a function of the output powers is

$$F_1 = C_T = \sum_{i=1}^{n_g} C_i = \sum_{i=1}^{n} c_i + b_i P_i + a_i P_i^2 \tag{4.33}$$

where C_T = total production cost

C_i = production cost of the i^{th} plant

P_i = generation level of the i^{th} plant

The generation levels are limited, so (33) is subject to the following constraints

$$P_{i(\min)} \leq P_i \leq P_{i(\max)} \tag{4.34}$$

with $P_{i(\min)}$ & $P_{i(\max)}$ the minimum and maximum generating levels of the plants

4.2.4.2 Active power losses

Since the system losses is taken into account, the total amount of generated power is given by the load demand plus the system losses and is given by

$$F_2 = \sum_{i=1}^{n} P_L = P_G - P_D \geq 0 \tag{4.35}$$

with P_D, P_L, P_G the total load, real losses (*Kron's*) and generation in the system.

4.2.4.3 Average voltage deviation from permitted range (AVDP)

The average voltage deviation from permitted range is the voltage deviation of the actual voltages at the busbars and the permitted voltage range of the system. This is given by

$$F_3 = V_{avg} = \frac{\sum_{i=1}^{n} \left| V_i - V_i^* \right|}{N} \tag{4.36}$$

with V_i = actual voltage at busbar *i*

V_i^* = desired voltage range at busbar *i* (0.95 pu - 1.05 pu)

N = number of busbars in power system

4.2.4.4 Average voltage deviation from ideal (AVDI)

The average voltage deviation from ideal is the voltage deviation of the actual voltages at the busbars from the ideal voltage level. i.e. 1 pu. This is given by

$$F_4 = V_{ideal} = \frac{\sum_{i=1}^{n} \left| V_i - v_{ideal} \right|}{N} \tag{4.37}$$

with V_i = actual voltage at busbar *i*

v_{ideal} = ideal voltage (1 pu)

N = number of busbars in power system

The optimization problem to solve is the following

$$F = \min\left[F_1 \quad F_2 \quad F_3 \quad F_4\right] \tag{4.38}$$

that is

$$F = \min\left[\sum_{i=1}^{n} c_i + b_i P_i + a_i P_i^2 \quad P_G - P_D \quad \frac{\sum_{i=1}^{n} \left| V_i - V_i^* \right|}{N} \quad \frac{\sum_{i=1}^{n} \left| V_i - v_{ideal} \right|}{N}\right] \tag{4.39}$$

subject to $P_{i(\min)} \le P_i \le P_{i(\max)}$ and the load flow equations:

$$\Delta P_i = \sum_{j=1}^{n} |V_i||V_j||Y_{ij}|\cos(\theta_{ij} - \delta_i + \delta_j) \text{ and } \Delta Q_i = -\sum_{j=1}^{n} |V_i||V_j||Y_{ij}|\sin(\theta_{ij} - \delta_i + \delta_j)$$

Figure 4.3 illustrates the process for the development of the training data.

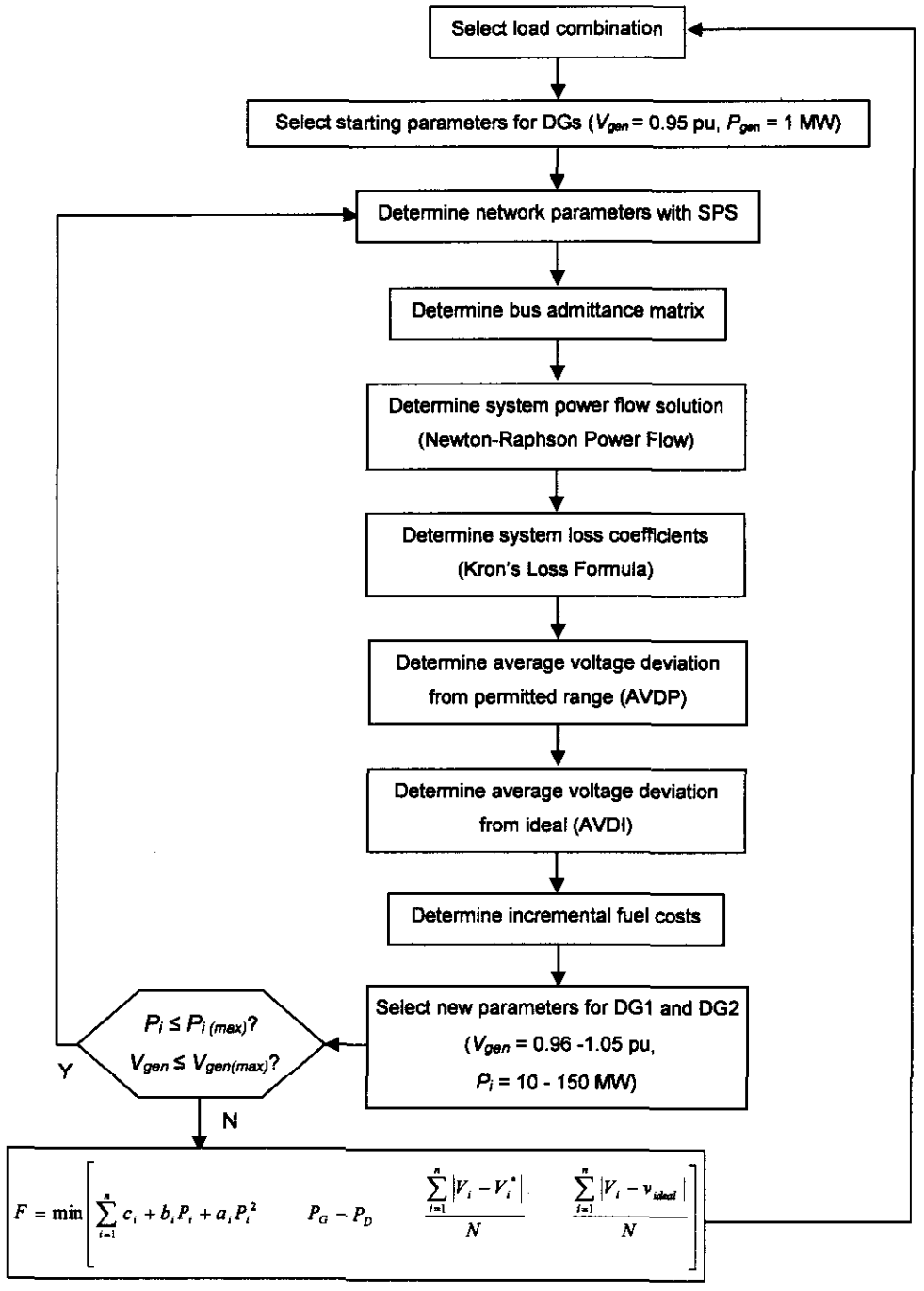

Figure 4.3 Flow diagram of the process for the development of the training data.

4.3 The formulated training data

As discussed in chapter 2, the training data must be randomly organised to prevent the ANN from classifying the data into certain groups. For the purpose of this study, the training data representing the network includes the following:

- Load conditions (seven loads that each has a real and reactive power value);
- Generator outputs (two DGs that each has a real power and voltage magnitude level).

All the loads (input variables) can take one of 3 different normalised values: 0, ½, 1. Since there are 7 loads, the training table consists of 3^7 = 2187 entries, i.e. 2187 different load combinations. The optimum generation levels for the two DGs need to be determined for each of these input combinations. The cost function is used for this optimisation process. The result of this optimisation process is the training data. This data is normalised to represent the training table for the ANN. Table 4.3 shows the normalised training table for the input load combinations. Take note that the input values are incremented in steps of ½. The output values of the DGs are determined by the cost function.

Input	*Normalised Inputs*							*Outputs*	
number	**L7**	**L6**	**L5**	**L4**	**L3**	**L2**	**L1**	**DG1**	**DG2**
1	0	0	0	0	0	0	0	?	?
2	0	0	0	0	0	0	½	?	?
3	0	0	0	0	0	0	1	?	?
4	0	0	0	0	0	½	0	?	?
5	0	0	0	0	0	½	½	?	?
6	0	0	0	0	0	½	1	?	?
7	0	0	0	0	0	1	0	?	?
8	0	0	0	0	0	1	½	?	?
9	0	0	0	0	0	1	1	?	?
10	0	0	0	0	½	0	0	?	?
11	0	0	0	0	½	0	½	?	?
12	0	0	0	0	½	0	1	?	?
13	0	0	0	0	½	½	0	?	?
⋮	⋮	⋮	⋮	⋮	⋮	⋮	⋮	⋮	⋮
2187	1	1	1	1	1	1	1	?	?

Table 4.3 Normalised training table.

The values corresponding to the normalised input values 0, ½ and 1, are discussed in chapter 5. To minimise the input combinations to the cost function to 2187, all the loads are set to operate at a power factor of 0.95. The reactive power can thus only vary in that ratio (the active and reactive power of the load is set to produce a power factor of 0.95).

4.3.1 Sequential optimistaion

The training data are determined for all 2187 different input states with the cost function. This is done by sequentially testing each output state for all 2187 input states. The two DGs in the power system can each operate with an incremental power of 10 MW and a maximum of 150 MW. This means that the output power can take on one of 16 different states (1 MW, 10 MW, 20 MW,..., 150MW). The DGs terminal voltage levels can be varied from 0.95 pu to 1.05 pu, which translates to 11 different states. Since there are 2187 input states, 2187*16*11*11 = 4 234 032 possible outputs must be tested. To minimise the different possible outputs that has to be determined by the cost function, the output powers of the DGs are the same. If not so and each DG could increment its power independently, the DGs output powers could take on one of 16^2 = 256 different combinations. For 2187 different input states, the cost function would have to evaluate 2187*256*11*11 = 67 744 512 states.

The program determines the cost function for each of the different outputs states (1936 times) for each of the input states (2187 times). The parameters used to determine the cost function are graphically displayed against the input state number below. This is done to visualise the training data as a behavioural pattern that the ANN should adopt. The parameters chosen to plot against the input state numbers are:

- the system real losses (P_L);
- the system average voltage deviation from permitted range (V_{avg});
- the system average voltage deviation from ideal (V_{ideal});

Figures 4.4 and 4.5 show some of the results of the cost function parameters plotted against the input state number. The output power of the DGs for the 2187 input states, are graphically displayed in figure 4.6. The maximum output powers of the DGs are limited to 150 MW per unit.

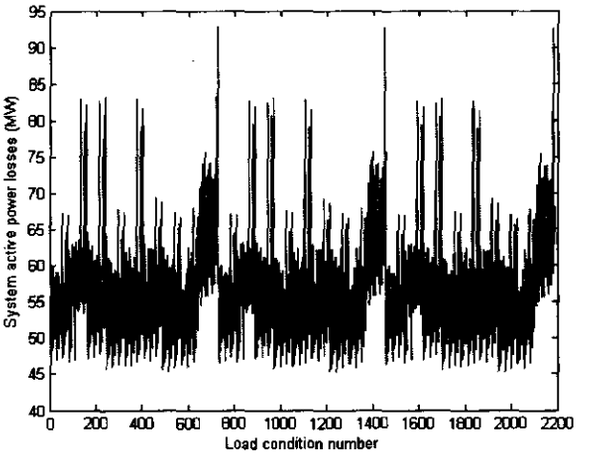

Figure 4.4 Power losses for the system versus the input state number.

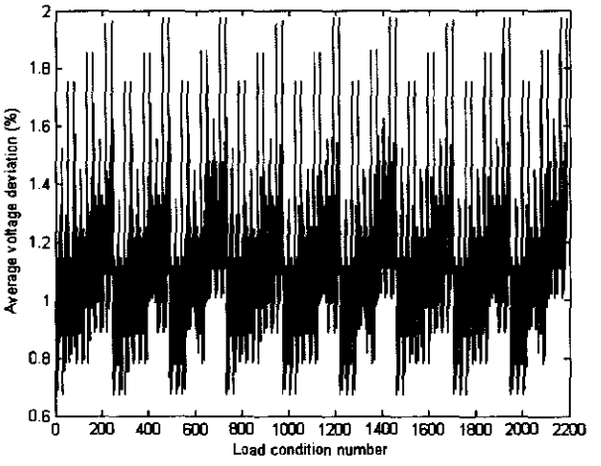

Figure 4.5 Average voltage deviations from ideal (1pu) versus the input state number.

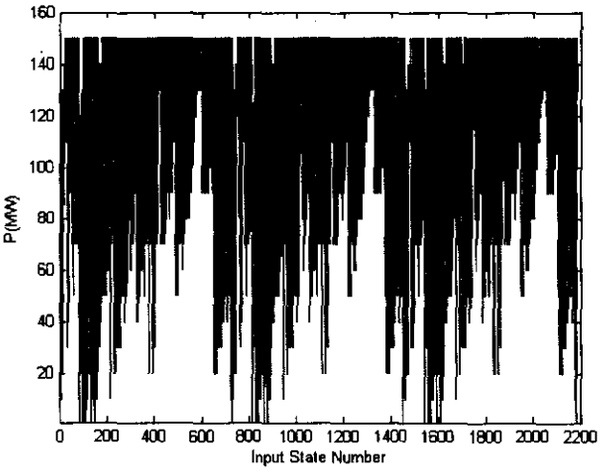

Figure 4.6 Output powers of the DGs versus the input state number.

4.4 Conclusions

The chapter describes the development of the training data for the ANN. To do this, the power system is firstly analysed and certain network parameters are measured and processed. Voltage and current magnitudes as well as phase angles are measured on each system bus. These measurements allow us to determine the active and reactive powers on each system bus. All these parameters are necessary to compute a power flow analysis of the power system. Two power flow environments are tested against each other, one in SimPowerSystems and the other with the Newton-Raphson Power Flow solution. Both these environments showed similar results and the power flow solution could be done with either. The Newton-Raphson Power Flow solution is chosen for the analysis.

The system power losses are determined with *Kron's Power Loss* formula. The loss formula is discussed and explained. The power losses of the system are used as a measurement in the cost function analysis. The cost function uses four different measurements to determine the suitability of each result. These results form the data used for the ANN training table. Sequential optimisation is used for the cost function optimisation technique. The technique allowed the cost function to test 1936 different output states for each of the 2187 input states. To minimise the different output states to only 1936, both DGs are incremented with the same generation level. If not so, the different output combinations would increase 16 times to 30 976 different output combinations for each input.

Chapter 5 - Training the ANN controller

5.1 Introduction

This chapter focuses on the use of an Artificial Neural Network (ANN) to optimally control the DGs in a power network. The ANN is firstly trained offline (not integrated in the power system) and then evaluated with the power system. The aim is mainly to let the ANN learn the generation patterns for the normalised training data. The ANN must then make decisions about optimal generation parameters for the DGs to improve system losses, bus voltage profiles and generation costs.

The internal structure of the ANN must firstly be determined, i.e. the hidden units. This ANN structure must ensure a minimum training and test error with the minimum number of epochs (training iterations). The main training data set is split into smaller data sets used for training and testing. The test data set is used to determine how well the ANN generalises for data it has not been trained with. Lastly, the ANN controller is optimised to evaluate minimum training versus maximum performance.

5.2 Compiling the training and test Data

5.2.1 Training data set

The training data set for the ANN is normalised to limit the input data to a certain domain. The data interval is limited to the domain between [0, 1]. The interval [0, 1] is thus associated with a minimum and maximum scaling or normalisation vector. Table 5.1 shows the input components and the appropriate minimum and maximum normalisation values. Table 5.2 shows a sample of the normalised input data table of the ANN. The following equation is applied to normalise the data set [27]:

$$d_{norm,i} = nv_{\min} + (nv_{\max} - nv_{\min}) \times \left(\frac{d_i - d_{\min}}{d_{\max} - d_{\min}} \right) \tag{5.1}$$

with $d_{norm,i}$ = The normalised data point;

$nv_{\min}, nv_{\max}$ = Minimum and maximum normalisation values e.g. 0 and 1;

$d_{\min}, d_{\max}$ = Minimum and maximum data point values.

It is very important to randomise the training data set, as to allow the training data set to equally represent the likelihood of each outcome. This means that the training set should contain all the dominant features of the entire input-output data space.

Component	Min. Nor. (P)	Max. Nor. (P)	Min. Nor. (Q)	Max. Nor. (Q)
Load 1	150 MW	250 MW	49.303 MVAr	82.171 MVAr
Load 2	300 MW	400 MW	98.605 MVAr	131.47 MVAr
Load 3	100 MW	160 MW	32.868 MVAr	52.589 MVAr
Load 4	200 MW	250 MW	65.737 MVAr	82.171 MVAr
Load 5	100 MW	130 MW	32.868 MVAr	42.729 MVAr
Load 6	200 MW	250 MW	65.737 MVAr	82.171 MVAr
Load 7	42 MW	50 MW	13.805 MVAr	16.434 MVAr

Table 5.1 Maximum and minimum normalisation values of the loads.

	Normalised Input Values						
	.....	**1513**	**1514**	**1515**	**1516**	**1517**	.....
Load 1 (P)	.....	0.8	0.6	1	0.8	0.8	.....
Load 2 (P)	.....	0.75	0.75	0.75	0.75	0.875	.....
Load 3 (P)	.....	0.62353	0.81177	0.62353	0.62353	0.81177	.....
Load 4 (P)	.....	1	0.89968	0.89968	0.89968	0.79936	.....
Load 5 (P)	.....	1	1	0.76786	1	1	.....
Load 6 (P)	.....	0.79936	0.79936	0.89968	0.79936	0.79936	.....
Load 7 (P)	.....	0.83728	1	1	1	1	.....
Load 1 (Q)	.....	0.8	0.6	1	0.8	0.8	.....
Load 2 (Q)	.....	0.75	0.75	0.75	0.75	0.875	.....
Load 3 (Q)	.....	0.62054	0.81027	0.62054	0.62054	0.81027	.....
Load 4 (Q)	.....	1	0.89902	0.89902	0.89902	0.79804	.....
Load 5 (Q)	.....	1	1	0.76503	1	1	.....
Load 6 (Q)	.....	0.79804	0.79804	0.89902	0.79804	0.79804	.....
Load 7 (Q)	.....	0.83148	1	1	1	1	.....

Table 5.2 Sample of the normalised input data set (load condition 1513 to 1517).

5.2.2 Test data set

When choosing a test data set to test the performance of the ANN, two important factors must be considered:

- The test set must have the same characteristics as the training set;
- The test and training sets must be mutually exclusive.

The test set must also be chosen to represent the entire input-output data space. The method used to choose a training and test set, is to generate a uniformly distributed random input-output data space. The data space is generated using Matlab's *Uniformly Distributed Random Generator* [21]. This data set is then subdivided into two mutually exclusive data sets, one for training, and one for testing. The size of the training set is much larger than the test set, typically around 70% of the entire data set. The test set is then made up of the remaining 30%. Since the entire input-output data set consists of 2187 entries, the size of test set is initially chosen as 655.

5.3 ANN structure

The structure of the ANN as discussed in chapter 2, is chosen as a multilayer feedforward network, i.e. multilayer perceptron (MLP). A MLP consist of a set of source nodes that constitute an input layer, one or more hidden layers and an output layer. The input signal propagates through the network layer by layer in a forward direction. The training of the network is done with the *error back-propagation algorithm* [15].

Firstly, the number of hidden layers and neurons must be determined. Most problems can be solved using only one hidden layer [28]. To find the optimum number of neurons in the hidden layer, two methods are used and compared. Firstly, a method named *constructive approach* or *network growing* [15] is used. The network is firstly trained with one hidden layer and one hidden neuron until the training error reaches a minimum and stabilises. The weights of the network are fixed and a hidden neuron is added. The network is retrained and tested. Eventually the training error will approach zero and the network will have learned the data exactly. This must be avoided because the network will generalise poorly for data not initially trained with. To stop adding hidden neurons, the network is tested with both the training and test data. If the performance error of both does not improve, the optimal number of neurons is reached. Adding more hidden neurons at this point, will improve the training error but to the detriment of the test error. All the training and testing of the network is done with the Neural Network Toolbox (Annexure D) in Matlab.

Table 5.3 summarises the sum squared errors of the constructive approach method and figures 5.1 - 5.8 shows the average training and test errors of some of these test runs.

No. Neurons	Hidden Layers	Epochs	Training Error	Test Error
14	1	150	3.130488	3.027082
15	1	150	5.342390	5.336285
16	1	150	3.613222	5.158387
17	1	150	3.754472	2.846106
18	1	134	2.360199	3.836269
19	1	129	1.996196	4.618863
20	1	150	3.238494	5.464665
21	1	150	3.117620	2.994529
22	1	150	4.475431	4.457668
23	1	106	1.326712	2.619345
24	1	105	1.289944	1.377203
25	1	78	2.595208	12.38539
26	1	92	1.821701	11.36163
27	1	131	2.235801	7.015050
28	1	86	2.008911	10.52061
29	1	63	3.003792	12.61006
30	1	93	1.627750	7.677910
50	1	150	1.538434	9.142491

Table 5.3 Training and test error versus number of neurons for the constructive approach method.

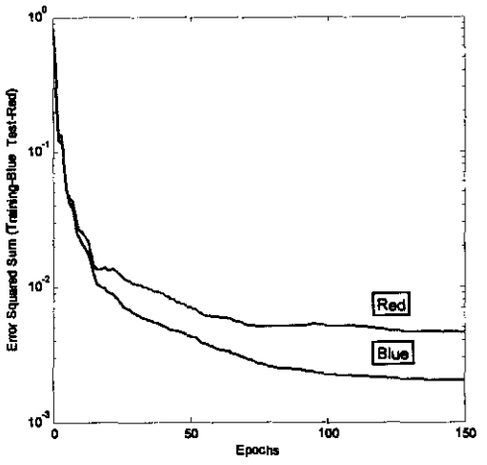

Figure 5.1 One hidden layer and 14 neurons.

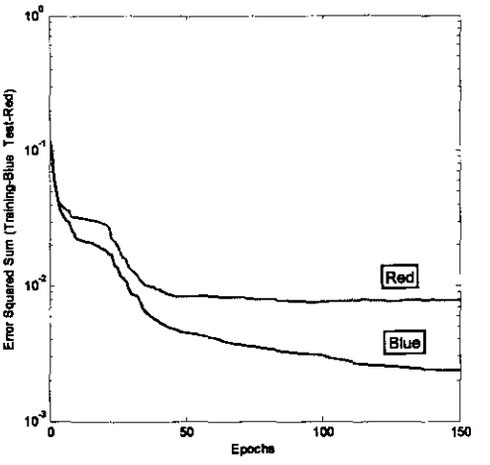

Figure 5.2 One hidden layer and 16 neurons.

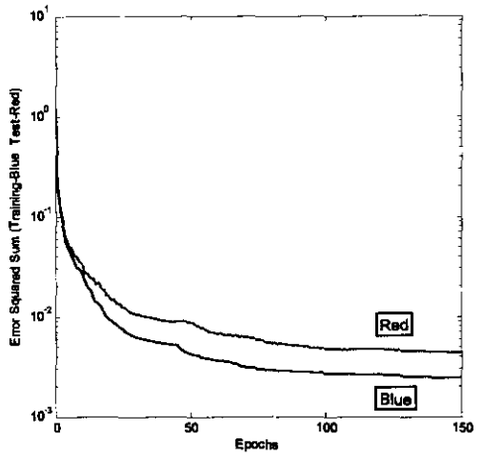

Figure 5.3 One hidden layer and 17 neurons.

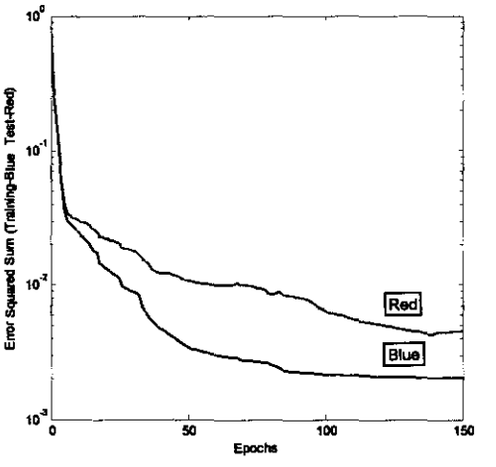

Figure 5.4 One hidden layer and 21 neurons.

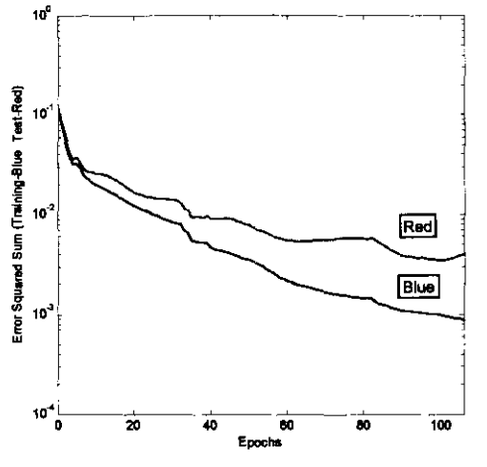

Figure 5.5 One hidden layer and 23 neurons.

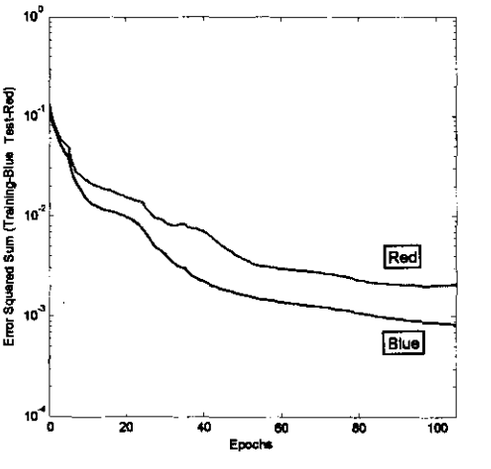

Figure 5.6 One hidden layer and 24 neurons.

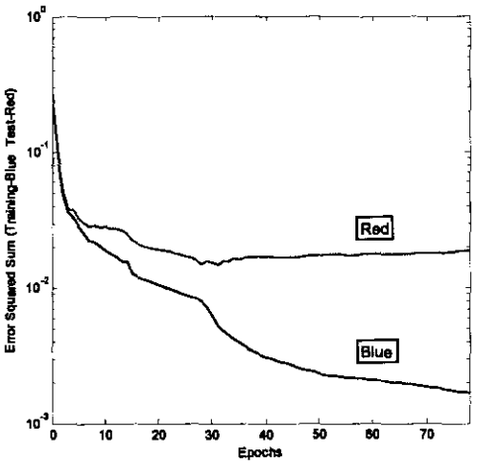

Figure 5.7 One hidden layer and 25 neurons.

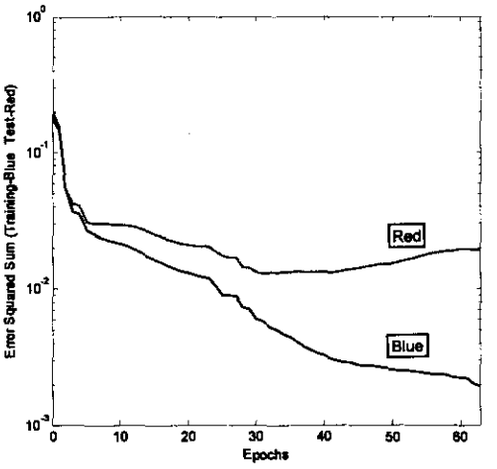

Figure 5.8 One hidden layer and 29 neurons.

Secondly, a method named the *leave-one-out method* is used [15]. The data set of (n - 1) examples are used to train the model, and the example left out is used to test the model. The training and testing is repeated for a total of n times (n is the number of examples in the entire data set), each time using a different test example. The training and testing error is then averaged over the n trial runs. The experiment is repeated for different numbers of neurons in the hidden layer. Figure 5.9 shows an illustration of the leave-one-out method.

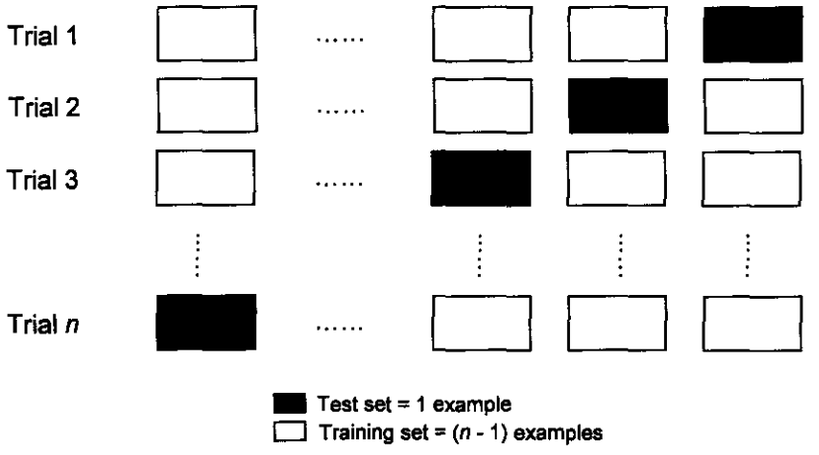

Figure 5.9 Illustration of the leave-one-out method.

Table 5.4 summarises the results of the leave-one-out method. The experiment is repeated for the same number of hidden neurons as for the constructive approach method summarised in table 5.3.

No. Neurons	Hidden Layers	Epochs	Training Error	Test Error
14	1	150	5.846112	11.57319
15	1	150	6.066413	20.11636
16	1	150	2.225536	18.13105
17	1	150	4.112041	5.502327
18	1	150	5.861585	5.846726
19	1	150	3.242324	3.943034
20	1	150	2.365254	20.71135
21	1	150	3.415287	15.01456
22	1	150	2.024997	2.270819
23	1	150	1.906267	2.623078
24	1	150	0.886568	1.271093
25	1	150	6.691622	24.49372
26	1	150	1.941044	9.931765
27	1	150	46.03966	44.08936
28	1	150	21.17224	13.66526
29	1	150	0.976956	1.894915
30	1	150	23.87464	16.98764

Table 5.4 Training and test error versus number of neurons for the leave-one-out method.

Table 5.3 and 5.4 shows that the optimum structure for the ANN is 14:24:4 representing 14 input layer neurons, 24 hidden layer neurons and 4 output layer neurons. Figure 5.10 shows a graphical representation of the ANN.

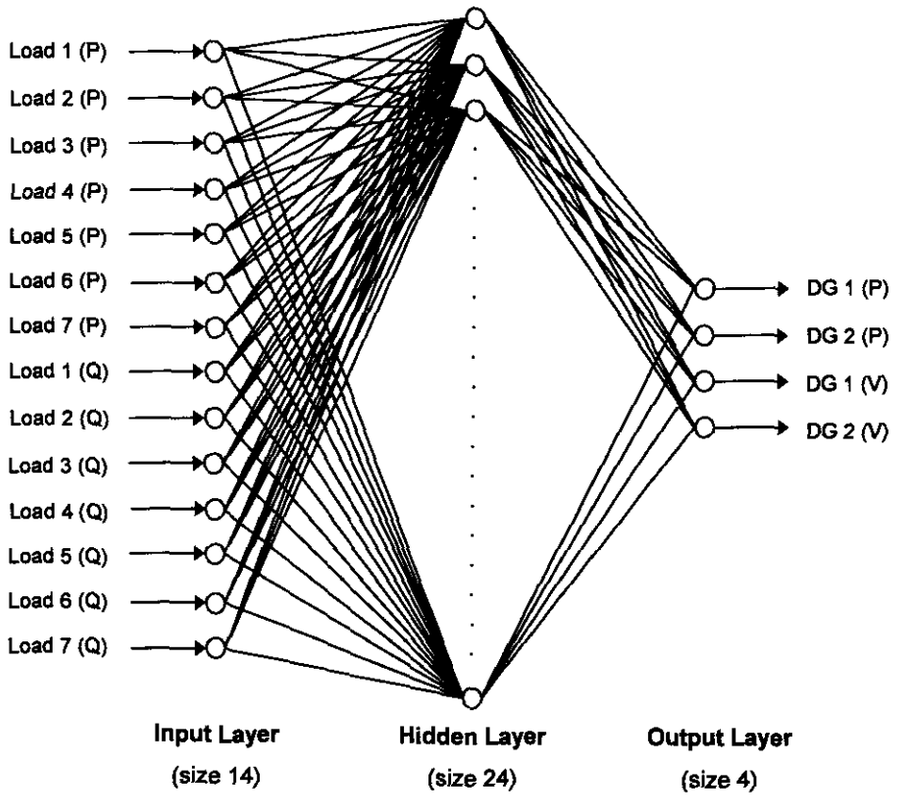

Figure 5.10 ANN structure.

5.4 Training the ANN

The training of the ANN is done off-line with Matlab. As discussed in section 5.2, the training data developed in chapter 4 are used for the training of the ANN. Finding the optimum training point of the ANN is done with the following procedure:

- The ANN is trained until the test error reaches a minimum whilst the training error is still decreasing;
- Test the ANN with several smaller new test sets.

Figure 5.11 graphically illustrates this training process in terms of the training and test errors.

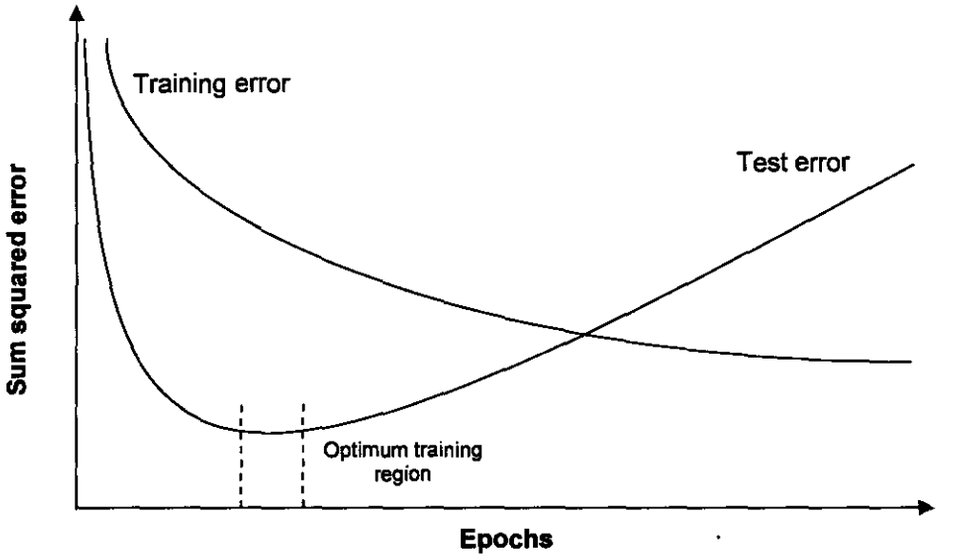

Figure 5.11 Training process in terms of the training and test errors.

The training error is defined as the sum of the squared errors between the output of the ANN and the desired target values for each output neuron over the entire training data set [15]. The test error is determined similarly between the test output of the ANN and the desired test values. The average training and test errors are the average of the training and test errors. This means that for four output neurons the test and training errors is the sum squared errors for each of the four output neurons over the test and training sets. The following equations show the training and test errors:

$$Training\ error = \sum_{i=1}^{1532}\sum_{j=1}^{4}\left(e_{ij(desired)} - e_{ij(ANN)}\right)^2 \tag{5.2}$$

with $e_{ij(desired)}$ the desired output of neuron j for the i^{th} training input value;

$e_{ij(ANN)}$ the ANN output of neuron j for the i^{th} training input value.

$$Test\ error = \sum_{i=1}^{655}\sum_{j=1}^{4}\left(e_{ij(desired)} - e_{ij(ANN)}\right)^2 \tag{5.3}$$

with $e_{ij(desired)}$ the desired output of neuron j for the i^{th} test input value;

$e_{ij(ANN)}$ the ANN output of neuron j for the i^{th} test input value.

To show the training process of the ANN, the average training and test errors are recorded for the ANN developed in section 5.3. Figure 5.12 shows the average training and test errors of the network plotted against the number of epochs. To show the average test error on a more visible scale, the error is plotted in figure 5.13 with a restricted range.

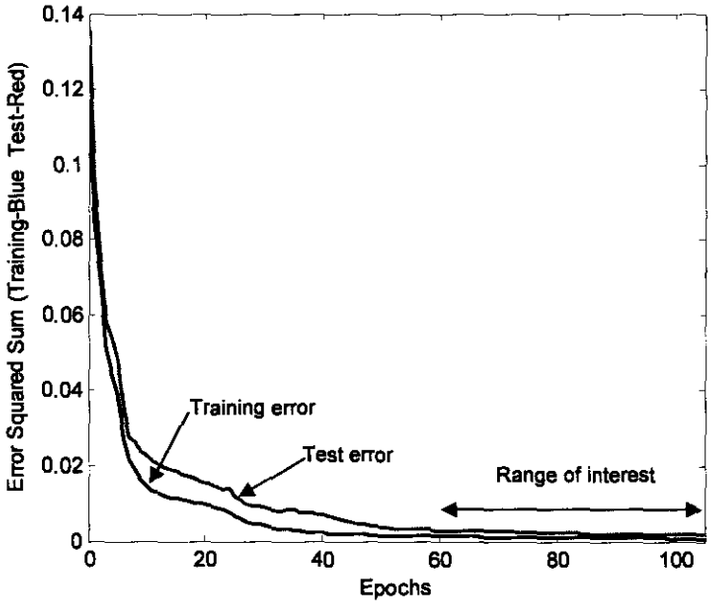

Figure 5.12 Average training and tests errors of the ANN versus the number of epochs.

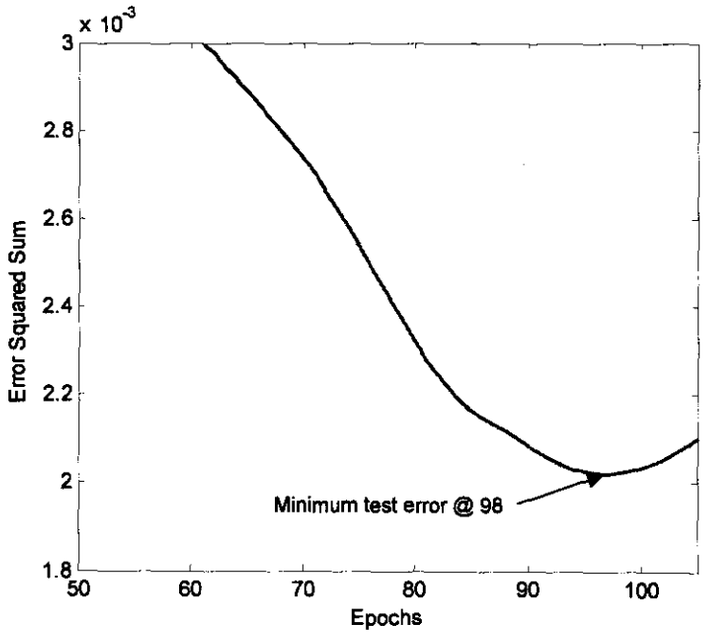

Figure 5.13 Average test error versus the number of epochs (restricted range).

To determine the optimum point of training, the ANN weights and biases are recorded for a few points beyond the point of the minimum test error. Table 5.5 shows the results of the training and test errors of these points.

Point	Training Error	Test Error
98(min. test error)	1.354885	1.324148
101	1.327263	1.333187
104	1.304069	1.354933
107	1.289974	1.377203

Table 5.5 Training data recorded for selected points beyond the minimum test error.

The weights and biases of these points can now be used for further evaluation of the ANN model. To verify the contents of the training data set, the ANN model is now tested with 100 random test sets, each of size 100. Figure 5.14, 5.15, 5.16 and 5.17 show the results of the average test errors for the different points.

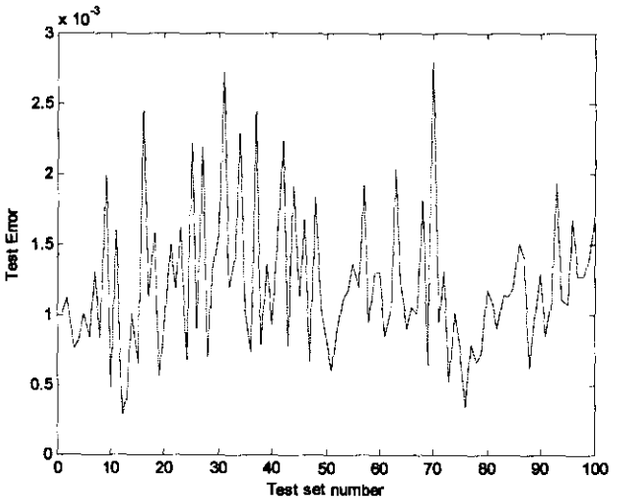

Figure 5.14 Average test errors versus test set numbers (weights and biases at point 98).

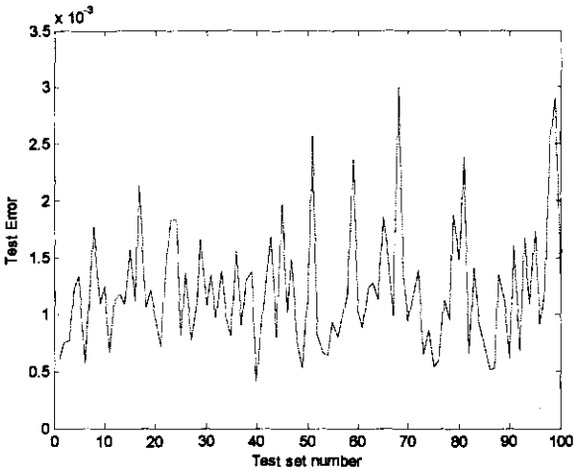

Figure 5.15 Average test errors versus test set numbers (weights and biases at point 101).

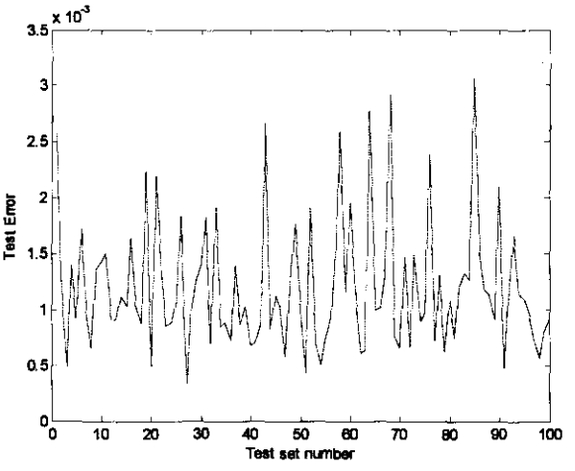

Figure 5.16 Average test errors versus test set numbers (weights and biases at point 104).

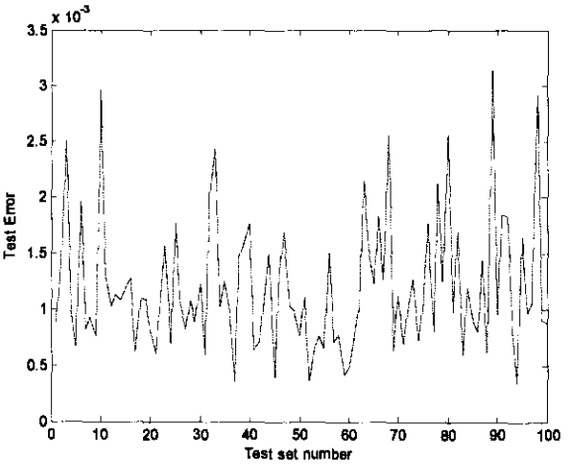

Figure 5.17 Average test errors versus test set numbers (weights and biases at point 107).

Table 5.6 summarises the results for the different points recorded in terms of the average and maximum test errors for the 100 test sets.

Point	Average Test Error (10e-3)	Maximum Test Error (10e-3)
98	1.2092	2.7903
101	1.2081	3.0049
104	1.2026	3.0644
107	1.1941	3.1382

Table 5.6 Results of the smaller test sets.

The results obtained from the different points show that there is no extreme test errors for the 100 smaller test sets. It shows that the contents of the training data set include all the dominant components of the DGs output space. From the results summarised in table 5.6, the optimum point of training of the model is not so easily seen. The results show that for points beyond the minimum test error, the average test error becomes smaller but to the detriment of a larger maximum test error. The point of minimum test error, i.e. 98, is thus used for further evaluation.

5.5 Optimisation of the ANN

This section aims at optimising the ANN controller with regards to the following:

- the training data set;
- the training parameters.

Optimising the controller means improving its performance. The back-propagation used in this section to train the ANN model, is based on minimising its cost function defined as the sum of the squared errors. The importance of this criterion is the ability of the network to generalise and its mathematical tractability [15]. A good ANN with minimum size is less likely to learn the noise in training data and may thus generalise better for new data. Also, improving the training data and training parameters of the model can improve the performance of the ANN controller. Improving the performance of the controller means minimising the training and test errors, thus improving the ability of the ANN controller to generalise.

5.5.1 Training data

To find the optimum training region in the data set (training and test errors a minimum), a process known as the hold-out method is used [15]. The entire data set of n examples is divided into k subsets, with $k > 1$. The model is then trained with $(k - 1)$ of the subsets and tested with the remaining subset for each of the k subsets. The performance of the model is assessed by averaging the test errors over all the subsets. Figure 5.18 illustrates the hold-out method for 5 subsets.

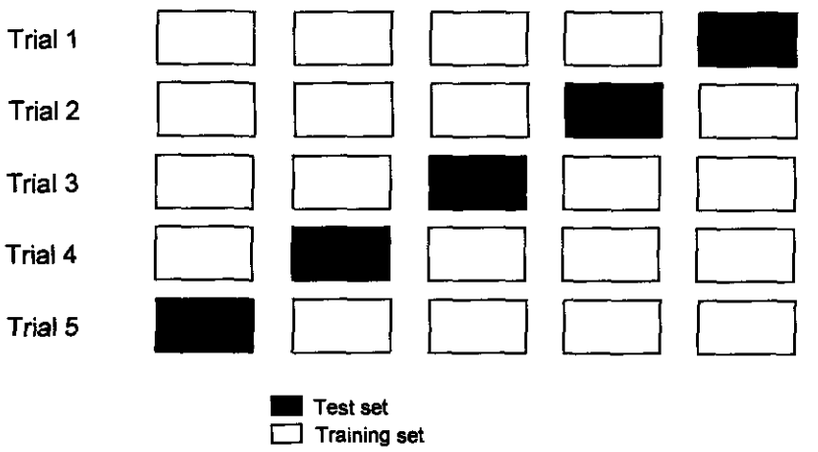

Figure 5.18 Illustration of the hold-out method.

For a data set size of 2187 examples, 9 subsets are selected for evaluation. Table 5.7 shows the results of the 9 trials and figure 5.19 the results of the selected subset with the best training and test errors.

Run no.	Average Training Error (10e-3)	Average Test Error (10e-3)	Average Minimum Test Error (10e-3)
1	1.1952	7.1226	4.8548
2	1.7252	7.0812	6.7846
3	1.0131	7.8964	2.8401
4	0.5852	2.0734	1.9801
5	2.6498	7.4807	7.1270
6	0.6673	6.3094	2.2529
7	0.8767	4.1989	4.1989
8	1.2294	21.573	7.4713
9	0.9128	4.2179	3.5167

Table 5.7 Average training and test errors for 9 different subsets.

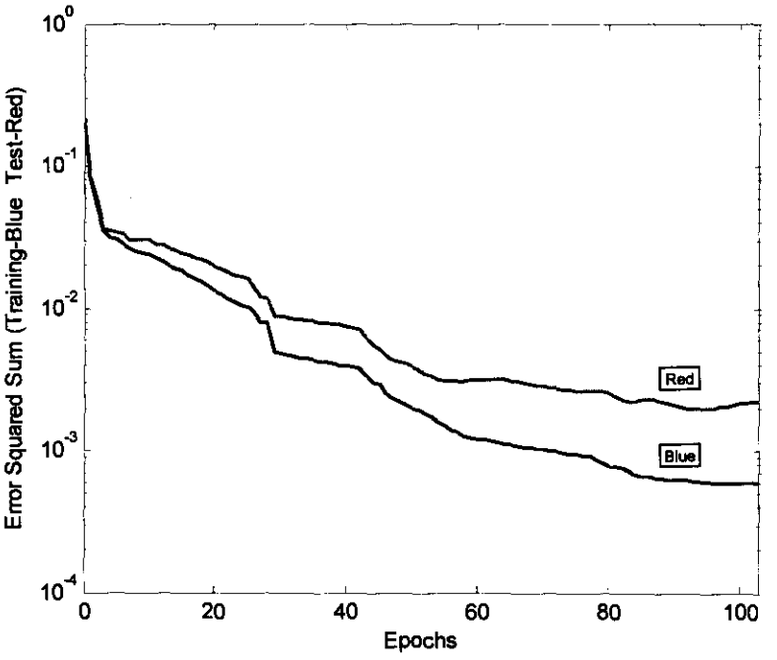

Figure 5.19 Average training and test errors for subsets no.4.

From the results shown in table 5.7 it is observed that the best training data set is no. 4 and that there is clearly a difference in the average training and test errors for the different subsets. Table 5.8 shows the improvement of the network outputs.

Training Set	Epochs	Training Error	Minimum Test Error
Old	98	1.3548851	1.324148
New	95	0.8965264	1.296965

Table 5.8 Network outputs for the new and old training sets.

To verify the contents of the new training data set, the ANN model is also tested with the 100 random test sets, each of size 100. Figure 5.20 shows the results of the average test errors for the new training set.

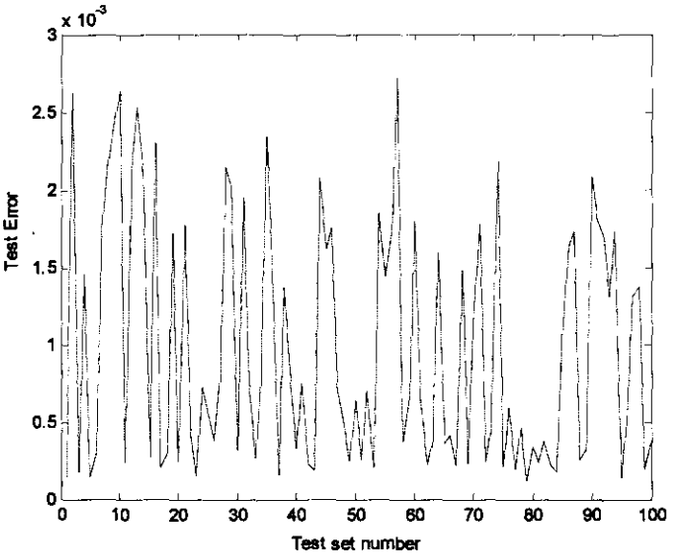

Figure 5.20 Average test errors versus test set numbers for 100 smaller test sets.

Table 5.9 summarises the results for the new training set in terms of the average and maximum test errors for the 100 smaller test sets.

Training Set	Average Test Error (10e-3)	Maximum Test Error (10e-3)
Old	1.20920	2.7903
New	0.98627	2.7276

Table 5.9 Results of the smaller test sets for the new and old training sets.

The results obtained from the 100 smaller test sets show that there are no extreme test errors. It is thus also concluded that the contents of the new training data set include all the dominant components of the DGs output space. The results summarised in table 5.8 and 5.9 shows that the new training set has smaller training and test errors and also revealed a decrease in the average and maximum test errors for the smaller test sets.

5.5.2 Model parameters

The back-propagation algorithm used in the training of the ANN provides an 'approximation' to the trajectory in its weight space. The delta rule for the correction $\Delta w_{ji}(n)$ applied to the synaptic weight connecting neuron *i* to neuron *j* is given by:

$$\Delta w_{ji}(n) = \alpha \Delta w_{ji}(n-1) + \eta \delta_j(n) y_i(n) \tag{5.4}$$

with η the learning-rate parameter and α the momentum constant.

The signal-flow diagram illustrating the effect of the learning-rate parameter and momentum constant is shown in figure 5.21.

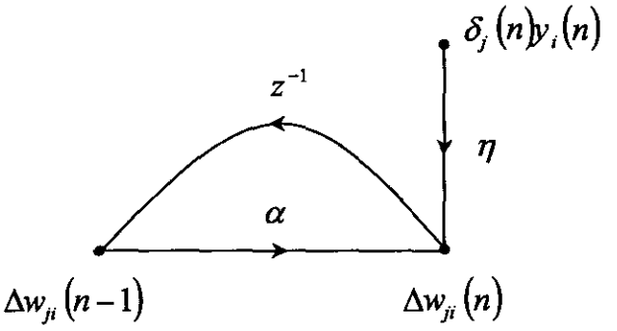

Figure 5.21 Signal-flow diagram of the delta rule.

The smaller we make the learning-rate parameter, the smoother the trajectory will be in weight space. This improvement is attained at the cost of a slower learning rate. The bigger we make it, the faster the learning process, but the network may become unstable (oscillatory). This problem is overcome by including the momentum constant. The inclusion of the momentum constant results in the following:

- it tends to accelerate descent;
- it has a stabilizing effect;
- it prevents the learning process from stopping in a small minimum on the error surface.

Using the 14:24:4 ANN and combinations of the learning-rate parameter $\eta \in \{0.01,0.1,0.5,0.9\}$ and momentum constant $\alpha \in \{0.01,0.1,0.5,0.9\}$, the network is simulated to find the best learning curves. Figure 5.22 shows the results of the average training and test errors of the best four combinations and table 5.10 summarises the results.

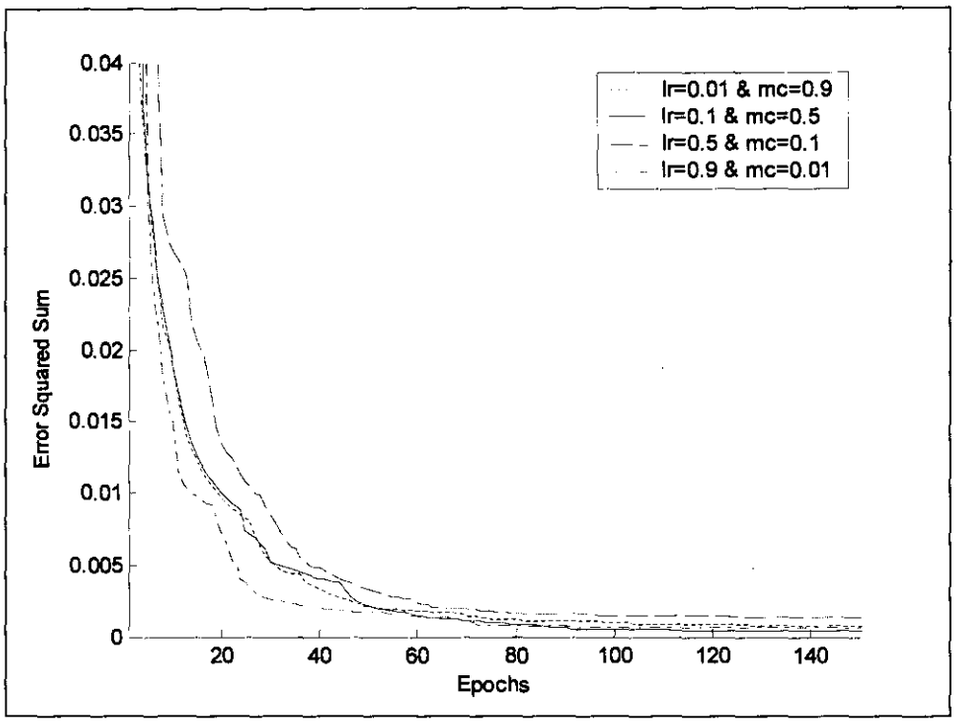

Figure 5.22 Learning curves of the network.

Combination	Learning-rate	Momentum	Training Error	Test Error
1	0.01	0.9	1.153125676	15.60734
2	0.1	0.5	0.645741064	1.242207
3	0.5	0.1	2.025089520	1.935787
4	0.9	0.01	0.947198832	12.83407

Table 5.10 Results of the learning-rate parameter and momentum constant combinations.

Table 5.11 shows the improvement of the network outputs (learning-rate = 0.1 and momentum constant = 0.5).

Training Set	Epochs	Training Error	Minimum Test Error
Old	95	0.8965264	1.296965
New	150	0.6457411	1.242207

Table 5.11 Network outputs for the new and old network parameters.

To verify the contents of the new network parameters, the ANN model is also tested with the 100 random test sets, each of size 100. Figure 5.23 show the results of the average test errors for the new network parameters.

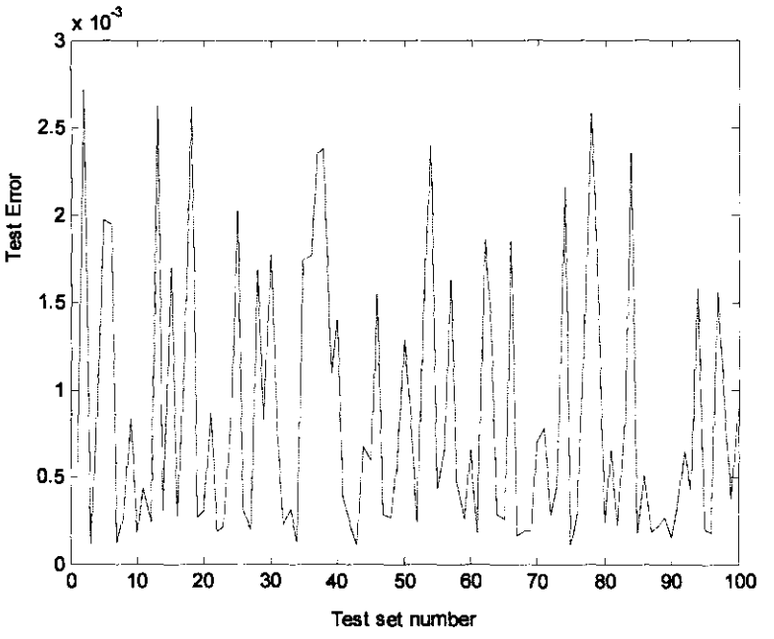

Figure 5.23 Average test errors versus test set numbers for 100 smaller test sets.

Table 5.12 summarises the results for the new training parameters in terms of the average and maximum test errors for the 100 smaller test sets.

Parameters	Average Test Error (10e-3)	Maximum Test Error (10e-3)
Old	0.98627	2.7276
New	0.87622	2.7125

Table 5.12 Results of the smaller test sets for the new and old training sets.

The results obtained from the new parameters showed that a smaller learning-rate parameter η resulted in a slower convergence, but it reached a smaller local minimum in the error surface. The use of a big learning-rate parameter and momentum constant α caused oscillation in the error surface and a higher value for the error at convergence. The best learning curve selected showed a smaller sum squared error, but took longer to converge to a minimum. As training of the ANN is done off-line and speed of convergence is not an issue, this curve is selected as the optimal learning curve of the model. The new network parameters summarised in table 5.11 and 5.12 shows that the new training set has smaller training and test errors and also revealed a decrease in the average and maximum test errors for the smaller test sets.

5.6 Conclusions

The training of the ANN is done off-line in this section and the performance of the model is evaluated. The training of the model suggested that it is good practice to check the system against data that it is not trained with. This practice improved the generalisation of the network for data not trained with. If the ANN is trained to an absolute minimum in the training error, the network showed good response to the data trained with, but made bad decisions upon new data. This is a typical characteristic of poor generalisation.

The ANN structure is determined by means of two methods, the *constructive approach* method and the *leave-one-out* method. Both these methods suggested that the best response of the network is with 24 neurons in the hidden layer. This structure showed a minimum in the error squared sum of the training and testing data. The network is tested against smaller test sets to evaluate the generalisation of the model. These tests showed similar results and it is concluded that the training data of the network included all the components of the DGs output space.

The network is finally optimised to improve the performance of the model. Firstly, the data set is divided into subsets by the *hold-out method* and trained with new subsets. This method showed that

the network performance in terms of the different training subsets improved. By selecting the correct training data, the sum squared errors of both the training and testing improved. Secondly, the network learning parameters are varied and the results showed that the model showed different learning curves with the different combinations of parameters. The improved learning curve showed better training and test errors.

The overall results of the model are satisfactory, but it still leaves much room for improvement. Further improvements would be to obtain better training and testing errors and train the system with real life data from the network, rather than simulated data. For the scope of this project, the model is feasible and the controller can be implemented in the power system.

Chapter 6 - Evaluation of the cost function and ANN controller

6.1 Introduction

The focus of this chapter is the evaluation of the Artificial Neural Network (ANN) controller controlling two optimally placed DGs in a power network. The power network modelled in chapter 3, serves as the basis for this analysis. The power network is characterised by large loads (in the MW region) switching on and off the grid, which results in undervoltages and overvoltages at certain points in the system. This power quality (PQ) problem is rectified by controlling the power flow in the network and thus regulating the voltage levels.

Chapter 4 showed that the optimal generation and voltage levels are determined by the active and reactive power drawn by the loads. As the active and reactive power consumed by the loads change, the DGs power and voltage levels determined by the ANN also changes. The optimal condition of the network is determined by means of a cost function developed in chapter 4. The behaviour of the ANN controller is also evaluated for operating states (load conditions) beyond the training region as well as the operating states trained with. These results will give an overall indication of the performance of the ANN controller.

This chapter is based on simulation only, as constructing a laboratory scale power network with two controlled DGs is not feasible. The latter is however not the objective of the project.

6.2 Integration of the ANN controller in the power system

The power system model illustrated in figure 3.1 of chapter 3 is used as basis for the analysis. The optimised 14:24:4 ANN (representing an ANN structure with 14 input layer neurons, 24 hidden neurons and 4 output neurons) developed in chapter 5 is used in the evaluations. The power network consists of seven linear loads with a total switching capacity of 398 MW. The two DGs are placed at optimal points in the network to control certain PQ parameters as shown in figure 3.4 of chapter 3. The ANN controller is integrated in the power system with regards to the following:

- Inputs - Measuring the PQ busses (loads);
- Outputs - Controlling the PV busses (DGs).

The power system is divided into two distinct radial transmission feeders. The switching capacity is divided as follows: 100 MW on the slack bus, 160 MW on feeder 1 and 138 MW on feeder 2. Figure 6.1 shows a line diagram of the power network with the integrated ANN controller.

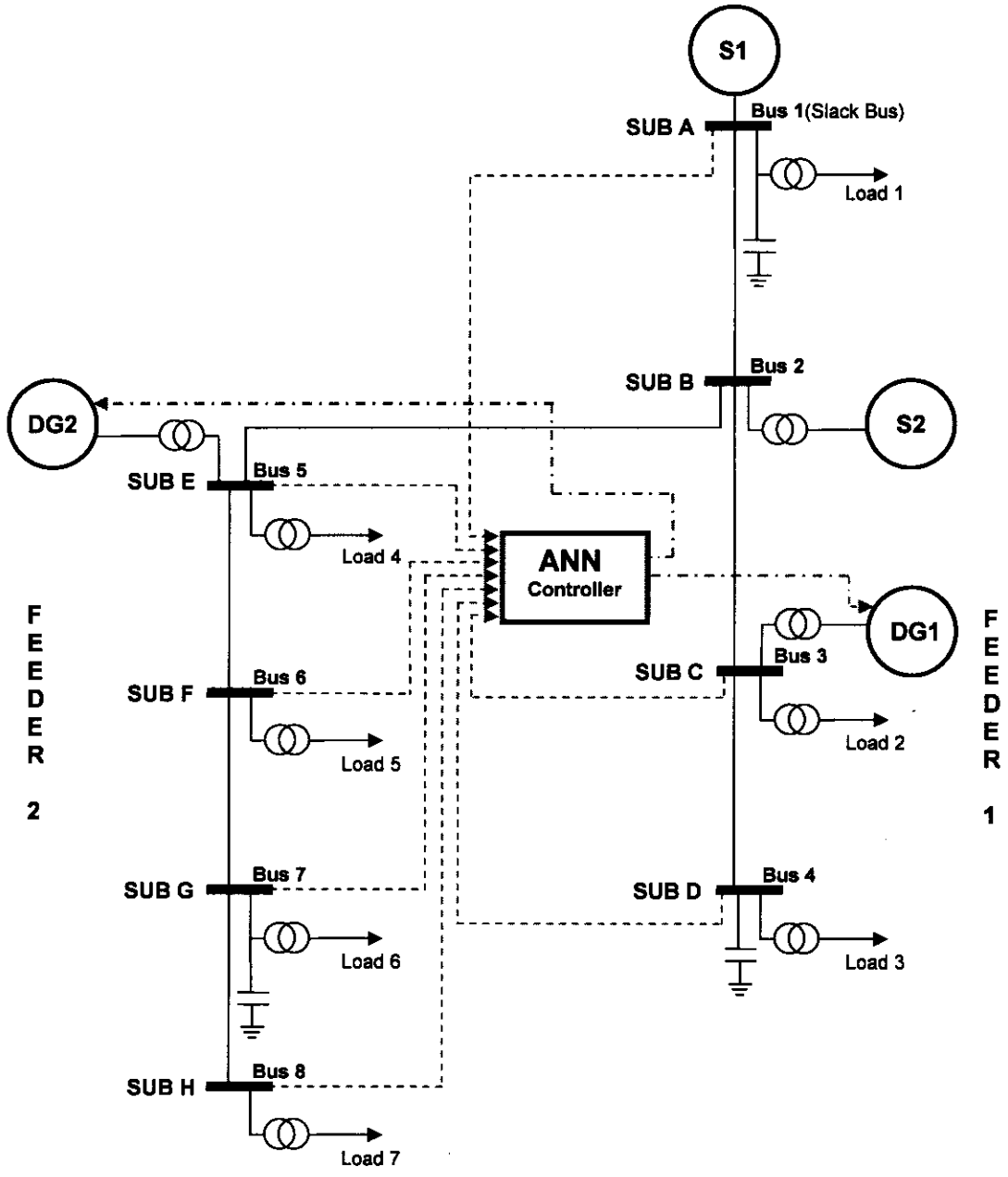

Figure 6.1 Line diagram of the power network with the integrated ANN controller.

6.3 Evaluation of the cost function

6.3.1 No DGs connected to power petwork

The cost function (CF) developed in chapter 4 selects the optimal control parameters for the DGs for a specific load condition. As discussed in chapter 4, the power system parameters are measured on each busbar in the system. The cost function then uses four objective functions to select optimal control parameters to improve the network conditions. The power network is firstly analysed without any voltage regulation (no DGs) with the loads switching over the entire spectrum of load capacity (transformer tap changers are fixed at 1 pu). The transformer tap changers are not used as control variables, as the effect of regulation and control with DG is investigated in this project. Figures 6.2 - 6.4 shows the CF objective functions over the load-switching spectrum. The blue figures visualise the CF objective functions as behavioural patterns of the load conditions and the red figures show the objective functions for increasing active power drawn by the loads (sum of all active power).

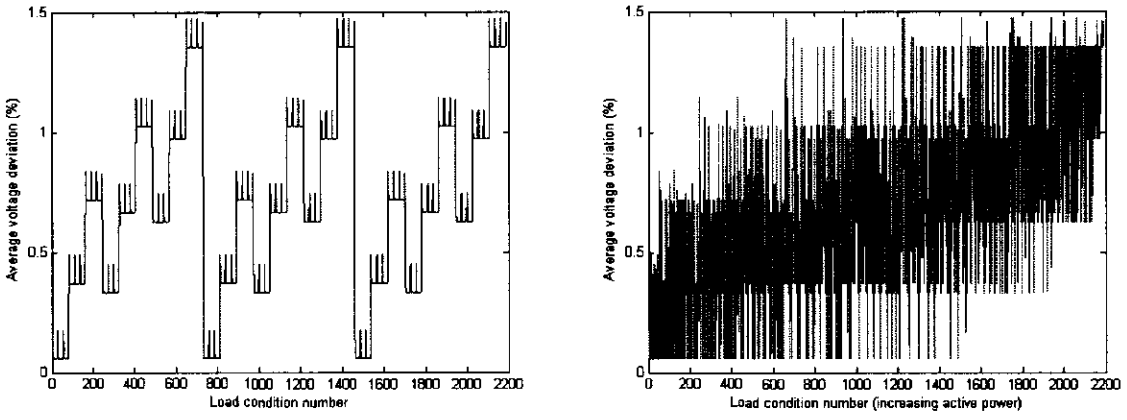

Figure 6.2 Average voltage deviations from permitted range (0.95 pu - 1.05 pu) (no DG).

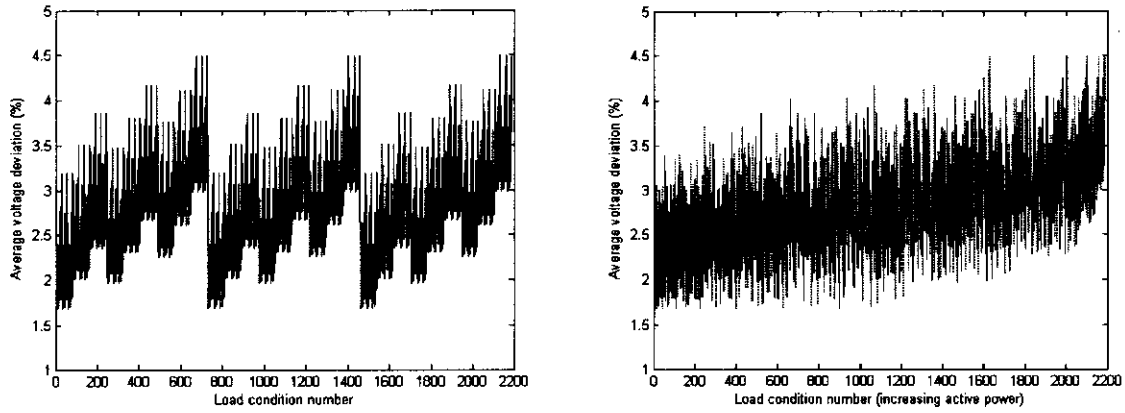

Figure 6.3 Average voltage deviations from ideal (1pu) (no DG).

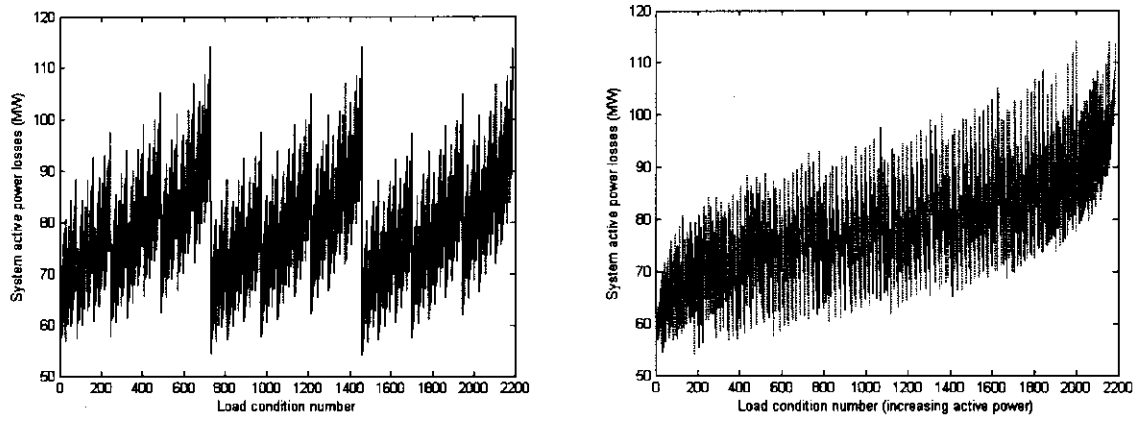

Figure 6.4 System active power losses (no DG).

From figures 6.2 - 6.4 (blue), three distinct sub-patterns are identified in each of the figures. These sub-patterns correspond to the three distinct levels of active power drawn by each load. Figures 6.2 - 6.4 (red) shows the objective functions against the load number for increasing active power. Load condition 0 is the minimum power drawn by the loads, i.e. 1092 MW and load condition 2188 is the maximum power drawn by the loads, i.e. 1490 MW. These figures give a better indication of what is happening in the power network with increasing power drawn by the loads. The voltage levels on feeder 1 results in undervoltages throughout the increase in power. Feeder 2 however shows under- and overvoltages throughout the increase in power. This was expected as there is no voltage regulation from the sources and onwards. Table 6.1 shows a summary of the line parameters for the two transmission feeders:

Parameter	Feeder 1	Feeder 2
L_{Total}	179 km	489 km
R	0.062 Ω/km	0.062 Ω/km
X	0.32 Ω/km	0.32 Ω/km
B	3.621e-6 mili mho/km	3.614e-6 mili mho/km
$V_{L\text{-}L}$	275 kV	275 kV
$\text{Load}_{(Min)}$	421 MVA	570 MVA
$\text{Load}_{(Max)}$	590 MVA	716 MVA

Table 6.1 Line parameters for the two transmission feeders.

To verify the results, the program **linepref** [18] is used to simulate the voltage profiles of the two transmission feeders with the line parameters given in table 6.1. Figures 6.5 and 6.6 show the results of the simulations.

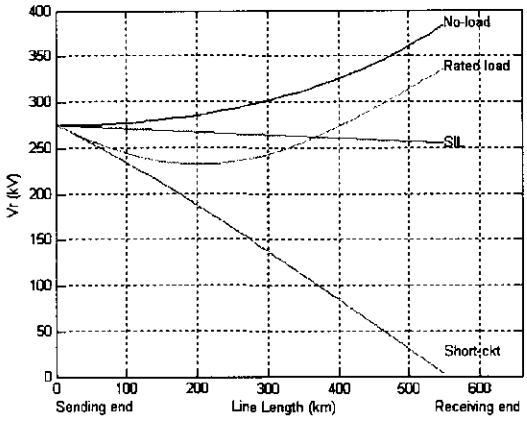

Figure 6.5 Voltage profile of feeder 1.

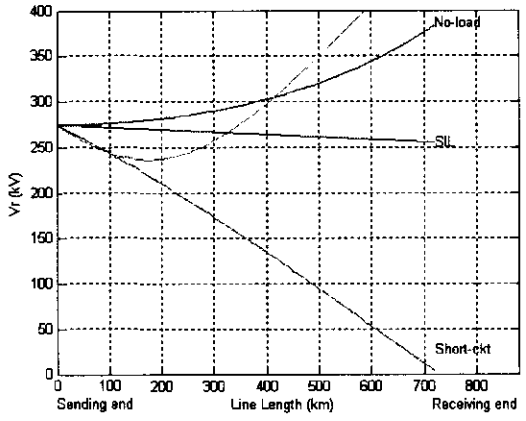

Figure 6.6 Voltage profile of feeder 2.

The simulations (light blue - Rated load) verify the results obtained by the cost function. Feeder 1 shows undervoltages at the end of the feeder (179 km from the source) for the given load condition. Feeder 2 however shows undervoltages close to the source, but overvoltages at the end of the feeder (489 km from the source). The system active loss pattern also shows a definite incline in the losses with the increase in load. This is because of larger currents drawn by the loads that results in the heating of lines and transformers. Proper voltage regulation is thus necessary to control under-and overvoltages in the network and reduce system losses. Reducing the system losses will prolong the life of network components.

Table 6.2 shows the bus voltage profiles of the power network with no DGs. It can be noticed that some system busses exceed the permissible limit of voltage drop up to 11.72 %. The average voltage drop for buses 3 and 4 is below the permitted range. The percentage of load conditions in the permitted range in table 6.2 reveals that only three of the eight buses stay within limits over the entire switching spectrum, and that the voltage profile of one bus never gets to the permissible range. This drop must be reduced within acceptable limits with the aid of DG and proper control.

Bus no.	Bus Voltage (kV)	Average Voltage Drop % (no DG, no tapping)	Maximum Voltage Drop/Rise % (no DG, no tapping)	In Range %
1	275	0	0	100
2	275	0	0	100
3	275	6.96	9.1	11.11
4	275	8.45	11.72	0
5	275	0	0	100
6	275	1.81	5.5	92.59
7	275	0.35	5.35	96.29
8	275	0	5.94 (rise)	88.89

Table 6.2 Bus voltage profiles of the power network with no DGs and no tapping.

6.3.2 DGs connected to power network with no control

To illustrate the effect of DG units in the power network, two DGs are connected to the network at proper positioning points as determined in chapter 3. The results for this paragraph are obtained with the DGs running at full capacity with no control. With no control, the output active power is set to the maximum capacity of the DG and the terminal voltage is set to 1 pu. The load conditions are varied over the same switching spectrum as used in sections 6.2 and 6.3.1. Figures 6.7 - 6.9 shows the CF objective functions over the load-switching spectrum for the network with two DGs running at full capacity. Table 6.3 shows a comparison between the network with no DGs and the network with DGs.

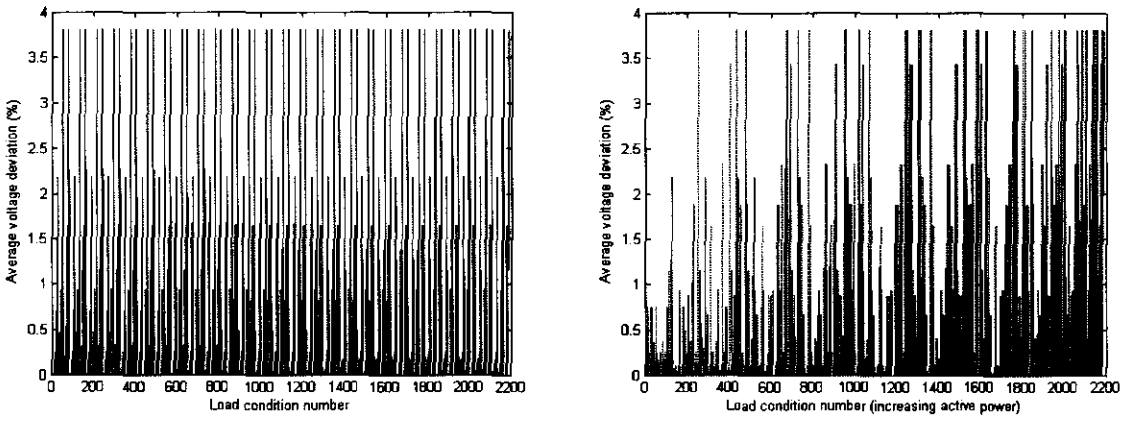

Figure 6.7 Average voltage deviations from permitted range (0.95 pu - 1.05 pu) (DG, no control).

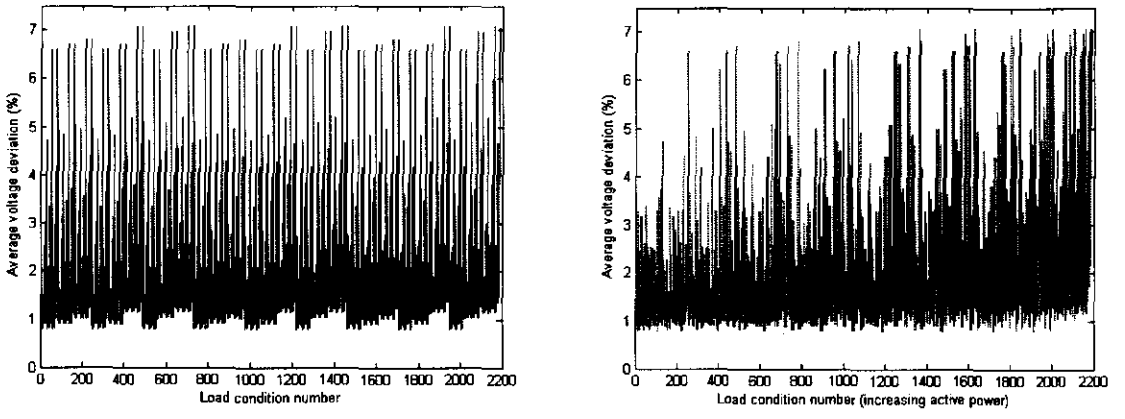

Figure 6.8 Average voltage deviations from ideal (1pu) (DG, no control).

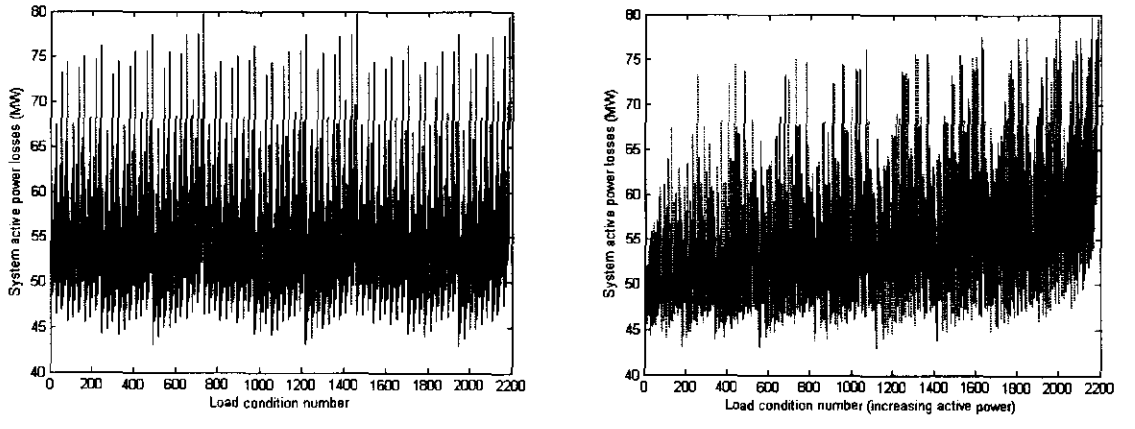

Figure 6.9 System active power losses (DG, no control).

Network (all busses)	Average voltage deviation (permitted range) (%)	Average voltage deviation (ideal) (%)	Power losses (MW)
No DGs	0.6898	2.8176	78.7110
2 DGs(no control)	0.3097	1.9743	54.7117

Table 6.3 Comparison between the networks with no DGs and two DGs with no control.

With the two DGs connected to the network, it is more difficult to identify the sub-patterns in figures 6.7 to 6.9 (blue). The figures (red) also reveal that there is a definite increase in the maximum voltage deviation and network active losses with the increase in load. The average voltage deviation from the permitted range rise to a maximum of 3.8%, mostly because of overvoltages at buses near the DGs and undervoltages at buses far from the DGs. This is an increase of 2.3%, whilst the deviation from ideal increased with 2.5%.

Table 6.3 shows that there is a decrease in the average deviation from the system with no DGs. The most positive effect of the DGs on the system is the decrease in the average power losses of 24 MW. Because the DGs are modelled as PV busses, they influence the flow of active and reactive powers in the network. The power flow simulations show a decrease in active and reactive power flows from the two main sources, thus a decrease in the network losses. The power losses at maximum load capacity also reveals a decrease from 115 MW to only 80 MW.

Table 6.4 shows the bus voltage profiles of the power network. The results show that the DGs bring feeder 1 within the permissible limits and that the average voltage drop for busses 3 and 4 is reduced by almost 6.5%. The DGs however degrade the performance of feeder 2. The percentage of load conditions within range is reduced by almost 15% for busses 6, 7 and 8. This is because of a maximum voltage drop increase of almost 10%. These large voltage drops are observed for the last few maximum load capacities.

The percentage of load conditions in the permitted range however reveals that five of the eight buses are now within limits. With the proper control of the DGs, busses 6, 7 and 8 can also be kept within the permissible limits. The bus average voltage drop/rise statistics show that all the busses have better voltage profiles, except for the few large load conditions. The implementation of the two DGs in the network shows that the network conditions, i.e. power losses and voltage profiles had successfully been improved.

Bus no.	Bus Voltage (kV)	Average Voltage Drop/Rise % (2 DGs, no tapping)	Maximum Voltage Drop/Rise % (2 DGs, no tapping)	In Range %
1	275	0	0	100
2	275	2.45 (rise)	3 (rise)	100
3	275	0.3	1	100
4	275	1.5	3.1	100
5	275	0.6	5	100
6	275	2.82	14.5	79
7	275	1.5	15.7	77.77
8	275	0	15.25	73.25

Table 6.4 Bus voltage profiles of the power network with two DGs with no control.

6.3.3 DGs connected to power network with cost function control

In section 6.3.2, the effect of the two DGs with no control is investigated. It revealed that some network parameters improved whilst others worsened. The need for control of the DGs is thus important. The results of this paragraph illustrate the effect of the DGs on the network with the proper control. The CF derived in chapter 4 is used to determine the optimal network conditions for a specific load condition and selects the best possible control parameters for each of the DGs. The DGs active power and terminal voltage are controlled as determined in chapter 3. The load conditions are varied over the same switching spectrum as used in sections 6.2 and 6.3.1. Figures 6.10 - 6.12 shows the CF objective functions over the load-switching spectrum for the two DGs with CF control. Table 6.5 shows a comparison between the network with DGs with no control and with CF control.

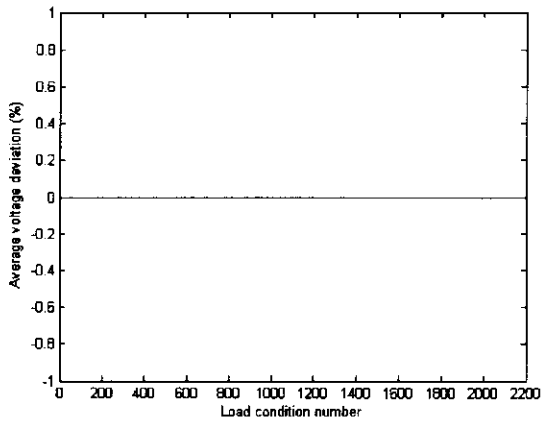

Figure 6.10 Average voltage deviations from permitted range (0.95 pu - 1.05 pu) (DG, CF control).

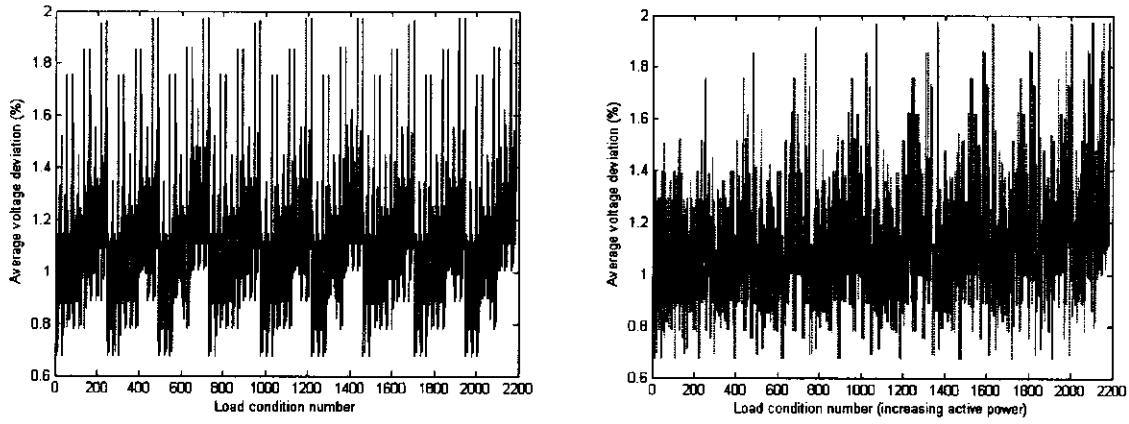

Figure 6.11 Average voltage deviations from ideal (1pu) (DG, CF control).

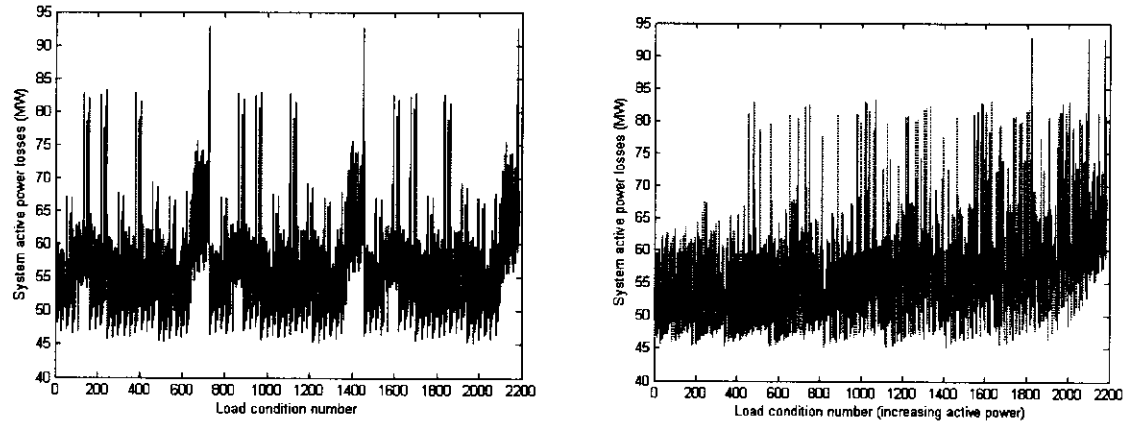

Figure 6.12 System active power losses (DG, CF control).

Network (all busses)	Average voltage deviation (permitted range) (%)	Average voltage deviation (ideal) (%)	Power losses (MW)
2 DGs(no control)	0.3097	1.9743	54.7117
2 DGs(CF control)	0	1.1107	54.6043

Table 6.5 Comparison between the networks with DGs with no control and with CF control.

From figures 6.11 - 6.12 (blue), the three sub-patterns that correspond to the three levels of power drawn by each load, can be identified. The figures also reveal that there is a slight increase in the average voltage deviation and network losses, but to a much smaller degree than shown in sections 6.3.1 and 6.3.2 for the other simulations. The CF keeps the objective functions much closer to a central operating point. The CF main objective goal to keep the voltage profile of all the network busses within the permissible range is accomplished. Figure 10 shows that the average voltage deviation from the permitted range is zero over the entire load-switching spectrum.

Table 6.5 shows that all three objective functions improved. The average voltage deviation from the ideal value reveals a decrease of 0.86%. The network power losses improved slightly with 0.1%. The overall result is a much improved voltage profile for the network over the entire load spectrum. The system power losses are also reduced by an average of 24 MW over the network with no DGs. From this optimum control of the DGs it is observed that the voltage profile of the network can be kept within the permissible limits with two proper positioned DGs.

Table 6.6 shows the bus voltage profiles of the power network. The results show that all the busses on both the transmission feeders are within the permissible limits. The big voltage drops on busses 6, 7 and 8 for maximum load capacity are significantly reduced from a maximum of 15.7 % to only 3.78 %. The average voltage drop for the busses is also improved and four busses reveal an average voltage drop/rise of 0% over the load switching spectrum.

Bus no.	Bus Voltage (kV)	Average Voltage Drop/Rise % (2 DGs, no tapping)	Maximum Voltage Drop/Rise % (2 DGs, no tapping)	In Range %
1	275	0	0	100
2	275	2.6 (rise)	5 (rise)	100
3	275	0	3 (rise)	100
4	275	0.8	2.04	100
5	275	0	2	100
6	275	1.6	3.87	100
7	275	0	3.5	100
8	275	1.4 (rise)	2.35	100

Table 6.6 Bus voltage profiles of the power network with DGs with CF control.

Since the main objectives of the CF control are to minimise system losses and improve the bus voltage profiles of the network, P_L and $V_{bus,i}$ are discussed. P_L is significantly reduced from a maximum of 115 MW to only 93 MW and P_{avg} to only 55 MW. The bus voltage profile of the busses showed an improvement of 6.7% and all the busses can be kept within the permissible limits with the introduction of DGs and CF control to the power system. This way under- and overvoltages are controlled over the load switching spectrum. Figure 6.13 illustrates the results of the bus voltage profiles and table 6.7 shows a summary of all the results for the power network.

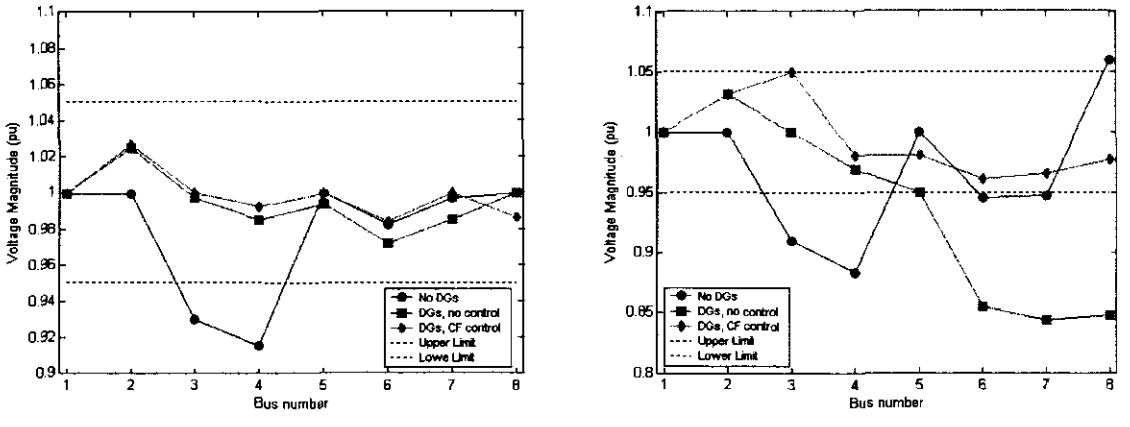

Figure 6.13 Bus voltage profiles of the power network (average and maximum drop/rise).

Bus no./ Objective function	No DGs			DGs, no control			DGs, CF control		
	Avg. drop %	Max. drop %	In range %	Avg. drop %	Max. drop %	In range %	Avg. drop %	Max. drop %	In range %
1	0	0	100	0	0	100	0	0	100
2	0	0	100	2.45	3	100	2.6	5	100
3	6.96	9.1	11.11	0.3	1	100	0	3	100
4	8.45	11.72	0	1.5	3.1	100	0.8	2	100
5	0	0	100	0.6	5	100	0	2	100
6	1.81	5.5	92.59	2.82	14.5	79	1.6	3.87	100
7	0.35	5.35	96.29	1.5	15.7	77.77	0	3.5	100
8	0	5.94	88.89	0	15.25	73.25	1.4	2.35	100
$V_{Avg,Permitted}$	0.6898			0.3097			0		
$V_{Avg,Ideal}$	2.8176			.1.9743			1.1107		
$P_{L,Avg}$	78.7110 MW			54.7117 MW			54.6043 MW		
Variable parameters	None			V_{DG1}, V_{DG2} = 1 pu			V_{DG1}, V_{DG2} = 0.98 pu - 1.05 pu		
				P_{DG1}, P_{DG2} = 150 MW			P_{DG1}, P_{DG2} = 1MW - 150 MW		

Table 6.7 Evaluation of the power network (Summary of results).

6.4 Evaluation of the ANN controller

The data used to train the ANN controller is developed in chapter 4 by the CF. The ANN controller is then trained in chapter 5 until optimum performance is reached for the training and test data. To evaluate the performance of the ANN controller, it is tested against the optimum solution of the power system as determined by the CF. The following criteria for comparison are selected:

- power system voltage profile for a selected operating state; and
- power system losses.

Since the ANN controller has been trained to the CF results, it is expected that they will perform better than the base case (no DGs) and close to the performance of the CF. Figures 6.14 - 6.15 shows the response of the ANN controller and the CF for the control variables of the DGs. A random load combination of 100 is chosen from the test data to show the results.

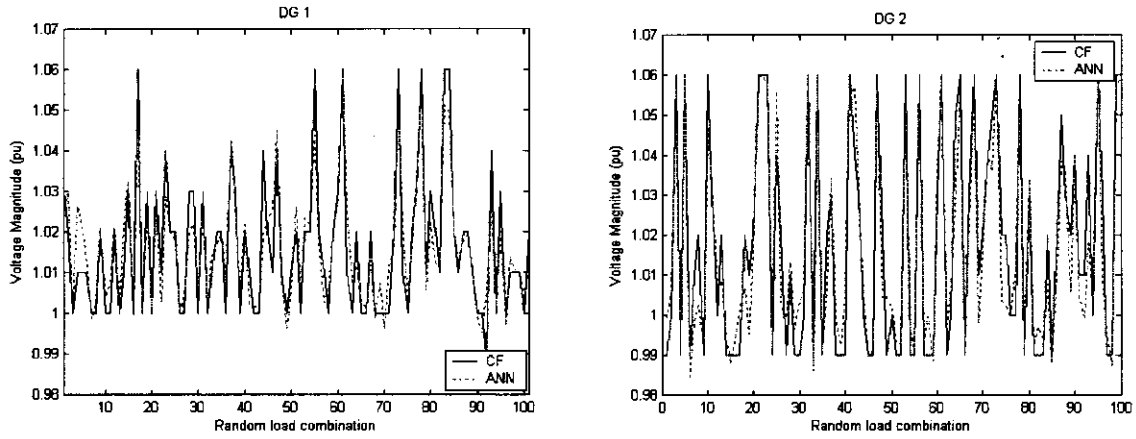

Figure 6.14 Voltage magnitudes of the DGs for a random load combination.

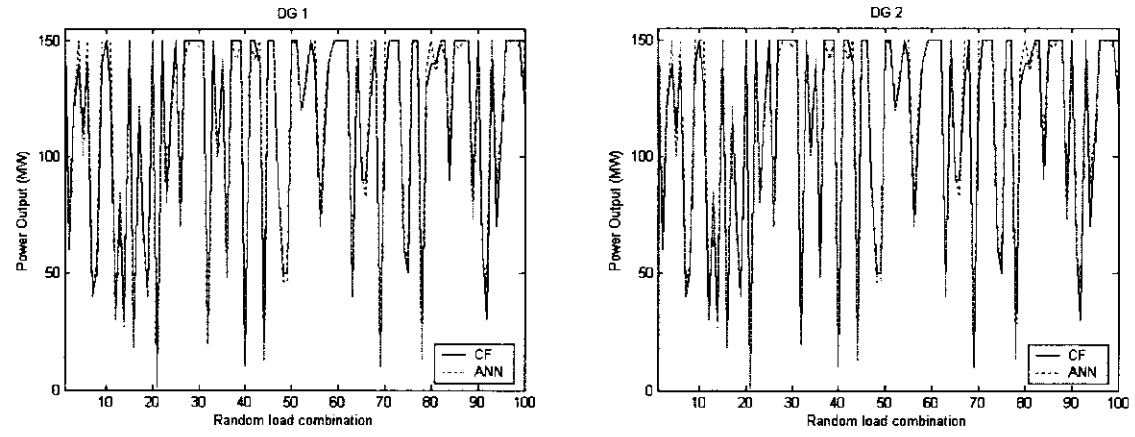

Figure 6.15 Power outputs of the DGs for a random load combination.

The response of the CF and ANN controller show a close resemblance. To show the performance of the ANN controller in the power system, the average voltage profiles of the network busses are investigated for the 2187 load combinations. In addition to the voltage profiles, a histogram comparison of the ANN controller performance to the CF results regarding reduction of active power losses over the base case is shown in figure 6.16. Histograms can illustrate the frequency of certain parameters (i.e. power losses/bus voltages levels) in a power system for all the operating states in the data set.

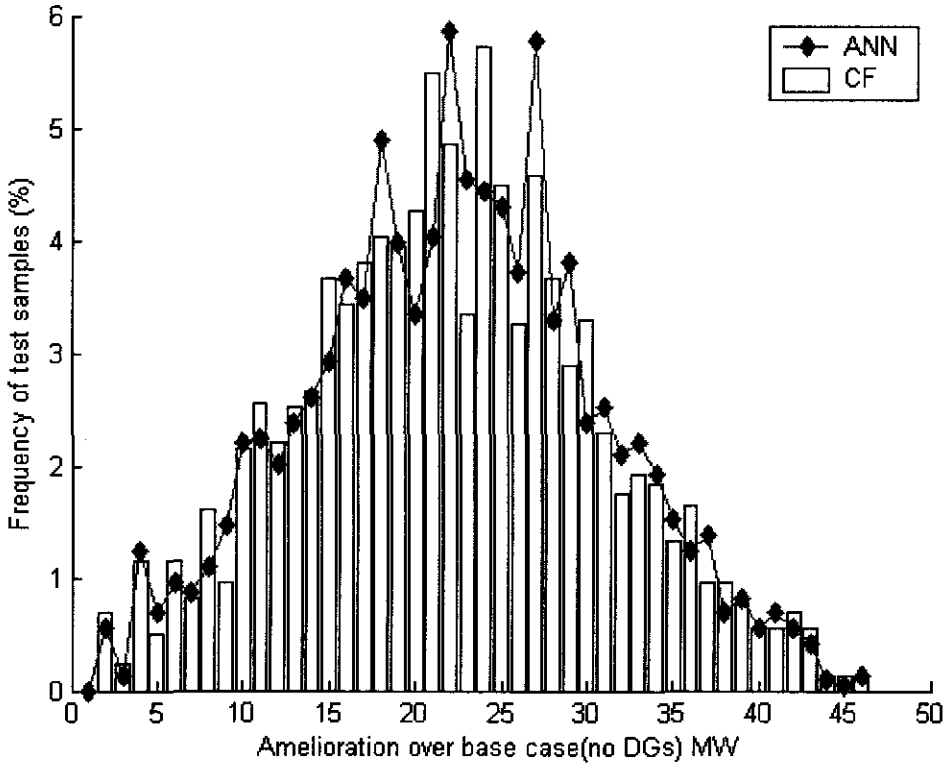

Figure 6.16 ANN and CF improvement of active power losses compared to base case (no DGs).

In figure 6.16, a significant improvement of the network power losses in percentage over the base case losses is evident, whereas the frequency distribution of the ANN controller results resembles the CF distribution. The frequency on the vertical axis describes the percent of the 2187 load conditions in the data set developed in chapter 4. The voltage profiles of the network busses are shown in figure 6.17 for the CF and the ANN controller. The figures show that the ANN controller kept the bus voltages between the permissible limits over the entire load switching spectrum. The voltage profiles of the network busses show that the results of the ANN controller closely resemble the results of the CF. A voltage histogram comparison between the ANN controller and CF is shown in figures 6.18 and 6.19.

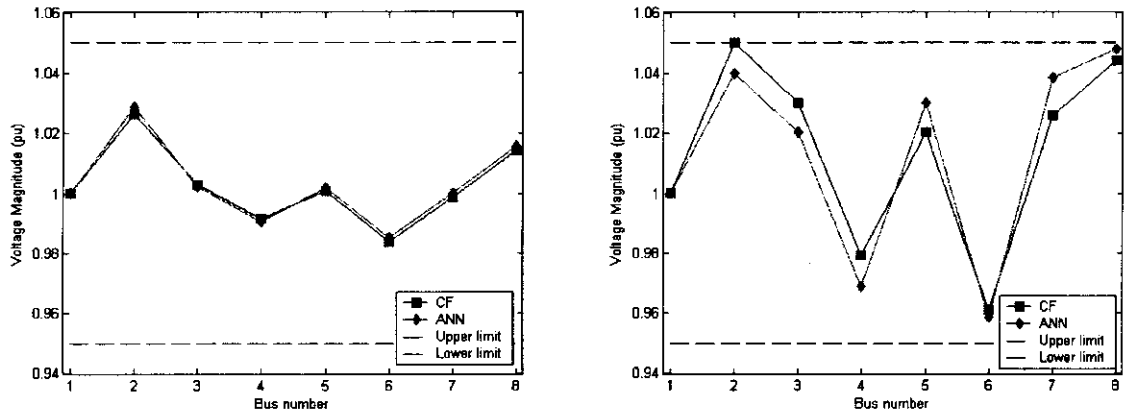

Figure 6.17 Bus voltage profiles of the network for the CF and ANN (avg. and max. drop/rise).

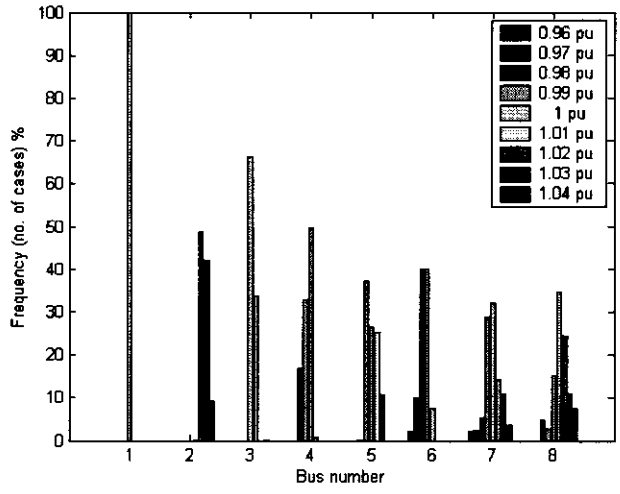

Figure 6.18 Voltage histogram (frequency of cases) for the CF.

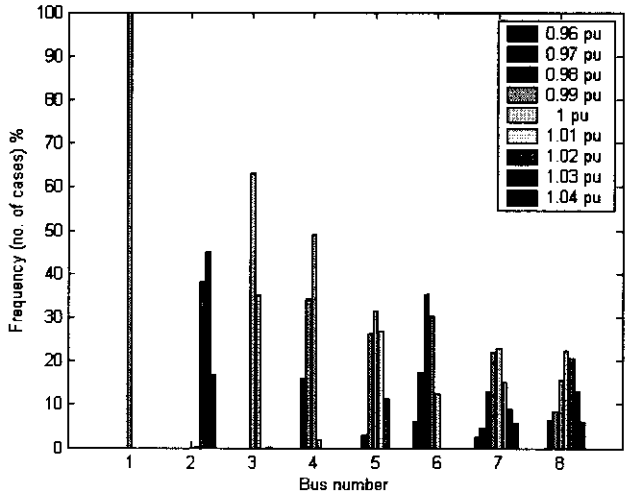

Figure 6.19 Voltage histogram (frequency of cases) for the ANN controller.

In figures 6.18 and 6.19, the frequency of voltage distribution for the ANN controller closely resembles that of the CF. The frequency on the vertical axis describes the percent of the load conditions for a specific voltage range. The frequency plot in figure 6.19 shows that the PV busses controlled by the DGs have a smaller voltage spectrum around 1 pu. This is expected because one of the CF objective functions and hence the ANN controller is to keep the bus voltage profiles as close to 1 pu as possible. Both frequency plots reveal that the voltage levels on busses 7 and 8 vary over a much bigger spectrum.

From the results shown in this section it is safe to conclude that the behaviour of the ANN controller closely mimics the response of the CF. The results of the ANN controller also revealed that the introduction of the controller and the DGs to the power system improved network conditions considerately over the base case where no DGs support the power system. These results however are limited to the restricted load-switching spectrum derived in chapter 4 (load variations are limited to only three operating states). The next section will evaluate the behaviour of the ANN controller over a much bigger load-switching spectrum. The integrity of the ANN controller will then be validated to make meaningful decisions about load conditions that are more likely to occur in real time.

6.5 Evaluation of the ANN controller beyond the training limits

Section 6.4 discussed the evaluation of the ANN controller and the power network. These results however were obtained with load conditions used in the original random data set (data set contains the training and testing load conditions) and the ANN controller may have been trained with the specific load conditions. This section deals with load conditions beyond the scope of the original data set, i.e. variable load conditions (loads are not restricted to only three operating states). The operating states of the loads are randomly varied with an incremental value of 10 MW. The performance of the ANN controller and the power network are now evaluated with these new random load conditions. Several simulation runs are performed as summarised in table 6.14, of which a few are discussed in the following sections.

6.5.1 Loads at 55% of switching capacity

The loads are varied with Matlab's random permutation ('randperm') command. The loads are randomly varied between the minimum and maximum switching capacity. This case still represents a load condition within the minimum and maximum training boundaries of the ANN controller, but not encountered before. Table 6.8 describes the load conditions of the network at 55 %. Figure 6.20 shows the response of the CF and the ANN controller for the control parameters of the DGs. Table 6.9 shows the results of the load conditions at 55% for the base case, CF, DGs with no control and response of

the ANN controller. The bus voltage profile of the network is shown in figure 6.21

	P_{load} (MW)	Q_{load} (Mvar)	Switch (%)
Load 1	210	69.024	60
Load 2	400	131.47	100
Load 3	120	39.442	33.3
Load 4	220	72.311	40
Load 5	100	32.868	0
Load 6	220	72.311	40
Load 7	44	14.312	25
L_{Total}	1314	431.73	55.77

Table 6.8 Load conditions for a total load-switch of 55 %.

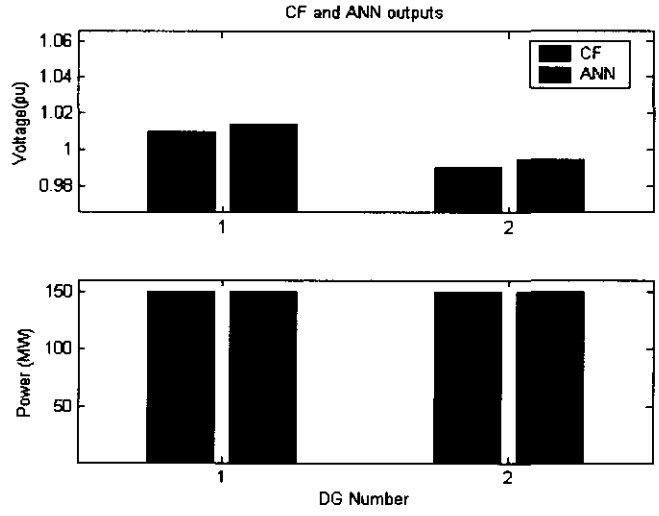

Figure 6.20 Response of the CF (left) and the ANN controller (right).

Statistics around 55 %	Average voltage deviation (permitted) %	Average voltage deviation (ideal) %	System active power loss (MW)
Base case (no DGs)	0.85348	2.8053	73.686
CF evaluation	0	0.96441	48.197
DGs (no control)	0	1.3162	48.685
DGs (ANN controller)	0	1.1304	48.409

Table 6.9 Results of the power network.

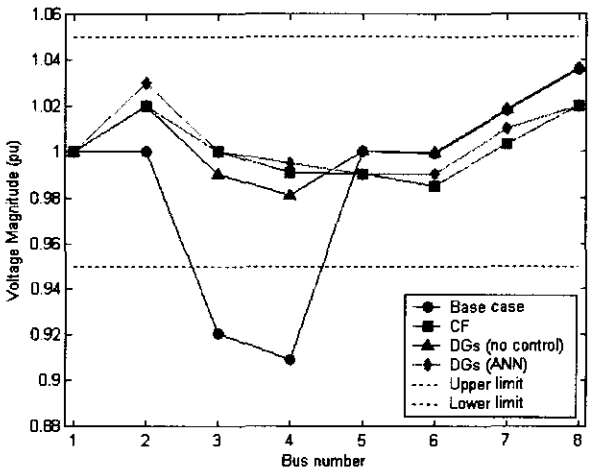

Figure 6.21 Bus voltage profiles of the power network.

From the results in figure 6.20 it is evident that the ANN controller could make a meaningful decision about the network load condition. The response of the ANN controller closely resembles that of the CF, but with a much better response time. The CF took 69 s (real-time) to find the optimum network condition and control variables, whereas the ANN controller took only 0.062 s (real-time). The results in table 6.9 show that the network conditions improved considerably over the base case. The average voltage deviations are established in the permissible range for both cases of DGs. This is expected because the power output parameters of the CF and ANN controller nears full power (DGs with no control run at full output power).

From the results in table 6.9, it is evident that control over the DGs improved the system power losses and the voltage deviation from 1 pu. Figure 6.21 shows that the bus voltage profiles improved over the base case, and that the voltage profiles for both cases of DGs are within the permissible limits. This concludes that the ANN controlled DGs improved network conditions and held the bus voltage profiles within the limits. As can be seen from these results, the behaviour of the ANN beyond the training load conditions showed a meaningful decision about the network conditions with much less computational time (compared to the CF).

6.5.2 Loads at 34% of switching capacity

The loads are randomly varied to 1228 MW within the boundaries of the load-switching spectrum. Table 6.10 describe the load conditions of the network at 34 %. Figure 6.22 show the response of the CF and the ANN controller for the control parameters of the DGs. Table 6.11 shows the results of the load conditions for the base case, CF, DGs with no control and response of the ANN controller. The bus voltage profile of the network is shown in figure 6.23.

	P_{load} (MW)	Q_{load} (Mvar)	Switch (%)
Load 1	160	52.589	10
Load 2	320	105.18	20
Load 3	130	42.729	50
Load 4	240	78.884	80
Load 5	110	36.155	33.3
Load 6	220	72.311	40
Load 7	48	15.777	75
L_{Total}	1228	403.62	34.17

Table 6.10 Load conditions for a total load-switch of 34 %.

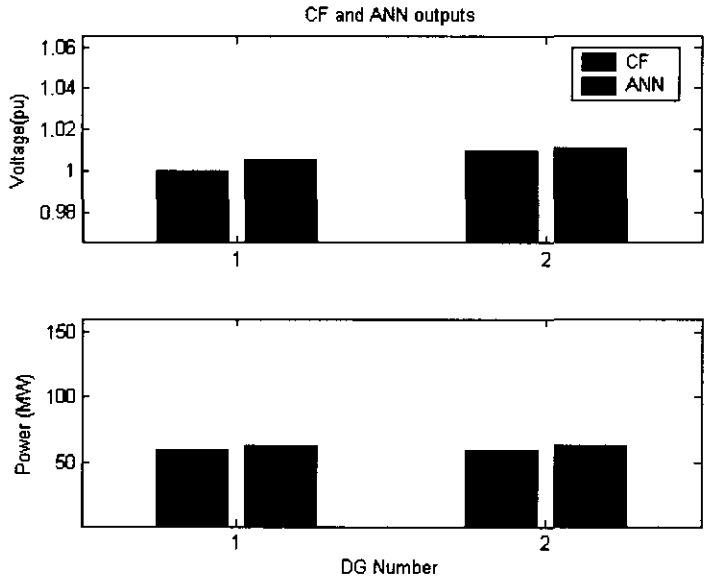

Figure 6.22 Response of the CF (left) and the ANN controller (right).

Statistics around 34 %	**Average voltage deviation (permitted) %**	**Average voltage deviation (ideal) %**	**System active power loss (MW)**
Base case (no DGs)	0.48597	2.1846	73.772
CF evaluation	0	0.84334	58.345
DGs (no control)	0	1.0108	58.814
DGs (ANN controller)	0	0.96834	58.606

Table 6.11 Results of the power network.

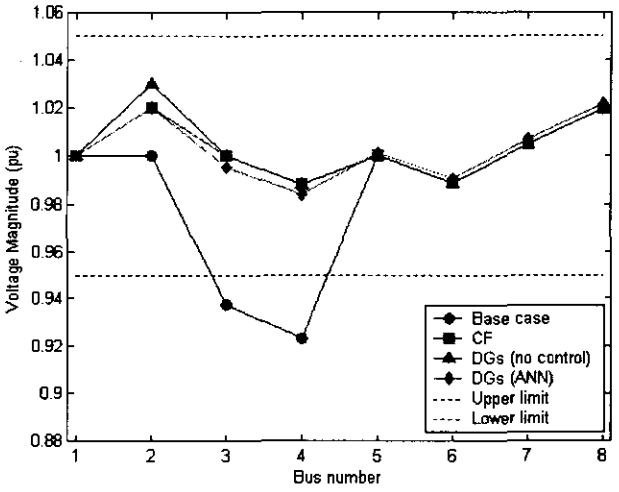

Figure 6.23 Bus voltage profiles of the power network.

The results in figure 6.22 show that the ANN controller and CF decisions about the network load conditions were closely matched. The response of the ANN controller and CF closely resembles each other. The results in table 6.11 show similar trends than the results in section 6.5.1. The network conditions improved considerably over the base case. The active network losses of the system are reduced by 15 MW, to only 58 MW. The average voltage deviation from the permissible range is also reduced to 0 % by the DGs. The results show that the DGs with ANN control produced better results over the DGs with no control. Figure 6.23 shows that the ANN controller improved the bus voltage profile over the base case for busses 3 and 4. The undervoltages at these busses are regulated within the permissible range with the ANN controller.

6.5.3 Loads at 70% of switching capacity

The loads in the power network are randomly varied to 1368 MW within the boundaries of the load-switching spectrum. Table 6.12 describes the new load conditions of the network at 70 % of the total rated switching spectrum. Figure 6.24 shows the response of the CF and the ANN controller for the control parameters of the DGs. Table 6.13 shows the results of the load conditions for the base case, CF, DGs with no control and of the ANN controller. The bus voltage profile of the network is shown in figure 6.25.

	P_{load} (MW)	Q_{load} (Mvar)	Switch (%)
Load 1	250	82.171	100
Load 2	380	124.9	80
Load 3	130	42.729	50
Load 4	210	69.024	20
Load 5	120	39.442	66.67
Load 6	230	75.597	60
Load 7	48	15.777	75
L_{Total}	1368	449.64	70

Table 6.12 Load conditions for a total load-switch of 70 %.

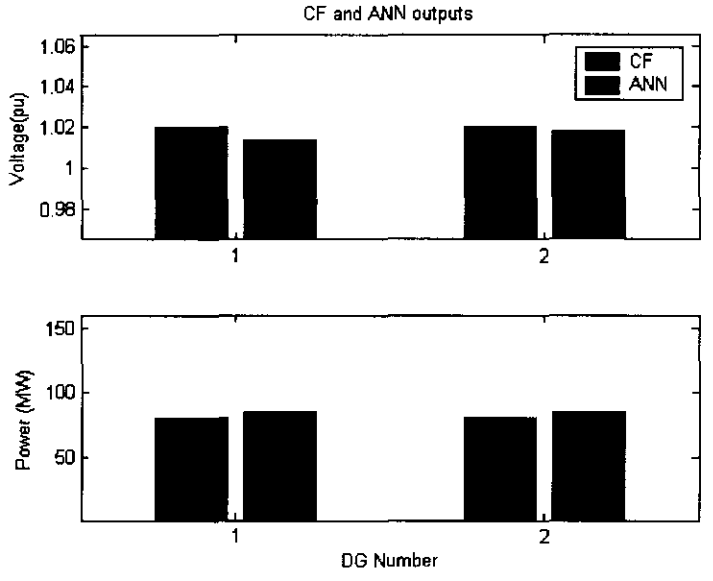

Figure 6.24 Response of the CF (left) and the ANN controller (right).

Statistics around 70 %	Average voltage deviation (permitted) %	Average voltage deviation (ideal) %	System active power loss (MW)
Base case (no DGs)	0.84647	2.6152	82.565
CF evaluation	0	0.91342	61.592
DGs (no control)	0	1.5199	62.615
DGs (ANN controller)	0	1.0691	61.789

Table 6.13 Results of the power network.

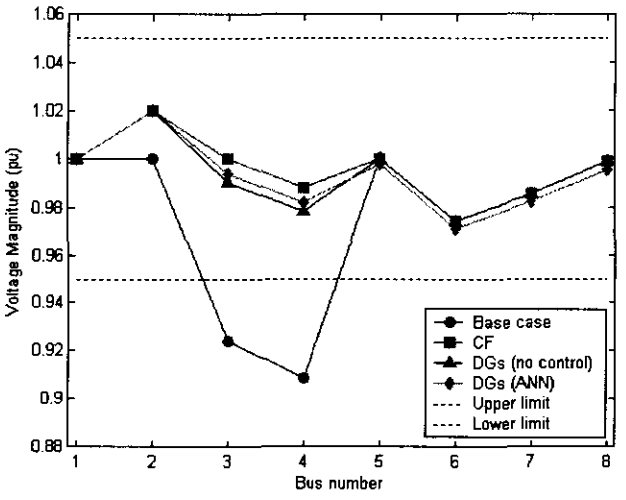

Figure 6.25 Bus voltage profiles of the power network.

Figure 6.24 describes the response of the CF and ANN controller to the load condition. The results reveal that the ANN controller closely mimics the response of the CF, thus making an appropriate decision again. The response shows that the best network conditions are achieved with the DGs running at about half-rated power. The time response of the ANN controller also topped the CF response with only 0.071s of computational time. Table 6.13 captures the statistics of the power network for this simulation run. The results obtained here also reveal that the network conditions improved over the base case. The rest of the findings are similar to the analysis of paragraphs 6.5.1 and 6.5.2 where the load conditions were set to other levels. Voltage levels are within the permissible range and the network power losses are minimized.

Figure 6.25 describes the voltage profile on all the system busses. The results reveal that the DGs improved the profile for all the busses over the base case. The profiles also reveal that the uncontrolled and controlled cases are more or less the same. The controlled case however shows better average deviation and network power losses. From all these results it is clear that the ANN controller chooses appropriate control parameters for the DGs for this simulation run.

6.5.4 Discussion of results

Results were obtained for changing load conditions in the power network and the adaptive behaviour of the ANN controller was investigated. The response of the ANN controller to such varying load conditions is the key issue to discuss. To facilitate the evaluation of the ANN controller, the results of the simulation runs are summarised in table 6.14.

The results of the ANN controller should primarily be compared to the base case, i.e. the original power network with no DGs. Since the main objectives of the ANN controller are to regulate the voltage profile of the network and minimise the active power losses, V_{avg}, V_{ideal} and P_L are evaluated. The base case showed that the voltage profile of busses 3, 4, 6, 7 and 8 drifted outside the limits for certain load conditions. In the simulation runs, busses 3 and 4 mainly posed a problem area in the network. The voltage profile of the network is improved for all the cases to within the permissible voltage range with the aid of the DGs and ANN control. The voltage parameters showed better results for all the simulations if the DGs were controlled.

The power losses of the system are significantly improved for all the cases over the base case. The lowest values are obtained with ANN control with a reduction of over 36 MW. This is a reduction of almost 40 % in the network power losses. This reduction is because sources closer to the load provide the necessary power and regulation as to central sources kilometres away. This concludes that the DGs with control reduce power flows in the power network and lines, thus reducing network losses.

As seen in table 6.14, the ANN controller made inadequate decisions on two occasions. The response of the ANN controller improved the network conditions over the base case, but degraded it for the case where no control over the DGs was active. The integrity of the ANN controller has to be improved to enable it to make meaningful decisions for any load condition in the switching spectrum. This could be achieved by analysing the power network with a much larger variety of load conditions and training the ANN controller to accommodate these conditions. This however would increase the training data considerably and may form the basis for future research.

Run no.	Load conditions								Base case			CF Output							ANN Output						
	L1 (MW)	L2 (MW)	L3 (MW)	L4 (MW)	L5 (MW)	L6 (MW)	L7 (MW)	Switch (%)	V_{avg} (%)	V_{ideal} (%)	P_L (MW)	DG1 V (pu)	DG1 P (MW)	DG2 V (pu)	DG2 P (MW)	V_{avg} (%)	V_{ideal} (%)	P_L (MW)	DG1 V (pu)	DG1 P (MW)	DG2 V (pu)	DG2 P (MW)	V_{avg} (%)	V_{ideal} (%)	P_L (MW)
1	210	400	120	220	100	220	44	55	0.85	2.81	73.68	1.01	150	0.99	150	0	0.96	48.19	1.015	150	0.995	150	0	1.13	48.41
2	160	320	130	240	110	220	48	34	0.49	2.18	73.77	1.00	60	1.01	60	0	0.84	58.34	1.005	65	1.012	65	0	0.96	58.61
3	250	380	130	210	120	230	48	70	0.85	2.61	82.57	1.02	80	1.02	80	0	0.91	61.59	1.015	83	1.018	83	0	1.07	61.78
4	150	340	130	230	110	200	46	28	0.60	2.88	67.50	1.00	150	0.99	150	0	1.19	48.20	1.002	149	0.991	149	0	1.33	47.89
5	250	300	130	210	110	230	42	45	0.37	2.03	68.73	1.00	40	1.02	40	0	0.80	59.26	1.003	46	1.022	46	0	1.00	57.84
6	190	330	160	250	100	220	48	51	0.90	2.69	78.38	1.01	70	1.01	70	0	1.05	59.58	1.014	65	1.009	65	0	1.18	60.59
7	210	330	150	210	100	210	42	40	0.78	3.09	65.88	1.01	150	0.99	150	0	1.27	48.07	1.012	150	0.991	150	0.008	1.75	47.01
8	170	380	140	230	120	240	48	60	0.97	3.19	92.21	1.04	150	1.04	150	0	1.10	57.22	1.028	150	1.042	150	0	1.09	56.98
9	240	390	150	240	130	220	42	81	1.16	2.84	90.08	1.03	140	1.00	140	0	1.02	55.54	1.037	137	1.005	137	0	1.17	56.33
10	160	320	110	200	110	210	44	15	0.27	2.27	61.78	1.00	130	0.99	130	0	0.98	49.29	1.003	133	0.993	133	0	1.13	48.86
11	230	370	150	240	100	220	46	66	1.03	2.87	79.45	1.01	150	0.99	150	0	1.01	51.36	1.009	148	0.991	148	0	1.01	51.38
12	230	350	130	210	120	200	44	48	0.66	2.81	67.49	1.00	150	0.99	150	0	1.16	48.51	1.003	150	0.991	150	0.009	1.29	48.17

Table 6.14 Evaluation of the adaptive behaviour of the ANN controller (Summary of results).

6.6 Conclusions

The results of the CF and ANN controller to optimise network parameters are evaluated in this chapter. The power network is firstly evaluated for the case where DGs are present in the network, but with no control. The results showed that the network environment in terms of voltage profiles improved to a certain extent for some busses, but to the detriment of other busses. The network power losses improved considerably over the base case. The CF is then used to analyze network conditions for a given load profile. The CF is tested against the base case, i.e. the original power system without the DGs. Using the CF to analyze and improve the network environment seems viable. The regulating requirements in terms of deviation from the permitted and ideal values are met while the network active power losses are kept to a minimum.

The ANN controller is evaluated for load conditions within the original data set developed by means of the CF. The ANN controller showed similar results as the CF and it is concluded that the ANN controller can make meaningful decisions for these load profiles. The ANN controller also made proper decisions for load conditions beyond the training limits. To improve the capabilities of the ANN controller, it should be trained with a broader spectrum of load possibilities. This would enable the ANN controller to make informed control decisions for a bigger region of load conditions. In practice this would be a requirement, but to the expense of a much bigger and more complex training data set. The ANN controller developed for the purpose of this project however showed adequate network conditions and improved power quality parameters.

Chapter 7 - Conclusion and Recommendations

7.1 Introduction

The traditional way of delivering power to a consumer is from a centralised utility. With the rapid growth of technology, generation of power at all levels is possible whether at transmission, distribution or at the end user level. The confluence of decentralisation with advances in distributed generation (DG) and artificial intelligence (AI) has opened new opportunities to deliver power closer to the point of consumption. The purpose of this research was to investigate the feasibility of using AI to control power quality (PQ) parameters through the optimal utilisation of DG in an electric power system. This chapter concludes the research conducted and summarises the significance of the study.

7.2 The significance of the research

The electric power system under investigation is characterised by large loads switching on-and off the electric grid. As described in the IEEE Std. P1433, these conditions are likely to cause PQ phenomena termed under-and overvoltages. These phenomena are the result of poor system voltage regulation capabilities and controls. The NRS 048 standard in South Africa demands that voltage regulation must comply within ±5 % of the nominal voltage level for voltage levels above 500 V. To find a solution to these conditions, DG with AI controls is evaluated in this research to regulate the voltage profile of the electric power system and reduce the active power losses.

To evaluate the behaviour of an Artificial Neural Network (ANN) controller controlling the DGs, a simulation model is developed which integrates the DGs and the electric power system. The strategic placement of the DGs in the power system is important to complement their voltage regulation capabilities. For the purpose of simulation, the Matlab® environment facilitates all the software tools necessary to analyse the power system and develop an AI controller. The electric power system is modelled in SimPowerSystems®, a toolbox integrated into Matlab to model electric networks and systems. This simulation model forms the basis for the analysis of the electric power system.

The ANN emerged as the most suitable AI technique for the control algorithm. Using ANN control is shown to minimise the network active power losses while optimising the bus voltage profile of the network in terms of the average voltage deviations from the permissible and ideal values. The cost function is initially used to develop training data for the ANN. This data incorporate load-switching patterns for the network and the optimal deployment of the DGs. The ANN is trained with this

randomised data set and the ANN topology used is 14:24:4 representing 14 input neurons, 24 hidden layer neurons and 4 output layer neurons.

The ANN controlled cases are compared to conditions of no control where the DGs are deployed at full power and a nominal voltage level of 1 pu. For the load conditions analysed by the cost function, the ANN controller proved to be very effective in controlling the DGs. The bus voltage profiles as well as the average voltage deviations are successfully kept within the permissible voltage range. From the results, the system active power losses are reduced by an average of 24 MW. Comparing the results obtained, the optimal utilisation of DGs showed that the network conditions improved vastly over the original power system.

The adaptive behaviour analysis of the ANN controller beyond the training limits reveals that the ANN controller can make meaningful output decisions when subjected to load conditions not in the training set. Beyond the training limits means that the load conditions are increased to different randomly selected power levels. What becomes clear from these analyses is that the behaviour of the ANN controller closely mimics the response of the cost function. This behaviour of the ANN justifies the ability of the cost function to select the optimal network conditions as the same improvements are seen in the network as discussed in the previous paragraph.

Table 7.1 describes the results of improvement in the network conditions over the original power network. The results conclude that the integrated power system with DGs could be controlled to eliminate under-and overvoltages due to the switching of large loads.

Electric Power System	Ave. voltage deviation - Permitted (%)	Max. voltage deviation - Permitted (%)	Ave. voltage deviation - Ideal (%)	Max. voltage deviation - Ideal (%)	Ave. active power losses (MW)
Original	0.6898	11.72	2.8176	4.501	78.7110
DGs with ANN controller	0	0	1.1107	1.982	54.6043
Improvement (%)	**100**	**100**	**60**	**56**	**31**

Table 7.1 Summary of the results of the research conducted.

7.3 Further research

Based on the research conducted during this study, the following areas can be improved or be recommended for future research:

a) Refinement of the ANN training data;
b) Other power network configurations;
c) DG penetration on distribution level;
d) The impact of DG on other power quality issues.

The training data developed by the CF are based on the same active output power for all the DGs. This constraint limited the output combinations of the DGs to an acceptable size. The output combinations of the DGs could be refined to a larger domain of output voltage and active power levels. This refinement would affect the developed model and ultimately the performance of the power network. The load boundaries of the network are set to the network load capacity and not to the current operational boundaries of the loads. Changing the training data to the operational boundaries and updating it as the boundaries change need to be devised.

The primary objective of distribution systems is to supply customers at a voltage that is within a prescribed range. Adding DGs on a distribution feeder at different locations and increasing the DG penetration level directly affects the control of voltage regulation devices like LTCs (load tap changers), SVRs (step voltage regulators) and switched capacitor banks. Devising an integrated control scheme can be used to assist these devices in the overall voltage regulation of the distribution feeder. Implementation of such a control scheme, however, requires a communication infrastructure not currently available in most distribution systems.

The primary power quality phenomena addressed in this research is under-and overvoltages. Adding DG to a power system potentially influences the quality of power provided to other customers connected to the grid. Some of the other power quality attributes that is of concern include harmonic distortion, flicker and voltage imbalance. These key issues could be considered in further investigations into the effect of DG on the quality of supply.

7.4 Closure

The conclusion of this dissertation is that the use of DGs with ANN control to optimise the power quality in an electric power system is meaningful. This is achieved through proper positioning and control. The evaluation of the power quality in the electric power system is however subject to power quality definitions used to optimise only certain parameters and it is recommended that further research be done on power quality and DG as discussed in section 7.3.

Transient A phenomenon or quantity that varies between two consecutive steady states during a time interval that is short compared to the time scale of interest.

Undervoltage A voltage having a value of at least 10% under the nominal voltage.

Voltage Change A variation of the rms value of a voltage between two consecutive levels.

Voltage Sag See *Sag*.

Voltage Distortion Distortion of the ac line voltage.

Voltage Fluctuation A series of voltage changes.

Voltage Unbalance A condition in which the three phase voltages differ in amplitude or are displaced from their normal 120° phase relationship.

Voltage Interruption Disappearance of the supply voltage on one or more phases.

Voltage Regulation The degree of control or stability of the rms voltage at the load.

Voltage Magnification The magnification of capacitor switching oscillatory transient voltage on the primary side by capacitors on the secondary side of a transformer.

Waveform Distortion A steady-state deviation from an ideal sine wave of power frequency.

B ESKOM case study

B.1 Substation diagrams

DETAILED DEFINITION OF PLANT & EQUIPMENT COMPRISING THE TRANSMISSION SYSTEM (TS)	Reference OS 1	Rev. 1	Page 71	Of 127

NORTH WESTERN REGION

BETA

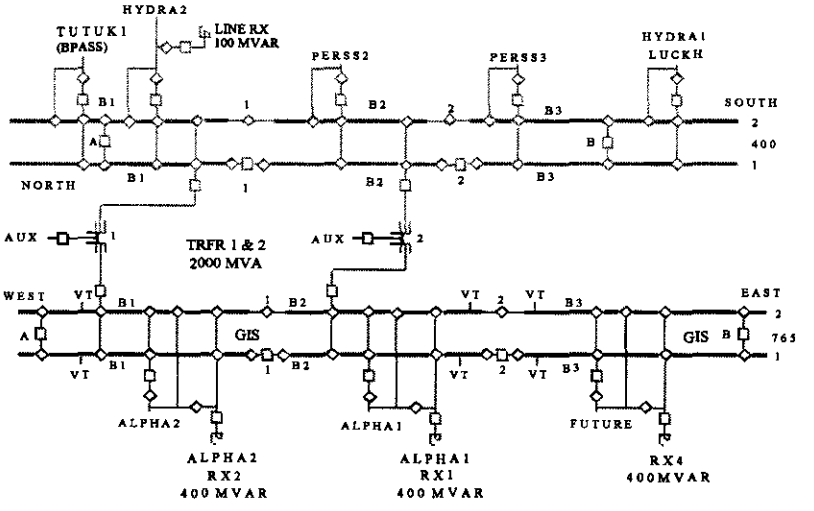

BOUNDARY

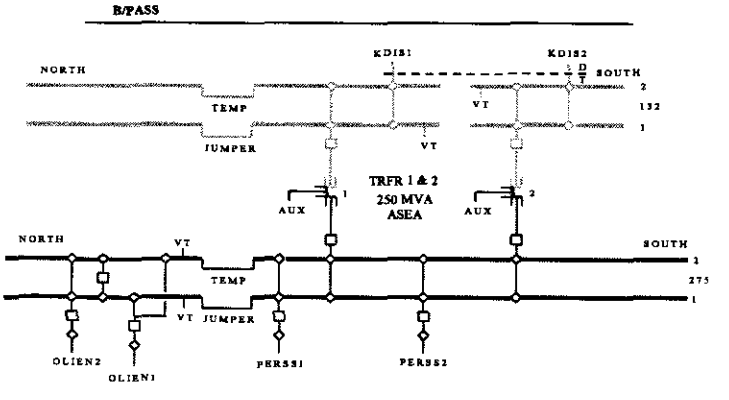

No. 1 Bypass will be shown on the drawing at bottom

Note : Updates can be sent to MRS LS J van Rensburg, PO Box 103 Germiston 1400, Room 418 National Control Building or Telephone (011) 871-3044 FACSIMILE (011) 871-3238

Figure B.1 Substation diagram of Boundary.

CARMEL

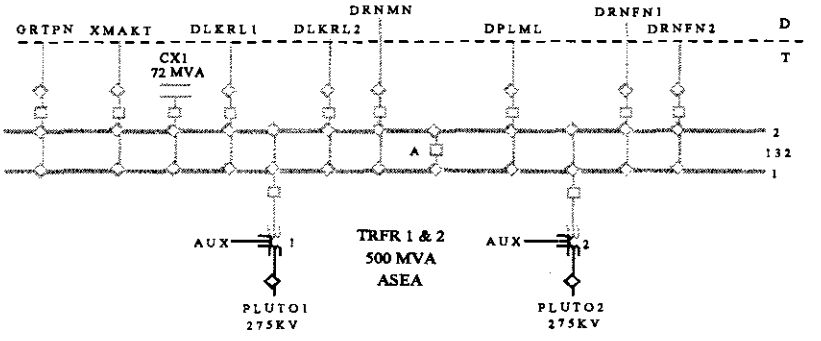

EVEREST

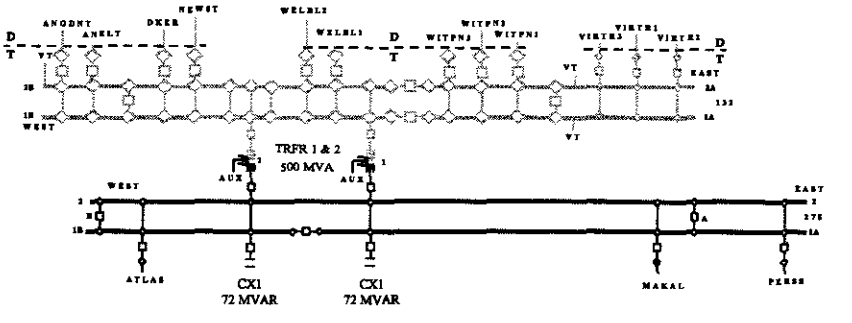

No. 1 Bypass will be shown on the drawing at bottom

Note : Updates can be sent to MRS LS J van Rensburg, PO Box 103 Germiston 1400, Room 418 National Control Building or Telephone (011) 871-3044 FACSIMILE (011) 871-3238

Figure B.2 Substation diagram of Everest.

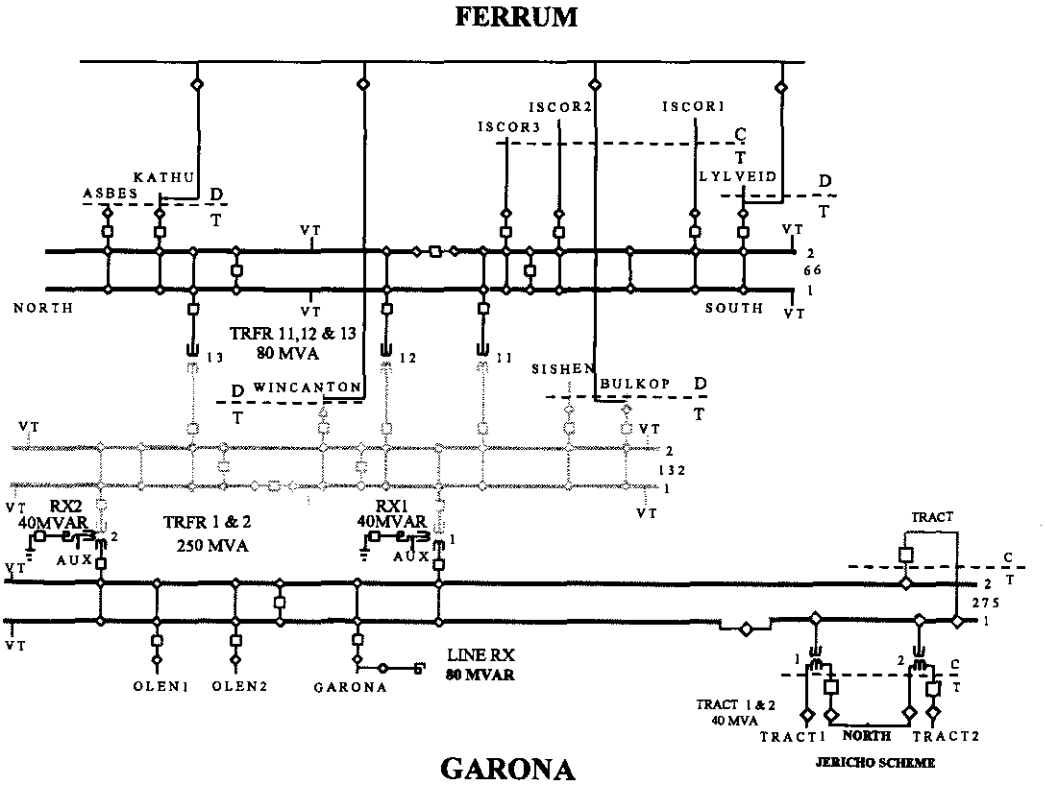

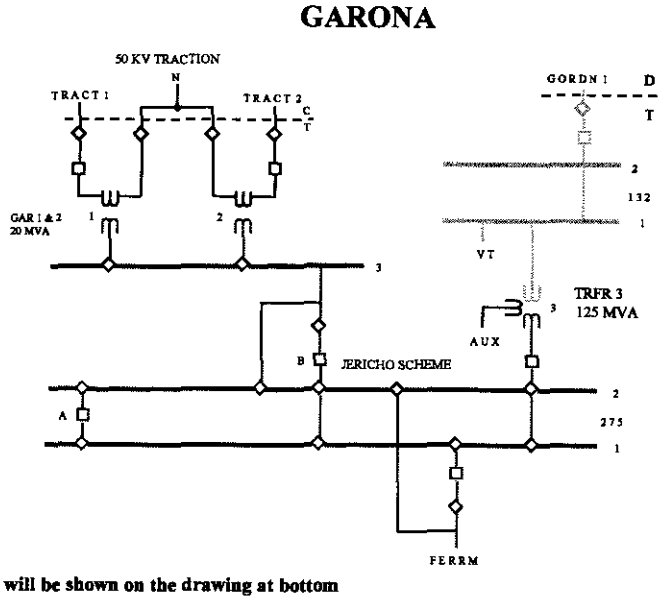

No. 1 Bypass will be shown on the drawing at bottom

Note : Updates can be sent to MRS LS J van Rensburg, PO Box 103 Germiston 1400, Room 418 National Control Building or Telephone (011) 871-3044 FACSIMILE (011) 871-3238

Figure B.3 Substation diagrams of Ferrum and Garona.

HARVARD

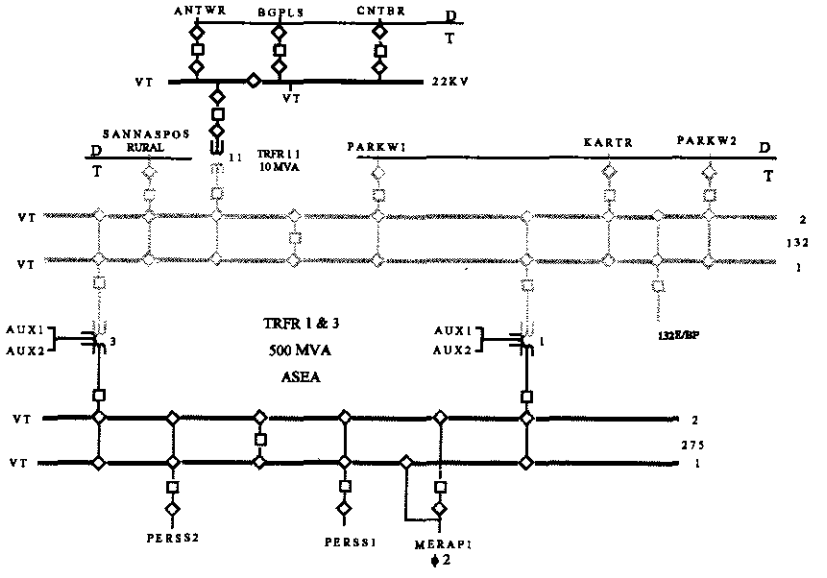

HERMES

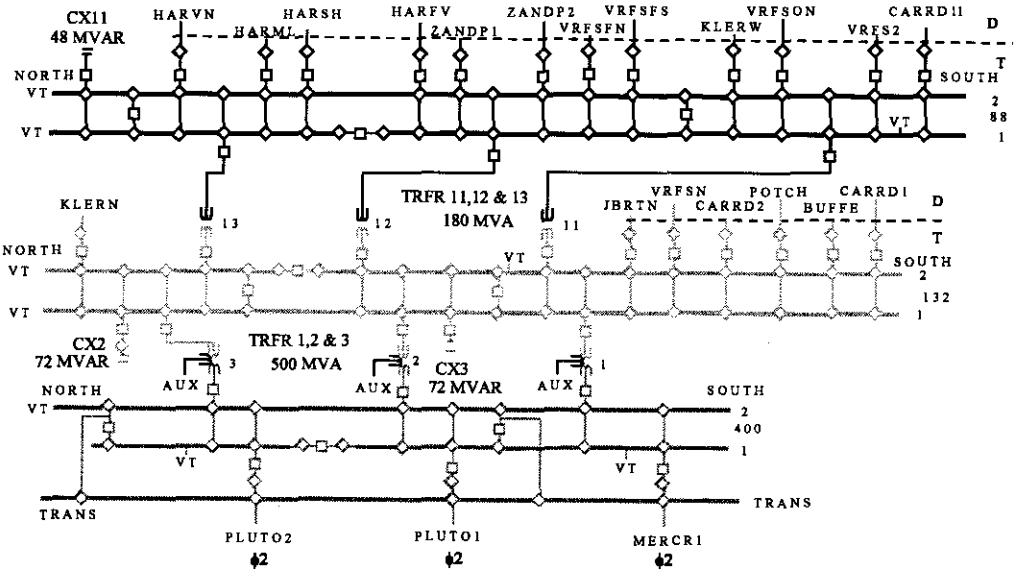

No. 1 Bypass will be shown on the drawing at bottom

Note : Updates can be sent to MRS LS J van Rensburg, PO Box 103 Germiston 1400, Room 418 National Control Building or Telephone (011) 871-3044 FACSIMILE (011) 871-3238

Figure B.4 Substation diagram of Harvard.

LEANDER

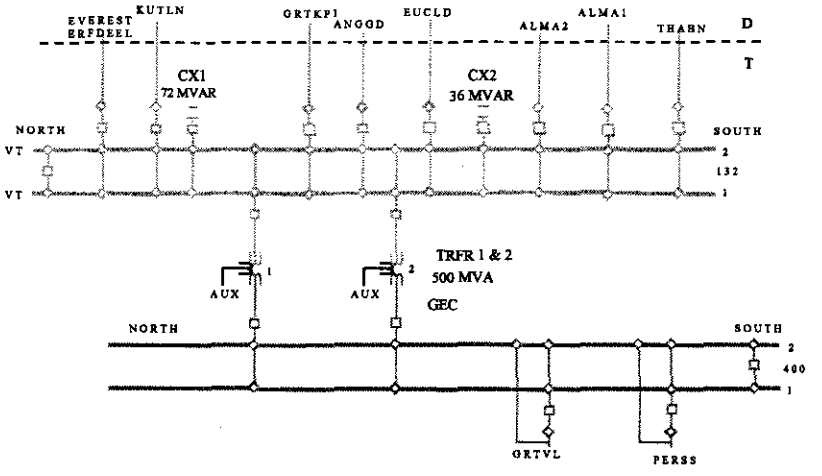

MERAPI

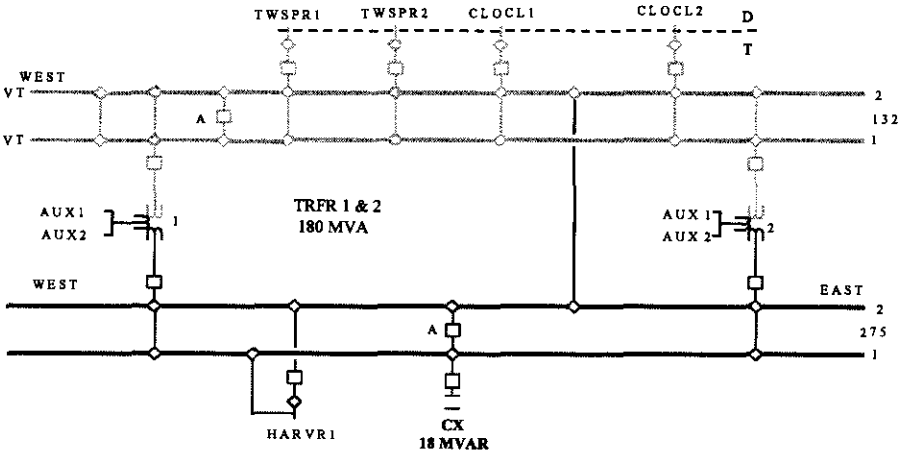

No. 1 Bypass will be shown on the drawing at bottom

Note : Updates can be sent to MRS LS J van Rensburg, PO Box 103 Germiston 1400, Room 418 National Control Building or Telephone (011) 871-3044 FACSIMILE (011) 871-3238

Figure B.5 Substation diagram of Merapi.

B.2 Line data transformation

The line data provided by ESKOM are shown in table B.1:

Line no.	Sub I	Sub J	*R* (pu)	*X* (pu)	*B* (pu)	*S* (MVA)	Length (km)
1	A	B	0.01207	0.06310	0.39655	478	147.01
2	B	C	0.00559	0.02888	0.18582	956	68.180
3	C	D	0.00909	0.04667	0.30279	478	110.47
4	B	E	0.007365	0.03783	0.24545	956	89.550
5	E	F	0.01096	0.05661	0.36608	956	133.905
6	F	G	0.00809	0.04110	0.27119	956	98.505
7	G	H	0.01365	0.07071	0.45483	478	166.80

Table B.1 Electric power network line data.

The line *R*, *X* and *B* values are in per unit on a 100 MVA (*S*) base. To calculate the line *R*, *L* and *C* transformations, the following formulas are used.

$$Z_{base} = R_{base} = X_{base} = V_{base} / I_{base} = V^2_{base} / S_{base} \quad \text{(B.1)}$$

$$Z_{base} \text{ @ } 275 \text{ kV} = 275^2 / 100 = 756.25$$

$$Y_{base} = 1 / Z_{base} = 1.322\text{e-}3$$

The *R*, *X* and *B* values for the full length of the line are:

$$R_{full} = R_{pu} \times Z_{base} \quad \text{(B.2)}$$

$$X_{full} = X_{pu} \times Z_{base} \quad \text{(B.3)}$$

$$B_{full} = B_{pu} \times Y_{base} \quad \text{(B.4)}$$

The new values of *R*, *X* and *B* per kilometer are:

$$R_{new} = R_{full} / \text{Line Length} \quad \text{(B.5)}$$

$$X_{new} = X_{full} / \text{Line Length} \quad \text{(B.6)}$$

$$B_{new} = B_{full} / \text{Line Length} \quad \text{(B.7)}$$

Table B.2 shows the *R*, *X* and *B* values of the lines per kilometer:

Line no.	*R* (Ω/km)	*X* (Ω/km)	*B* (mili mho/km)
1	6.2e-2	3.25e-1	3.567E-6
2	6.2e-2	3.20e-1	3.604E-6
3	6.2e-2	3.19e-1	3.624E-6
4	6.2e-2	3.19e-1	3.624E-6
5	6.2e-2	3.20e-1	3.615E-6
6	6.2e-2	3.16e-1	3.640E-6
7	6.2e-2	3.21e-1	3.606E-6

Table B.2 Line *R*, *X* and *B* per kilometer.

Table B.3 shows the *R*, *L* and *C* values of the lines per kilometer:

Line no.	*R* (Ω/km)	*L* (H/km)	*C* (F/km)
1	6.2e-2	1.0345e-3	1.14e-8
2	6.2e-2	1.0186e-3	1.15e-8
3	6.2e-2	1.0154e-3	1.15e-8
4	6.2e-2	1.0154e-3	1.15e-8
5	6.2e-2	1.0186e-3	1.15e-8
6	6.2e-2	1.0059e-3	1.16e-8
7	6.2e-2	1.0218e-3	1.15e-8

Table B.3 Line *R*, *L* and *C* per kilometer.

B.3 Loads and capacitance in ESKOM power network

Capacitor banks are installed at various places in the electric power network. The sizes and locations of the capacitor banks are shown in table B.4.

Location	Size (MVAr)	Voltage Level (kV)
Everest	144	275
Merapi	18	275
Ferrum	80	275

Table B.4 Capacitor banks and sizes.

The load capacities in the electric power network are shown in table B.5.

Load	Current load (MW)	Max. load (MW)	Switching capacity (MW)
Load 1 (Sub A)	150	250	100
Load 2 (Sub C)	300	400	100
Load 3 (Sub D)	100	160	60
Load 4 (Sub E)	200	250	50
Load 5 (Sub F)	100	130	30
Load 6 (Sub G)	200	250	90
Load 7 (Sub H)	42	50	8
Total	**1092**	**1490**	**398**

Table B.5 Load capacities in the electric power network.

The generating capacities of the feeding transmission lines are shown in table B.6.

Source	Max. capacity (MVA)
275 kV Trans. line	1000
400 kV Trans. line	1500

Table B.6 Power capacities of the feeding transmission lines.

All the load values supplied by ESKOM are only the real power values. Assuming a 0.95 power factor at all the loads, the following formulas are used to calculate the reactive power values.

$$PF = \cos(\theta) \tag{B.8}$$

$$\theta = 18°$$

$$\sin(18°) = 0.309$$

$$S = P + jQ$$

$$S = |V||I|\cos(\theta) + j|V||I|\sin(\theta) \tag{B.9}$$

$$P = |V||I|\cos(\theta) \tag{B.10}$$

$$|V||I| = P/0.95$$

$$Q = (P/0.95) \times (0.309)$$

C Power flow analysis

To validate the two simulation environments, a smaller network was created with only one source and one DG. A flow diagram of the system is shown in figure C.1.

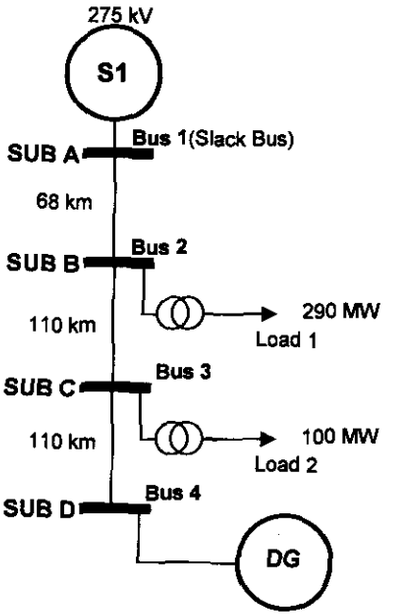

Figure C.1 Test network used for the power flow simulation.

The test network is firstly analysed with SimPowerSystems. The flow diagram of the network is shown in figure C.2.

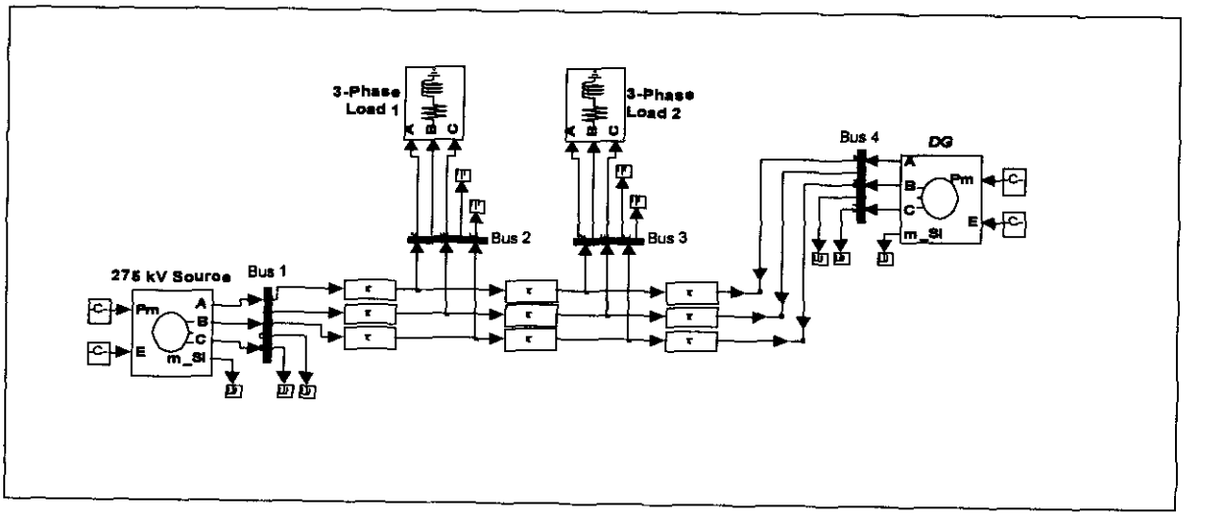

Figure C.2 Test network modelled in SimPowerSystems.

The test network is secondly modelled with the Newton-Raphson Power Flow solution. The results of the two simulations are shown in table C.1.

Bus no.	Parameter	SimPowerSystems	Newton-Raphson
Bus 1 (Slack)	V_1 (pu)	1.00	1.00
	δ_1 (deg.)	0.000	0.000
Bus 2	V_2 (pu)	0.970	0.967
	δ_2 (deg.)	-6.29	-6.671
Bus 3	V_3 (pu)	0.981	0.984
	δ_3 (deg.)	-9.18	-9.810
Bus 4 (DG)	V_4 (pu)	1.00	1.00
	δ_4 (deg.)	-9.41	-9.989

Table C.1 Results of the two power flow solutions.

The results show a close resemblance and the credibility of the two modelling environments are verified.

D Matlab neural network toolbox

The Matlab 'Neural Network Toolbox (NNT)' is used in to train the model described in chapter 5. The simulations are done using both the graphical user interface (GUI) and the command line. The GUI allows the user to quickly and easily do the following:

- Create new networks with different parameters and learning algorithms;
- Initialize, train, and test networks;
- Export the training and testing results from the GUI to the command line workspace.

The GUI is user friendly and figures A.1 – A.4 shows the different windows of the GUI.

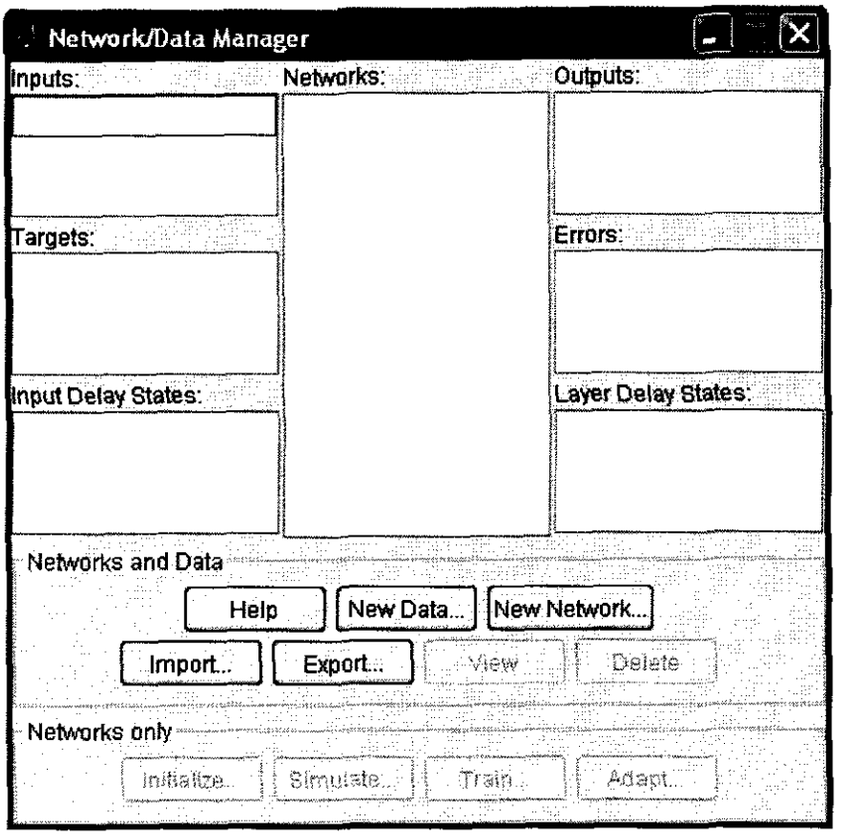

Figure D.1 Network manager of the NNT GUI.

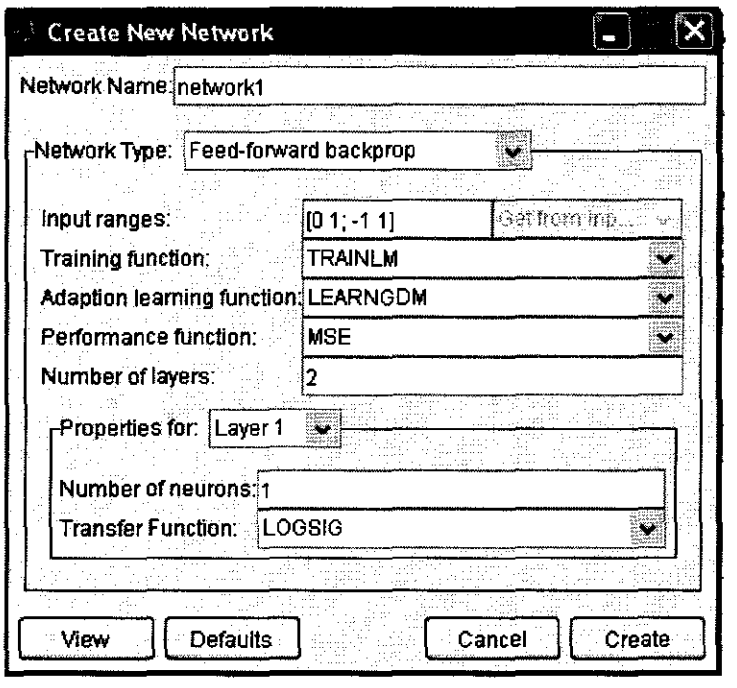

Figure D.2 Window in the GUI to create a new network.

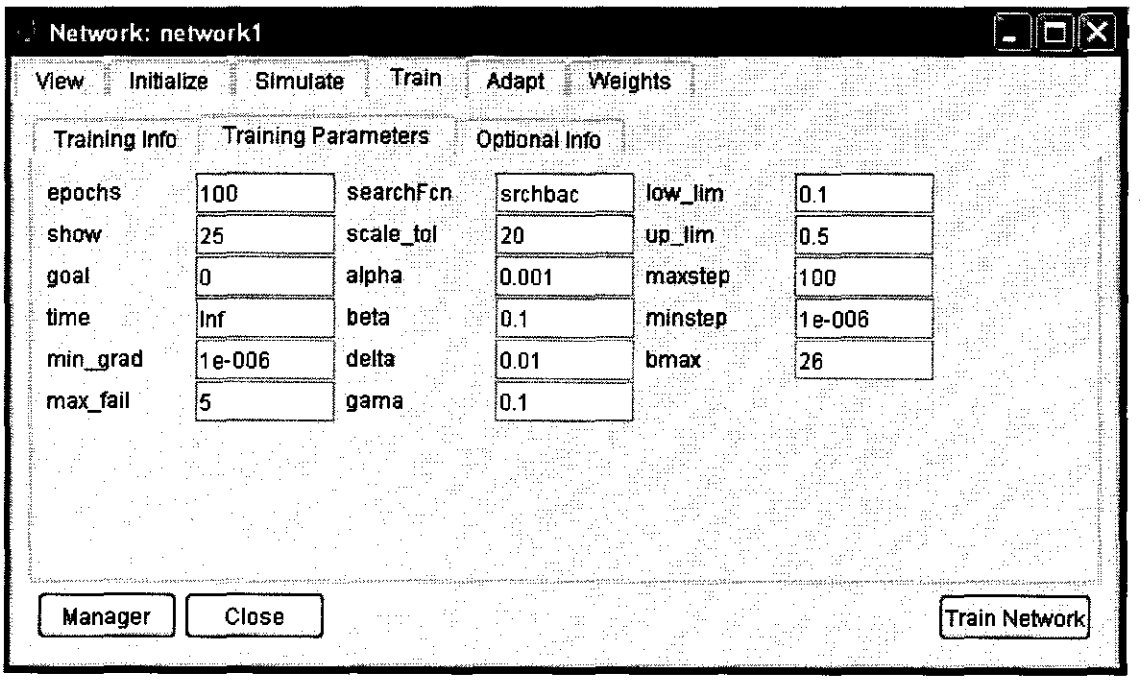

Figure D.3 Window in the GUI to train the network.

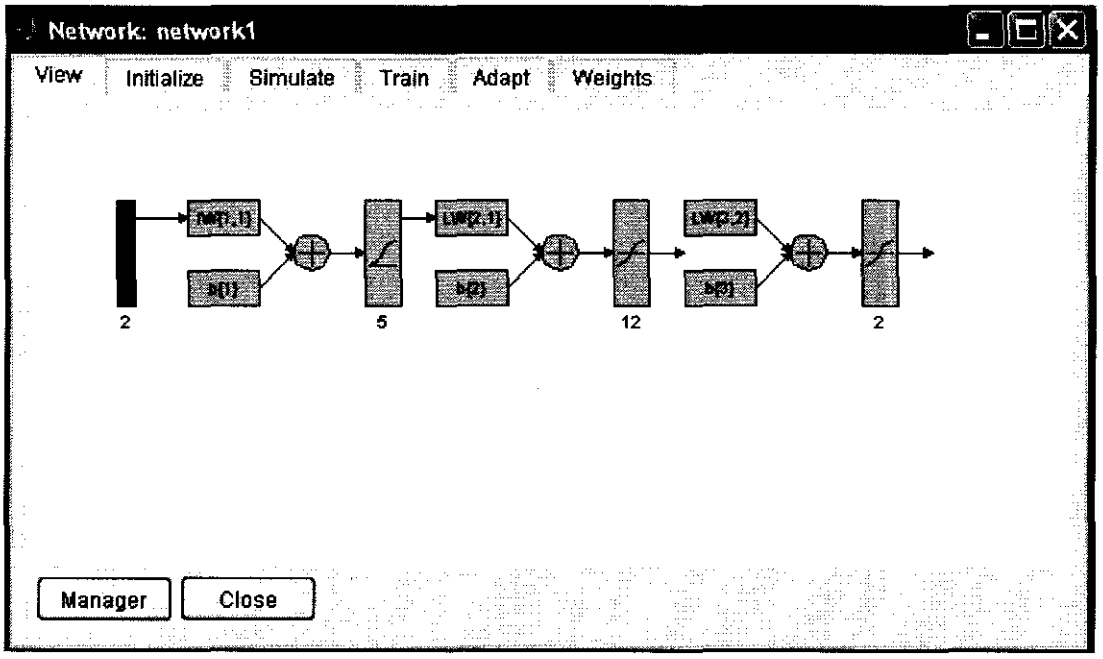

Figure D.4 A graphical view of the network created.

E Simulation model

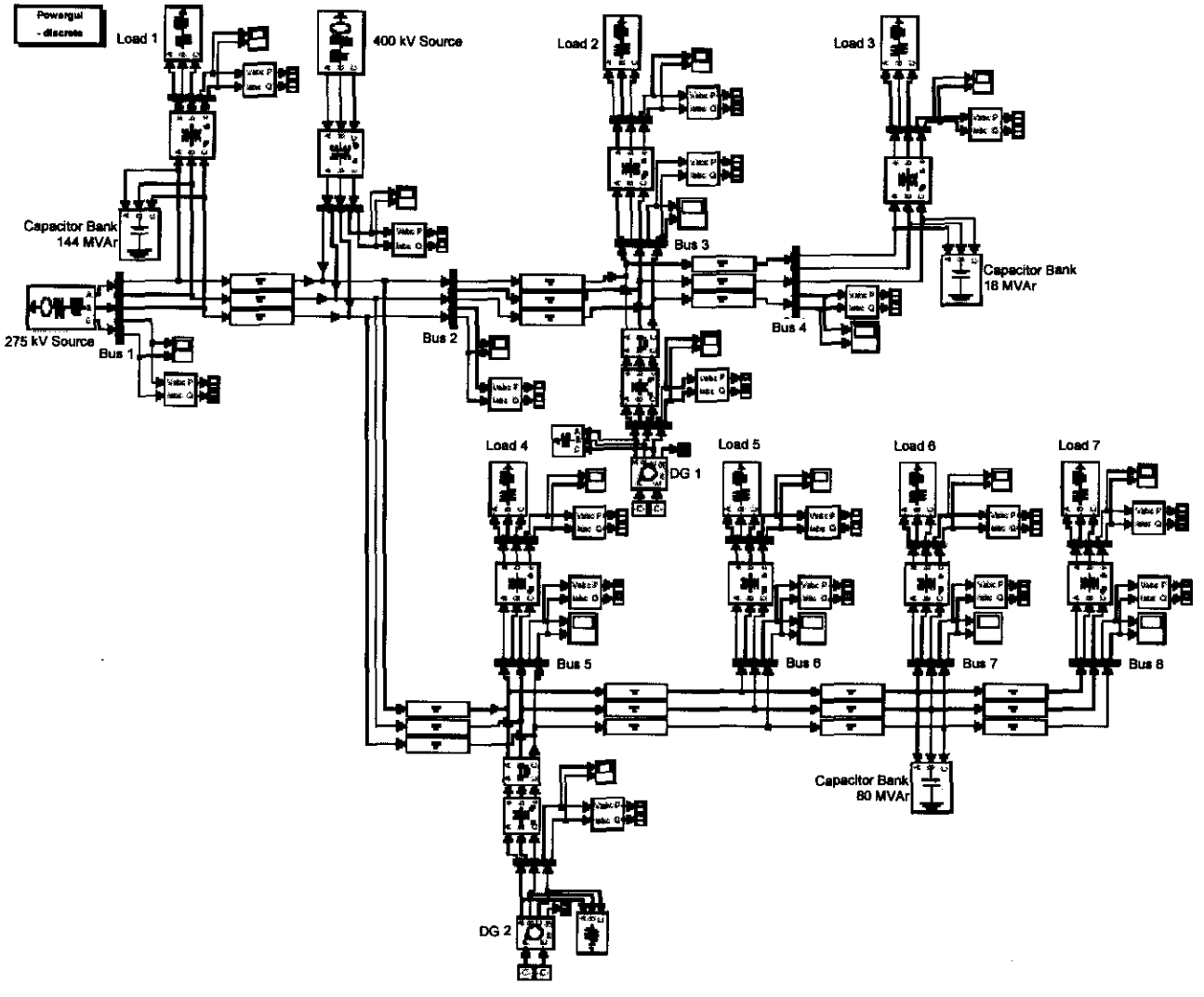

Figure E.1 Simulink model of the electric power network.

Bibliography

1. CIRED report (International Conference on Electricity Distribution), "*Dispersed generation*", Working Group WG04, Brussels, Belgium, June 1999.
2. Anis Ibrhim, M.M. Morcos, "*Electric power quality and artificial intelligence: Overview and applicability*". IEEE Power engineering review, 5-10 June 1999.
3. R.C. Dugan, M.F. McGranaghan, H.W. Beaty, "*Electric Power Systems Quality*", McGraw-Hill, 1996.
4. IEEE Std. 1159 –1995, "*Recommended Practice for Monitoring Electric Power Quality*".
5. GE Corporate Research and Development, "*DG Power Quality, Protection and Reliability Case Studies Report*", September 2001.
6. V. Del Toro, "*Electric Power Systems, Optimal Economic Dispatch of Generators*", Prentice Hall, 1992.
7. See the "*Electric Power Research Institute (EPRI)*" web – page http://www.epri.com/gg/newgen/disgen/index.html .
8. Gas Research Institute, "*Distributed Power Generation: A strategy for a competitive energy industry*", Gas Research Institute, Chicago, USA 1998
9. D. Sharma, R. Bartels, "*Distributed electricity generation in competitive energy markets*", in: The Energy Journal: Distributed Resources: Toward a new paradigm of the electricity business, Cleveland, Ohio, USA 1998, p.17 – 40.
10. CIRED, "*Impact of increasing contribution of dispersed generation on power systems*", CIGRE Study Committee no 37, September 1998.
11. C.P. du Rand, "*Capita Selecta – Distributed generation*", North-West University, Potchefstroom, 2004.
12. Electrical Power Research Institute (EPRI), "*Power quality impacts of distributed generation: Guidelines*", Final Report, California, USA, December 2000.
13. "*Draft 2 NRS 048-2*", 2002.
14. T.J. Ross, "*Fuzzy logic with engineering applications*", McGraw-Hill, USA 1995.
15. S. Haykin, "*Neural Networks: A comprehensive foundation*", Prentice Hall, New Jersey, USA 1999.
16. W.R. Anis, M.M. Morcos, "*Electric power quality and artificial intelligence: applicability and overview*," Proceedings of the 1998 Large Engineering Systems Conference on Power Engineering, Halifax, Nova Scotia, Canada, pp.107-111.
17. R. Caldon, F. Rossetto, A. Scala, "*Reactive power control in distribution system with dispersed generators: a cost based method*", Italy, Aug 2002.
18. H. Saadat, "*Power System Analysis*", 1999.

19. Kundur, P, "*Power System Stability and Control* ", McGraw-Hill, New York, 1994.
20. Dommel, H.W. and Tinney,W. F., "*Optimal power flow solutions. IEEE Transactions on Power Apparatus and Systems*", vol. PAS-87, no. 10, pp. 1866–76., 1968.
21. "*Matlab 6.5R13 Help Manual*", The Mathworks, June 2000.
22. "*Power System Blockset - For use with Simulink*", The Mathworks, September 2000.
23. H.L. Willis, W.G. Scott, "*Distributed Generation - Planning and Evaluation*", Marcel Dekker, New York, 2000.
24. Borbely, A, Kreider, J.F.,"*Distributed Generation - The power paradigm for the new millennium*", CRC Press, Florida, 2001.
25. J. Vallejos, R. Ramos, B. Baran, "*Multi-Objective Optimization in Reactive Power Compensation*", Paraguay, 2001.
26. R. Caldon, F. Rossetto, A. Scala, "*Reactive power control in distribution system with dispersed generators: a cost based method*", Italy, Aug 2002.
27. H. Demuth, M. Beale, "*Neural Network Users Guide v.4*", The Mathworks, January 2003.
28. C.C. Klimasauskas, "*Applying Neural Networks*", Vol. 5 no. 3, May/June 1991.

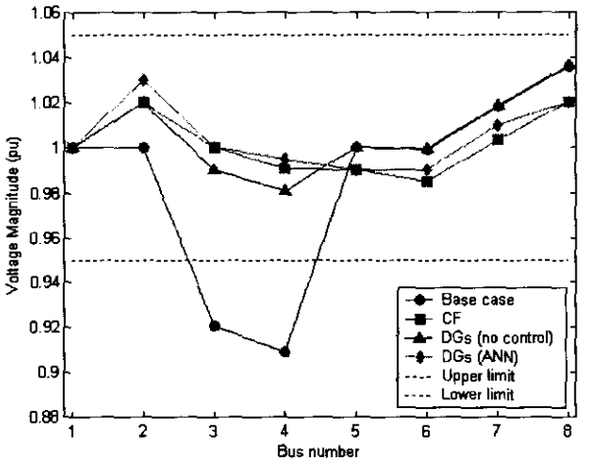

Figure 6.21 Bus voltage profiles of the power network.

From the results in figure 6.20 it is evident that the ANN controller could make a meaningful decision about the network load condition. The response of the ANN controller closely resembles that of the CF, but with a much better response time. The CF took 69 s (real-time) to find the optimum network condition and control variables, whereas the ANN controller took only 0.062 s (real-time). The results in table 6.9 show that the network conditions improved considerably over the base case. The average voltage deviations are established in the permissible range for both cases of DGs. This is expected because the power output parameters of the CF and ANN controller nears full power (DGs with no control run at full output power).

From the results in table 6.9, it is evident that control over the DGs improved the system power losses and the voltage deviation from 1 pu. Figure 6.21 shows that the bus voltage profiles improved over the base case, and that the voltage profiles for both cases of DGs are within the permissible limits. This concludes that the ANN controlled DGs improved network conditions and held the bus voltage profiles within the limits. As can be seen from these results, the behaviour of the ANN beyond the training load conditions showed a meaningful decision about the network conditions with much less computational time (compared to the CF).

6.5.2 Loads at 34% of switching capacity

The loads are randomly varied to 1228 MW within the boundaries of the load-switching spectrum. Table 6.10 describe the load conditions of the network at 34 %. Figure 6.22 show the response of the CF and the ANN controller for the control parameters of the DGs. Table 6.11 shows the results of the load conditions for the base case, CF, DGs with no control and response of the ANN controller. The bus voltage profile of the network is shown in figure 6.23.

	P_{load} (MW)	Q_{load} (Mvar)	Switch (%)
Load 1	160	52.589	10
Load 2	320	105.18	20
Load 3	130	42.729	50
Load 4	240	78.884	80
Load 5	110	36.155	33.3
Load 6	220	72.311	40
Load 7	48	15.777	75
L_{Total}	1228	403.62	34.17

Table 6.10 Load conditions for a total load-switch of 34 %.

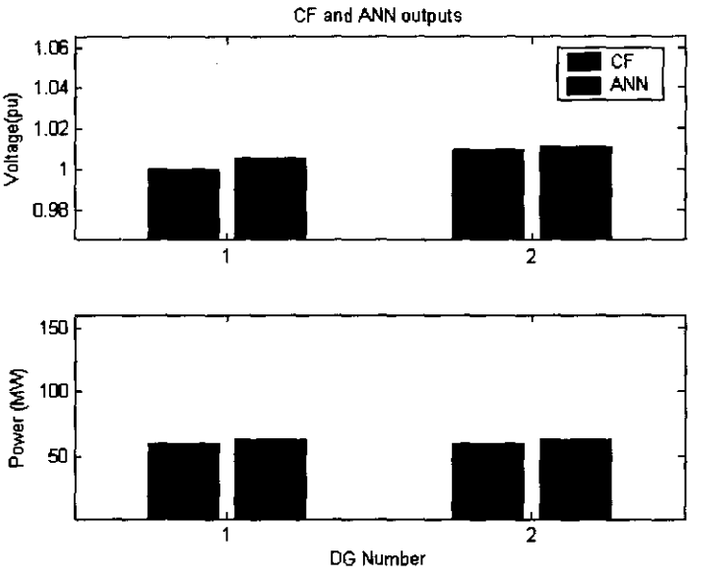

Figure 6.22 Response of the CF (left) and the ANN controller (right).

Statistics around 34 %	Average voltage deviation (permitted) %	Average voltage deviation (ideal) %	System active power loss (MW)
Base case (no DGs)	0.48597	2.1846	73.772
CF evaluation	0	0.84334	58.345
DGs (no control)	0	1.0108	58.814
DGs (ANN controller)	0	0.96834	58.606

Table 6.11 Results of the power network.

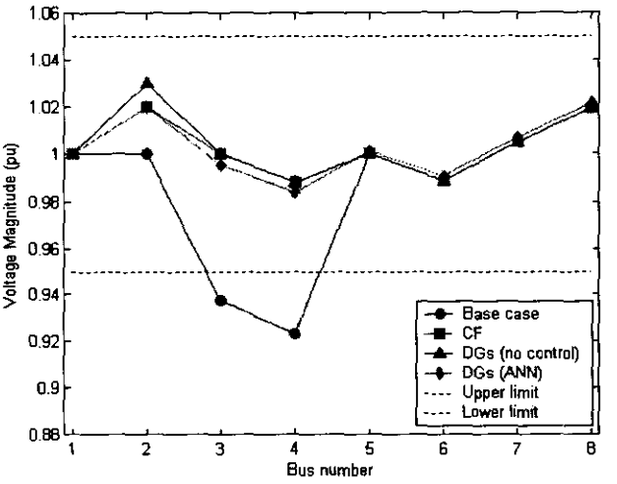

Figure 6.23 Bus voltage profiles of the power network.

The results in figure 6.22 show that the ANN controller and CF decisions about the network load conditions were closely matched. The response of the ANN controller and CF closely resembles each other. The results in table 6.11 show similar trends than the results in section 6.5.1. The network conditions improved considerably over the base case. The active network losses of the system are reduced by 15 MW, to only 58 MW. The average voltage deviation from the permissible range is also reduced to 0 % by the DGs. The results show that the DGs with ANN control produced better results over the DGs with no control. Figure 6.23 shows that the ANN controller improved the bus voltage profile over the base case for busses 3 and 4. The undervoltages at these busses are regulated within the permissible range with the ANN controller.

6.5.3 Loads at 70% of switching capacity

The loads in the power network are randomly varied to 1368 MW within the boundaries of the load-switching spectrum. Table 6.12 describes the new load conditions of the network at 70 % of the total rated switching spectrum. Figure 6.24 shows the response of the CF and the ANN controller for the control parameters of the DGs. Table 6.13 shows the results of the load conditions for the base case, CF, DGs with no control and of the ANN controller. The bus voltage profile of the network is shown in figure 6.25.

	P_{load} (MW)	Q_{load} (Mvar)	Switch (%)
Load 1	250	82.171	100
Load 2	380	124.9	80
Load 3	130	42.729	50
Load 4	210	69.024	20
Load 5	120	39.442	66.67
Load 6	230	75.597	60
Load 7	48	15.777	75
L_{Total}	1368	449.64	70

Table 6.12 Load conditions for a total load-switch of 70 %.

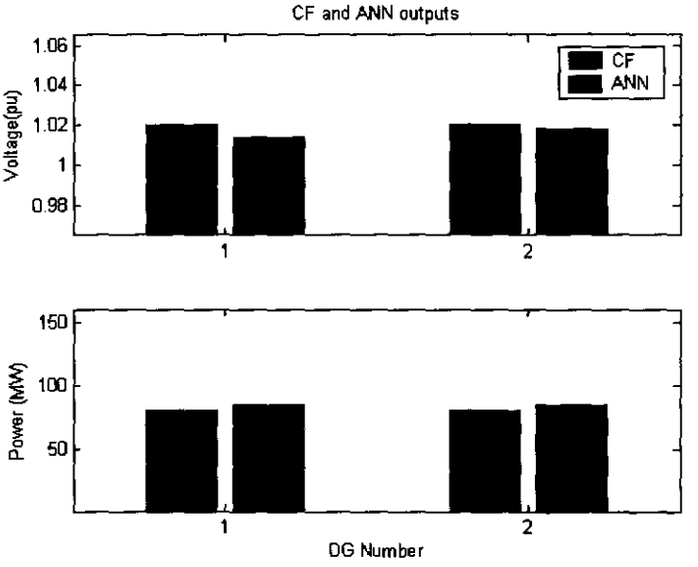

Figure 6.24 Response of the CF (left) and the ANN controller (right).

Statistics around 70 %	**Average voltage deviation (permitted) %**	**Average voltage deviation (ideal) %**	**System active power loss (MW)**
Base case (no DGs)	0.84647	2.6152	82.565
CF evaluation	0	0.91342	61.592
DGs (no control)	0	1.5199	62.615
DGs (ANN controller)	0	1.0691	61.789

Table 6.13 Results of the power network.

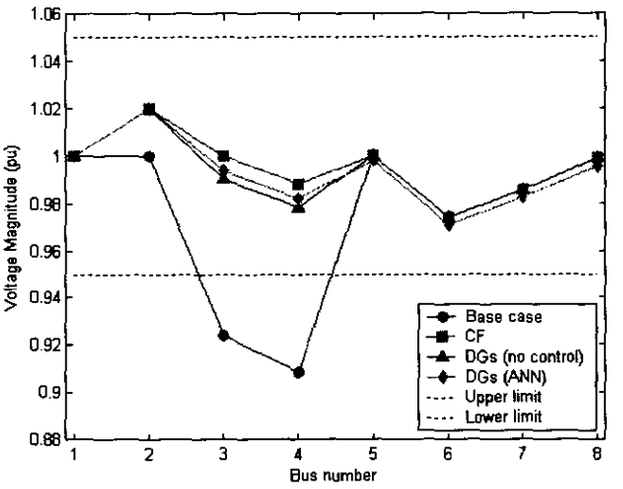

Figure 6.25 Bus voltage profiles of the power network.

Figure 6.24 describes the response of the CF and ANN controller to the load condition. The results reveal that the ANN controller closely mimics the response of the CF, thus making an appropriate decision again. The response shows that the best network conditions are achieved with the DGs running at about half-rated power. The time response of the ANN controller also topped the CF response with only 0.071s of computational time. Table 6.13 captures the statistics of the power network for this simulation run. The results obtained here also reveal that the network conditions improved over the base case. The rest of the findings are similar to the analysis of paragraphs 6.5.1 and 6.5.2 where the load conditions were set to other levels. Voltage levels are within the permissible range and the network power losses are minimized.

Figure 6.25 describes the voltage profile on all the system busses. The results reveal that the DGs improved the profile for all the busses over the base case. The profiles also reveal that the uncontrolled and controlled cases are more or less the same. The controlled case however shows better average deviation and network power losses. From all these results it is clear that the ANN controller chooses appropriate control parameters for the DGs for this simulation run.

6.5.4 Discussion of results

Results were obtained for changing load conditions in the power network and the adaptive behaviour of the ANN controller was investigated. The response of the ANN controller to such varying load conditions is the key issue to discuss. To facilitate the evaluation of the ANN controller, the results of the simulation runs are summarised in table 6.14.

The results of the ANN controller should primarily be compared to the base case, i.e. the original power network with no DGs. Since the main objectives of the ANN controller are to regulate the voltage profile of the network and minimise the active power losses, V_{avg}, V_{ideal} and P_L are evaluated. The base case showed that the voltage profile of busses 3, 4, 6, 7 and 8 drifted outside the limits for certain load conditions. In the simulation runs, busses 3 and 4 mainly posed a problem area in the network. The voltage profile of the network is improved for all the cases to within the permissible voltage range with the aid of the DGs and ANN control. The voltage parameters showed better results for all the simulations if the DGs were controlled.

The power losses of the system are significantly improved for all the cases over the base case. The lowest values are obtained with ANN control with a reduction of over 36 MW. This is a reduction of almost 40 % in the network power losses. This reduction is because sources closer to the load provide the necessary power and regulation as to central sources kilometres away. This concludes that the DGs with control reduce power flows in the power network and lines, thus reducing network losses.

As seen in table 6.14, the ANN controller made inadequate decisions on two occasions. The response of the ANN controller improved the network conditions over the base case, but degraded it for the case where no control over the DGs was active. The integrity of the ANN controller has to be improved to enable it to make meaningful decisions for any load condition in the switching spectrum. This could be achieved by analysing the power network with a much larger variety of load conditions and training the ANN controller to accommodate these conditions. This however would increase the training data considerably and may form the basis for future research.

Run no.	Load conditions								Base case			CF Output							ANN Output						
	L1 (MW)	L2 (MW)	L3 (MW)	L4 (MW)	L5 (MW)	L6 (MW)	L7 (MW)	Switch (%)	V_{avg} (%)	V_{ideal} (%)	P_L (MW)	DG1 V (pu)	DG1 P (MW)	DG2 V (pu)	DG2 P (MW)	V_{avg} (%)	V_{ideal} (%)	P_L (MW)	DG1 V (pu)	DG1 P (MW)	DG2 V (pu)	DG2 P (MW)	V_{avg} (%)	V_{ideal} (%)	P_L (MW)
1	210	400	120	220	100	220	44	55	0.85	2.81	73.68	1.01	150	0.99	150	0	0.96	48.19	1.015	150	0.995	150	0	1.13	48.41
2	160	320	130	240	110	220	48	34	0.49	2.18	73.77	1.00	60	1.01	60	0	0.84	58.34	1.005	65	1.012	65	0	0.96	58.61
3	250	380	130	210	120	230	48	70	0.85	2.61	82.57	1.02	80	1.02	80	0	0.91	61.59	1.015	83	1.018	83	0	1.07	61.78
4	150	340	130	230	110	200	46	28	0.60	2.88	67.50	1.00	150	0.99	150	0	1.19	48.20	1.002	149	0.991	149	0	1.33	47.89
5	250	300	130	210	110	230	42	45	0.37	2.03	68.73	1.00	40	1.02	40	0	0.80	59.26	1.003	46	1.022	46	0	1.00	57.84
6	190	330	160	250	100	220	48	51	0.90	2.69	78.38	1.01	70	1.01	70	0	1.05	59.58	1.014	65	1.009	65	0	1.18	60.59
7	210	330	150	210	100	210	42	40	0.78	3.09	65.88	1.01	150	0.99	150	0	1.27	48.07	1.012	150	0.991	150	0.008	1.75	47.01
8	170	380	140	230	120	240	48	60	0.97	3.19	92.21	1.04	150	1.04	150	0	1.10	57.22	1.028	150	1.042	150	0	1.09	56.98
9	240	390	150	240	130	220	42	81	1.16	2.84	90.08	1.03	140	1.00	140	0	1.02	55.54	1.037	137	1.005	137	0	1.17	56.33
10	160	320	110	200	110	210	44	15	0.27	2.27	61.78	1.00	130	0.99	130	0	0.98	49.29	1.003	133	0.993	133	0	1.13	48.86
11	230	370	150	240	100	220	46	66	1.03	2.87	79.45	1.01	150	0.99	150	0	1.01	51.36	1.009	148	0.991	148	0	1.01	51.38
12	230	350	130	210	120	200	44	48	0.66	2.81	67.49	1.00	150	0.99	150	0	1.16	48.51	1.003	150	0.991	150	0.009	1.29	48.17

Table 6.14 Evaluation of the adaptive behaviour of the ANN controller (Summary of results).

6.6 Conclusions

The results of the CF and ANN controller to optimise network parameters are evaluated in this chapter. The power network is firstly evaluated for the case where DGs are present in the network, but with no control. The results showed that the network environment in terms of voltage profiles improved to a certain extent for some busses, but to the detriment of other busses. The network power losses improved considerably over the base case. The CF is then used to analyze network conditions for a given load profile. The CF is tested against the base case, i.e. the original power system without the DGs. Using the CF to analyze and improve the network environment seems viable. The regulating requirements in terms of deviation from the permitted and ideal values are met while the network active power losses are kept to a minimum.

The ANN controller is evaluated for load conditions within the original data set developed by means of the CF. The ANN controller showed similar results as the CF and it is concluded that the ANN controller can make meaningful decisions for these load profiles. The ANN controller also made proper decisions for load conditions beyond the training limits. To improve the capabilities of the ANN controller, it should be trained with a broader spectrum of load possibilities. This would enable the ANN controller to make informed control decisions for a bigger region of load conditions. In practice this would be a requirement, but to the expense of a much bigger and more complex training data set. The ANN controller developed for the purpose of this project however showed adequate network conditions and improved power quality parameters.

Chapter 7 - Conclusion and Recommendations

7.1 Introduction

The traditional way of delivering power to a consumer is from a centralised utility. With the rapid growth of technology, generation of power at all levels is possible whether at transmission, distribution or at the end user level. The confluence of decentralisation with advances in distributed generation (DG) and artificial intelligence (AI) has opened new opportunities to deliver power closer to the point of consumption. The purpose of this research was to investigate the feasibility of using AI to control power quality (PQ) parameters through the optimal utilisation of DG in an electric power system. This chapter concludes the research conducted and summarises the significance of the study.

7.2 The significance of the research

The electric power system under investigation is characterised by large loads switching on-and off the electric grid. As described in the IEEE Std. P1433, these conditions are likely to cause PQ phenomena termed under-and overvoltages. These phenomena are the result of poor system voltage regulation capabilities and controls. The NRS 048 standard in South Africa demands that voltage regulation must comply within ±5 % of the nominal voltage level for voltage levels above 500 V. To find a solution to these conditions, DG with AI controls is evaluated in this research to regulate the voltage profile of the electric power system and reduce the active power losses.

To evaluate the behaviour of an Artificial Neural Network (ANN) controller controlling the DGs, a simulation model is developed which integrates the DGs and the electric power system. The strategic placement of the DGs in the power system is important to complement their voltage regulation capabilities. For the purpose of simulation, the Matlab® environment facilitates all the software tools necessary to analyse the power system and develop an AI controller. The electric power system is modelled in SimPowerSystems®, a toolbox integrated into Matlab to model electric networks and systems. This simulation model forms the basis for the analysis of the electric power system.

The ANN emerged as the most suitable AI technique for the control algorithm. Using ANN control is shown to minimise the network active power losses while optimising the bus voltage profile of the network in terms of the average voltage deviations from the permissible and ideal values. The cost function is initially used to develop training data for the ANN. This data incorporate load-switching patterns for the network and the optimal deployment of the DGs. The ANN is trained with this

randomised data set and the ANN topology used is 14:24:4 representing 14 input neurons, 24 hidden layer neurons and 4 output layer neurons.

The ANN controlled cases are compared to conditions of no control where the DGs are deployed at full power and a nominal voltage level of 1 pu. For the load conditions analysed by the cost function, the ANN controller proved to be very effective in controlling the DGs. The bus voltage profiles as well as the average voltage deviations are successfully kept within the permissible voltage range. From the results, the system active power losses are reduced by an average of 24 MW. Comparing the results obtained, the optimal utilisation of DGs showed that the network conditions improved vastly over the original power system.

The adaptive behaviour analysis of the ANN controller beyond the training limits reveals that the ANN controller can make meaningful output decisions when subjected to load conditions not in the training set. Beyond the training limits means that the load conditions are increased to different randomly selected power levels. What becomes clear from these analyses is that the behaviour of the ANN controller closely mimics the response of the cost function. This behaviour of the ANN justifies the ability of the cost function to select the optimal network conditions as the same improvements are seen in the network as discussed in the previous paragraph.

Table 7.1 describes the results of improvement in the network conditions over the original power network. The results conclude that the integrated power system with DGs could be controlled to eliminate under-and overvoltages due to the switching of large loads.

Electric Power System	Ave. voltage deviation - Permitted (%)	Max. voltage deviation - Permitted (%)	Ave. voltage deviation - Ideal (%)	Max. voltage deviation - Ideal (%)	Ave. active power losses (MW)
Original	0.6898	11.72	2.8176	4.501	78.7110
DGs with ANN controller	0	0	1.1107	1.982	54.6043
Improvement (%)	**100**	**100**	**60**	**56**	**31**

Table 7.1 Summary of the results of the research conducted.

7.3 Further research

Based on the research conducted during this study, the following areas can be improved or be recommended for future research:

a) Refinement of the ANN training data;
b) Other power network configurations;
c) DG penetration on distribution level;
d) The impact of DG on other power quality issues.

The training data developed by the CF are based on the same active output power for all the DGs. This constraint limited the output combinations of the DGs to an acceptable size. The output combinations of the DGs could be refined to a larger domain of output voltage and active power levels. This refinement would affect the developed model and ultimately the performance of the power network. The load boundaries of the network are set to the network load capacity and not to the current operational boundaries of the loads. Changing the training data to the operational boundaries and updating it as the boundaries change need to be devised.

The primary objective of distribution systems is to supply customers at a voltage that is within a prescribed range. Adding DGs on a distribution feeder at different locations and increasing the DG penetration level directly affects the control of voltage regulation devices like LTCs (load tap changers), SVRs (step voltage regulators) and switched capacitor banks. Devising an integrated control scheme can be used to assist these devices in the overall voltage regulation of the distribution feeder. Implementation of such a control scheme, however, requires a communication infrastructure not currently available in most distribution systems.

The primary power quality phenomena addressed in this research is under-and overvoltages. Adding DG to a power system potentially influences the quality of power provided to other customers connected to the grid. Some of the other power quality attributes that is of concern include harmonic distortion, flicker and voltage imbalance. These key issues could be considered in further investigations into the effect of DG on the quality of supply.

7.4 Closure

The conclusion of this dissertation is that the use of DGs with ANN control to optimise the power quality in an electric power system is meaningful. This is achieved through proper positioning and control. The evaluation of the power quality in the electric power system is however subject to power quality definitions used to optimise only certain parameters and it is recommended that further research be done on power quality and DG as discussed in section 7.3.

Annexures

A Power quality definitions

Current Distortion Distortion in the ac line current. See also *Distortion.*

Distortion Any deviation from the normal sine wave for any ac quantity.

Dropout Voltage The voltage at which a device ceases operation.

Flicker Impression of unsteadiness of visual sensation induced by a light stimulus whose luminance or spectral distribution fluctuates with time.

Frequency Deviation An increase or decrease in the power frequency.

Frequency Response In power quality usage, it refers to the variation of impedance as a function of frequency.

Fundamental (Component) The component of order one of the Fourier series of a periodic quantity.

Ground A conducting component by which the circuit is connected to the earth.

Harmonic (Component) The component of order greater than one of the Fourier series of a periodic quantity.

Harmonic Content The quantity obtained by subtracting the fundamental component from an alternating quantity.

Harmonic Distortion Periodic distortion of the sine wave.

Harmonic Number An integer multiple of the fundamental frequency.

Harmonic Resonance A condition were the power system resonates near one of the major harmonics produced by non-linear components.

Interharmonic (Component) A frequency component of a periodic quantity that is not an integer multiple of the fundamental frequency.

Low-Side Surges A current surge that's injected into the transformers secondary terminals upon a lightning strike to the grounded conductors in the vicinity.

Noise Unwanted electrical signals that produce undesirable effects in the circuits.

Non-Linear Load Electrical load whose impedance varies throughout the cycle of the ac input voltage.

Notch A switching disturbance of the normal power voltage; lasting less than a half cycle.

Oscillatory Transient A sudden, non-power frequency change in the steady-state condition of the voltage or current.

Overvoltage A voltage having a value of at least 10% above the nominal voltage.

Phase Shift Displacement in time of one voltage waveform relative to another.

Sag A decrease to between 0.1 and 0.9 pu in rms voltage or current.

Swell A temporary increase in the rms voltage or current of more than 10% the nominal voltage.